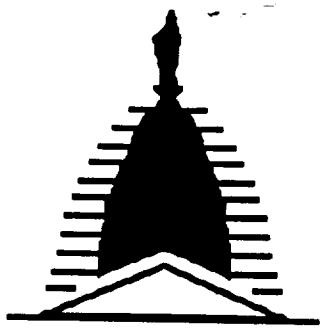

UNIVERSITY of
NOTRE DAME

# NASA/USRA UNIVERSITY ADVANCED DESIGN PROGRAM 1991-1992

## UNIVERSITY SPONSOR
## BOEING COMMERCIAL AIRPLANE COMPANY

# FINAL DESIGN PROPOSAL

# ARROW 227

Air Transport System Design Simulation

May 1992

Department of Aerospace and Mechanical Engineering
University of Notre Dame
Notre Dame, IN 46556

# ARROW 227

## Final Proposal

May 4, 1992


Michael Bontempi
Dave Bose
Georgeann Brophy
Timothy Cashin
Michael Kanarios
Steve Ryan
Timothy Peterson

# A. EXECUTIVE SUMMARY

The Arrow 227 is a commercial transport designed for use in an overnight package delivery network. The major goal of the concept was to provide the delivery service with the greatest potential return on investment.

The first step was to conduct a detailed mission evaluation followed by a thorough market analysis. The market analysis of AEROWORLD led to the implementation of a hub system of delivery with the hub located at city K. The analysis also revealed that service to cities C, D, and O should be excluded due to small runways and a negative profit margin due to excessive fuel costs. For this arrangement, the Arrow 227 will be required to fly intercontinental flights with a minimum range of 9720 feet and a minimum endurance of 6 minutes. The flight route suggested by the producers of the Arrow 227 requires a fleet of 16 aircraft. The fleet services twelve cities in AEROWORLD and each craft carries a maximum volume load of 1000 $in^3$ to each city. This proposed service also requires the Arrow 227 must also takeoff within a distance of 60 feet due to restrictions at AEROWORLD's city B airport. Finally, the RFP also required a minimum turn radius of 60 ft and a packaging constraint of 5'x3'x2'.

The design objectives of the Arrow 227 was based on three parameters; production cost, payload weight, and aerodynamic efficiency. Low production cost helps to reduce initial investment. Increased payload weight allows for a decrease in flight cycles and, therefore, less fuel consumption than an aircraft carrying less payload weight and requiring more flight cycles. In addition, fewer flight cycles will allow a fleet to last longer. Finally, increased aerodynamic efficiency in the form of high L/D will decrease fuel consumption.

The aerodynamics of the design were driven mainly by the desire for the minimization of drag and production cost. The wing planform was designed to minimize induced drag through the use of an

# TABLE OF CONTENTS

# A. EXECUTIVE SUMMARY

The Arrow 227 is a commercial transport designed for use in an overnight package delivery network. The major goal of the concept was to provide the delivery service with the greatest potential return on investment.

The first step was to conduct a detailed mission evaluation followed by a thorough market analysis. The market analysis of AEROWORLD led to the implementation of a hub system of delivery with the hub located at city K. The analysis also revealed that service to cities C, D, and O should be excluded due to small runways and a negative profit margin due to excessive fuel costs. For this arrangement, the Arrow 227 will be required to fly intercontinental flights with a minimum range of 9720 feet and a minimum endurance of 6 minutes. The flight route suggested by the producers of the Arrow 227 requires a fleet of 16 aircraft. The fleet services twelve cities in AEROWORLD and each craft carries a maximum volume load of 1000 $in^3$ to each city. This proposed service also requires the Arrow 227 must also takeoff within a distance of 60 feet due to restrictions at AEROWORLD's city B airport. Finally, the RFP also required a minimum turn radius of 60 ft and a packaging constraint of 5'x3'x2'.

The design objectives of the Arrow 227 was based on three parameters; production cost, payload weight, and aerodynamic efficiency. Low production cost helps to reduce initial investment. Increased payload weight allows for a decrease in flight cycles and, therefore, less fuel consumption than an aircraft carrying less payload weight and requiring more flight cycles. In addition, fewer flight cycles will allow a fleet to last longer. Finally, increased aerodynamic efficiency in the form of high L/D will decrease fuel consumption.

The aerodynamics of the design were driven mainly by the desire for the minimization of drag and production cost. The wing planform was designed to minimize induced drag through the use of an

aspect ratio equal to 10.52. A rectangular configuration was implemented to reduce production cost. The GO-508 airfoil was selected on the basis that it enabled cruise at the minimum point of the airfoil drag curve. Also, its simple shape helped to reduce production cost. Drag minimization was also apparent in the component drag breakdown. The fuselage and landing gear were designed to minimize their contribution to total parasite drag of the aircraft.

The design of the propulsion system was driven by three main objectives: 60 ft takeoff distance, minimal weight, and minimal current draw. The Astro 15 engine was chosen because it provided enough power to allow the aircraft to takeoff under 60 feet. The Zinger 10-6 was chosen as the systems propeller because it performed close to its maximum efficiency at cruise, and it provided enough thrust to takeoff within 60 feet. Twelve 900 mah batteries were used to provide enough power to the engine during takeoff.

The Arrow 227 is stabilized by employing a horizontal tail, a vertical tail, and dihedral. A convention configuration design was chosen for the Arrow 227 since the stability of the aircraft would be less sensitive to the center of gravity shift that occurs in cargo aircraft. The wing location and the location of the loaded aircraft CG were positioned so that no trim drag occurred at the cruise conditions which would increase the aerodynamic efficiency. Longitudinal and lateral control is achieved through the use of an elevator and a rudder. Ailerons were not employed since they would introduce additional cost and weight. Instead, lateral control was obtained by coupling the yaw and roll axis by using a high wing with 8 degrees of dihedral.

The structure of the aircraft is a major factor of the weight and must therefore be lightweight in order to meet our weight objective. With this in mind the fuselage was designed as an all balsa wood, truss structure and with all unnecessary support beams eliminated. The Arrow 227 is a cargo plane flying at low velocities and not expected to fly high g-maneuvers. Therefore the limit

load factor is only 1.5. This allowed the wing and fuselage to be designed as light as possible resulting in a structural weight fraction of less than 30%.

The strengths of the Arrow 227 are:

1) Large payload volume
2) Low Weight
3) Large Payload Fraction
4) Simplicity of design

The aircraft design was based on a 1000 $in^3$ cargo hold. The desire for a maximum cargo hold was to decrease the number of flights in order to increase profit for G-Dome Enterprises. The 1000 $in^3$ cargo hold can carry maximum capacity at an average package weight of .032 ounce per $in^3$. The totla aircraft weight of 6 lbs loaded achieved in the design of the Arrow 227 was due to material selection and careful desing of the fuselage and wing construction. By excluding control surfaces on the wing and implementing dihedral, added weight due to hinges and control rods was eliminated.

The weaknesses of the Arrow 227 are:

1) Inability to service all of AEROWORLD
2) Possible lack of thrust at takeoff due to small propeller size

The aircraft was designed to have a maximum full weight of 6.0 lbs carrying 100 $in^3$ of cargo. However, this payload volume and projected range and endurance do not allow all of AEROWORLD to be served. The cargo volume carried to and from each of the the three cities eliminated from service was not sufficient to provide a profit for G-Dome Enterprises and these cities did not have sufficient runway lengths to accomodate the Arrow 227. The Zinger 10-6 was chosen as the propeller for the Arrow 227. The propeller was designed to provide enough thrust at takeoff but there were two factors that led to uncertainty in these findings. The first was the high friction coefficient, 0.15, of the flight test range which would increase the takeoff thrust

requirement. The second was the size of the fuselage. The fuselage cross section was 7.5 x 4.0 in. Considering the diameter of the propeller was only 10 inches, the affect of fuselage interference on the propeller was uncertain.

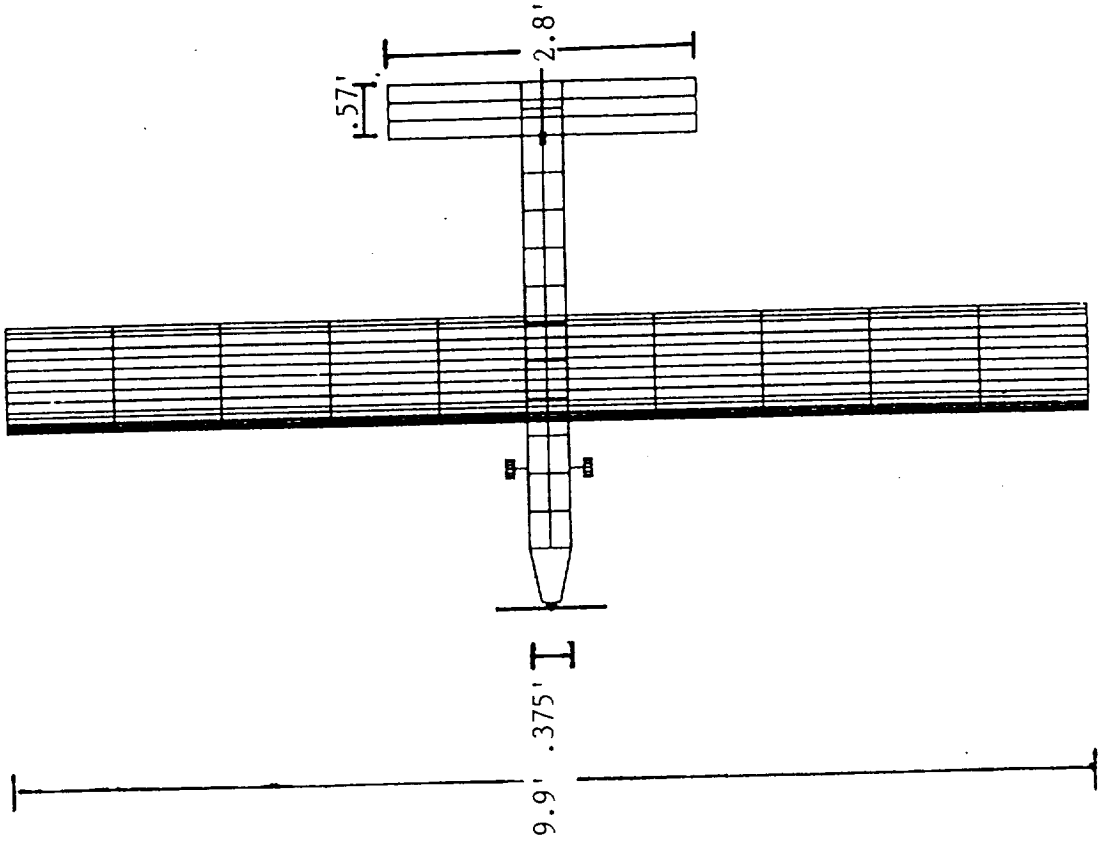


SCALE = 1 : 21.5

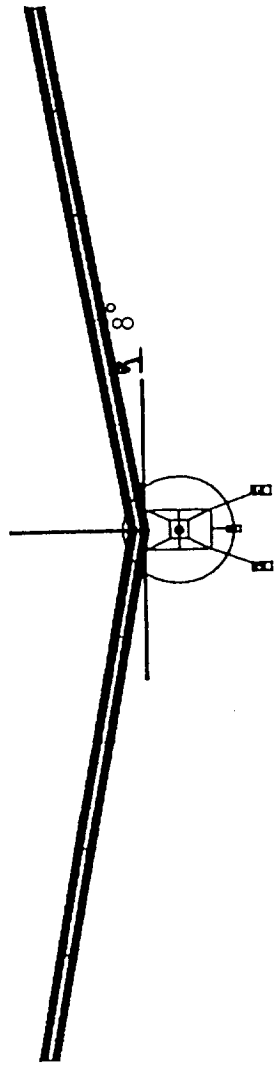


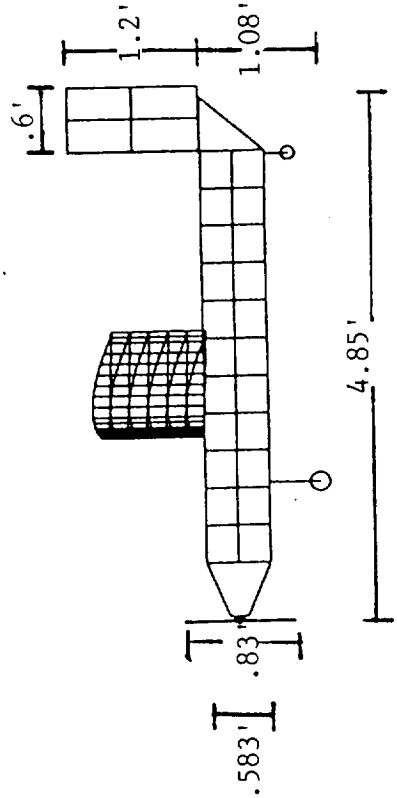

# B. MISSION "SCOPING" STUDY AND DR&O

## B.1 Introduction

The request for proposals states, "the project goal will be to design a commercial transport which will provide the greatest potential return on investment." The analysis of the RFP indicates that the plane design is primarily motivated by three factors: production cost, payload weight, and aerodynamic efficiency . These factors most directly affect the design approach. The production cost is important since the maximum expected life of the plane is less than 700 flight cycles. This maximum life was determined by accepting a minimum working stress reduction factor of .6. Using a stress reduction facto below .6 did not significantly increase the life of the aircraft. With this in mind, the production cost could be considered a cost per flight and was estimated to be over $400. Initially, the production cost was thought to exceed the total estimated maintenance, operation, and fuel costs per flight. Unfortunately, the same production cost is incurred per flight regardless of the distance travelled and the size of the payload. Therefore, the plane should be produced at a minimal cost and the number of flight cycles required to complete the mission should be minimized.

The second motivating factor, payload weight, is related to the first. The plane must carry the largest payload possible to lower the number of flight cycles necessary to deliver the cargo. It is not the volume of the payload, rather it is the weight that motivates the design. While a payload volume of 1.0 $ft^3$ can be achieved, the coinciding maximum possible payload weight of 4.3 lbs cannot reasonably be carried by a plane under the constraints set forth in the RFP. The gross weight of the aircraft is mainly limited by a minimum takeoff distance, the maximum wing size, and the cost of high lift devices.

The third motivating factor, aerodynamic efficiency, was determined after the initial DR&O. Soon after the initial DR&O, the cost of fuel was determined to be the largest component of the cost per flight. Therefore, it was necessary to make the aircraft as aerodynamically efficient as possible in

order to reduce drag and fuel consumption. The high cost of fuel per flight further emphasizes the need for a large payload capacity in order to reduce the number of flight cycles.

With the constraints of the RFP considered, the following design requirements and objectives were established.

## B.2 General Configuration

The data base of old design reports was consulted to make a reasonable total weight estimate for the aircraft These reports indicated that a plane was more likely to be successful if its takeoff weight was limited to under 5 lb. However, since the profitability of the aircraft increases proportionally with its payload capacity, an ambitious total takeoff weight of up to 6 lb was established. This allowed for a cargo weight of 2 lb and an operational empty weight of 4 lb. Allowing for an average cargo weight of 0.032 oz/$in^3$, the payload volume was then set at 1000 $in^3$.

## B.3 Service Market

A market analysis was performed to determine the feasability of servicing the various cities in Aeroworld. The market analysis considered each city's market size, runway length, and location relative to the other cities and/or a possible hub. The market analysis was performed considering a payload volume of 1000 $in^3$, and resulted in the removal of cities C, D, and O from the flight schedule to maximize profits. Short runways, small markets, and long flight distances were the factors considered in this decision. A hub was established at city K because of its central location and large market.

The market analysis indicated two options for a flight plan. Both flight plans attempt to reduce the number of flight cycles necessary to transport the available cargo. The first option maximized the return on the investment by insuring that each flight operated with a maximum payload. The flight plan requires 38 GAG cycles and delivers 22,000$in^3$ which results in 579 $in^3$ per GAG cycle. Even though this first option does not deliver all the available cargo between the serviced cities, it can be used as an initial flight plan to maximize the return on a limited investment. More routes can later be added to service the entire market and increase the total profit.

The second flight plan maximizes the profit by moving all the cargo between the serviced cities. Figure B.1 shows the second flight plan which requires 58 GAG cycles and delivers 30,930 $in^3$ . This distribution plan results in an average of 533 $in^3$ delivered per GAG cycle.

## B.4 Performance

Several performance requirements were established in the RFP. In order for the aircraft to service the designated cities, it must be able to takeoff on a 60 ft runway. In addition, the technology demonstrator must have the ability to perform a sustained level 60 ft radius turn. Finally, the disassembled aircraft must fit into a 2' x 3' x 5' box.

The minimum range and endurance were determined by considering the need to satisfy the requirement of a one minute loiter time after flying the farthest route and diverting to the nearest city. A minimum range of 9720 ft and a minimum endurance of 6 minutes satisfy the aforementioned requirements. These calculations were performed with a design cruise velocity of 27 ft/s.

## B.5 Cost

As mentioned earlier, the production cost is an important component of the total cost per flight. Again, previous design reports as well as the component and material costs were used to estimate the cost of the prototype and the man-hours involved in construction. The estimate production cost is $300,000 for each prototype.

# Figure B.1

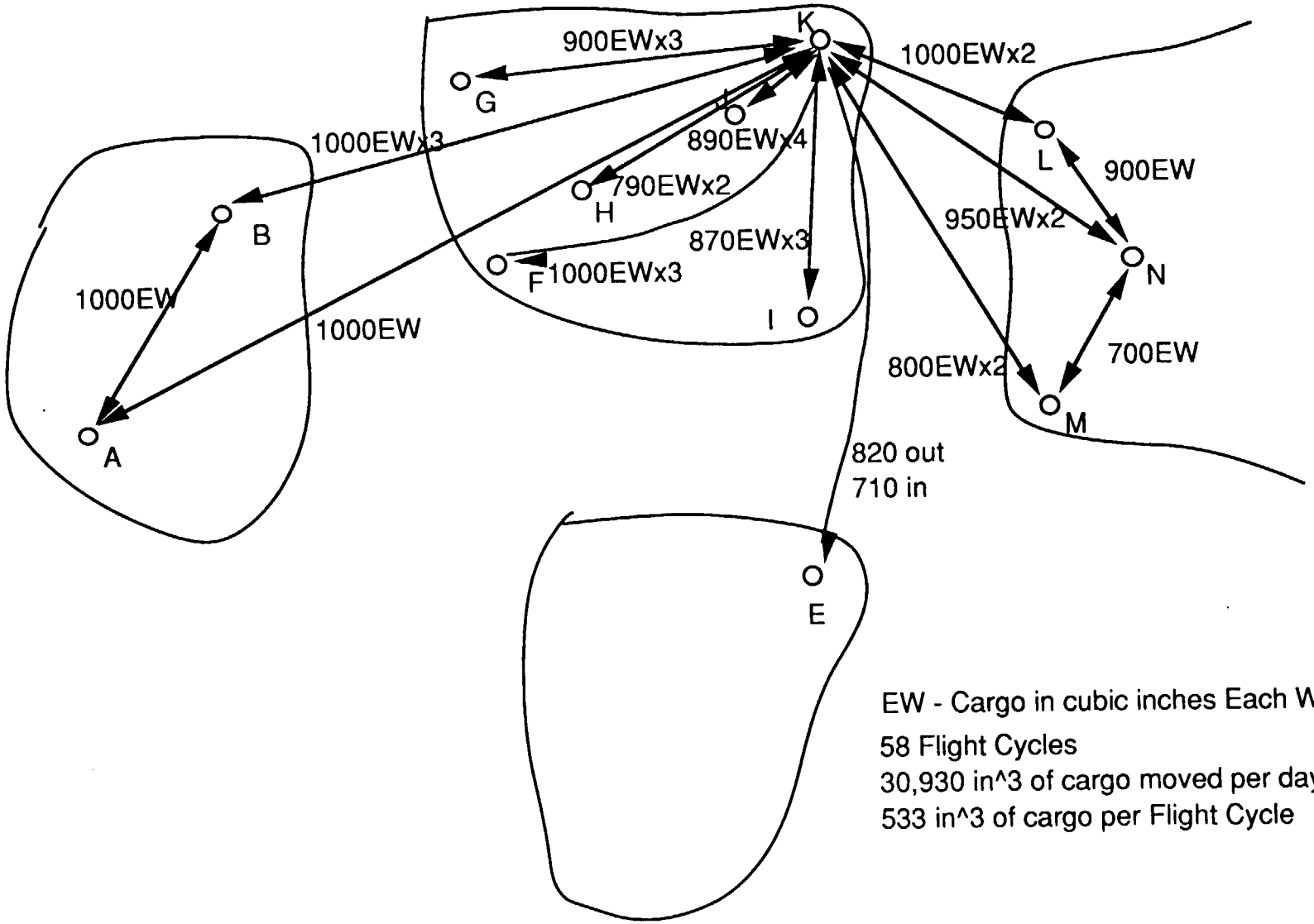
K
900EWx3
1000EWx2
G
J
890EWx4
1000EWx3
L
900EW
790EWx2
H
950EWx2
B
870EWx3
F
1000EWx3
N
1000EW
I
1000EW
800EWx2
700EW
M
A
820 out
710 in
E
EW - Cargo in cubic inches Each Way
58 Flight Cycles
30,930 in^3 of cargo moved per day
533 in^3 of cargo per Flight Cycle

# C. CONCEPT SELECTION STUDIES

## C.1 Canard Configuration

Among the first configurations conceptualized to meet the standards set in the DR&O was a canard aircraft (Figure C.1). It was believed at first that the canard would provide more lifiting surfaces and thus allow more cargo to be transported for G-Dome Enterprises. However, upon closer inspection, it turned out that the canard configuration may actually be less efficient than a conventional configuration aircraft. Specifically, the canard interferes with the main wing and thus lowers aerodynamic efficiency. Also, control of such an aircraft would prove quite difficult since the stability of a canard configuration is more sensitive to a center of gravity shift which occurs in cargo aircraft. The increased sensitivity is due to the fact that the center of gravity is located between the aerodynamic center of the wing and the horizontal tail instead of on or near the aerodynamic center of the wing as in a conventional configuration aircraft. For a cargo vessel, it is essential that the plane be readily controllable for a number of possible center of gravity shifts. The canard concept studied did not have a sufficient static margin for safety. A further drawback to this concept is the increased Research and Development and manufacturing costs inherent in such an advanced design. The canard concept created far more problems than benefits, and thus the concept was eliminated from consideration.

**Figure C.1**
**Canard Aircraft**

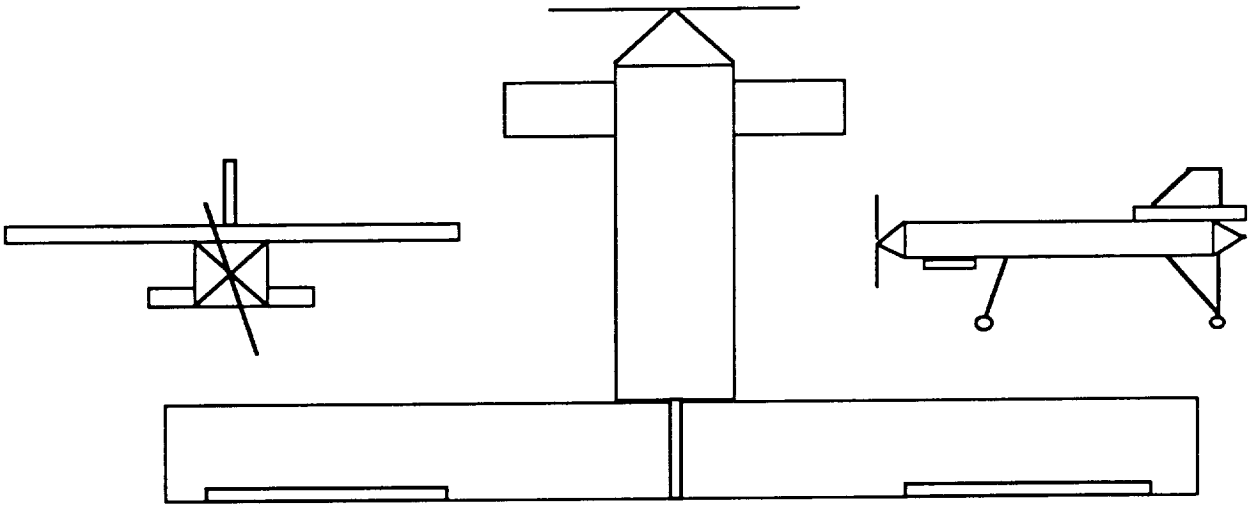

## C.2 Dirigible Configuration

The second configuration under consideration was that of a dirigible (See Figure C.2). This concept was considered mainly because the DR&O seemed to define a large, slow moving aircraft with short landing and takeoff distances. Nothing matched this description better than a blimp. A blimp was considered to be the ideal craft to meet these types of performance objectives. A properly designed zeppelin could meet the two pound cargo goal while maintaining a cruise velocity under 30 ft/s and taking off in under 60 feet. To do this with a blimp, however, necessitates an extremely large helium volume, which requires a larger engine to meet the overnight requirements (cruise velocity of ~27ft/s), which requires an even larger dirigible. The size of the concept would balloon greatly in order to meet the cargo and speed requirements, causing a great increase as well in the fuel cost per flight. These deficiencies indicated that this concept was inadequate to meet the mission requirements.

**Figure C.2**
**Zeppelin Concept**

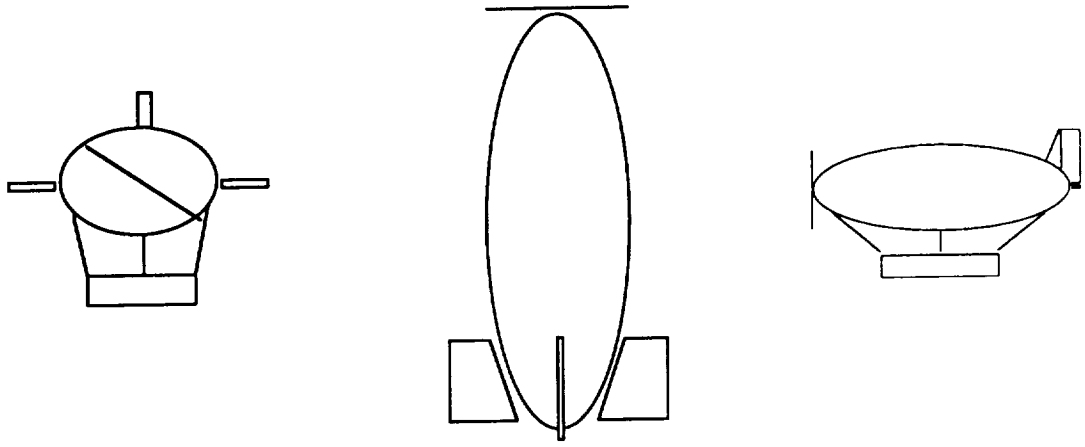

## C.3 Conventional Configuration

The third concept under consideration was a conventionally configured RPV (See Figure C.3). The team believed that using the wide data base which is accessible for this type of craft, the DR&O could be met with careful design. A conventional design would allow a large cargo volume to be carried with no penalty to aerodynamic efficiency or to stability with a shift in the center of gravity. Use of the large data base would also assist in keeping the manufacturing process simpler and could thus allow the team to present a more inexpensive RPV to G-Dome enterprises. Perhaps the greatest strength of this concept was that with proper design, it could have none of the weaknesses of the other two configurations under consideration.

The original conventional concept was to be controlled by ailerons, an elevator, and a rudder. This would require three servos for control, in addition to one for the motor (a total of four). Preliminary sizing included a 5 ft fuselage, a 10 ft wing span, and an empty weight of 4 lbs.

**Figure C.3**
**Conventional Aircraft**

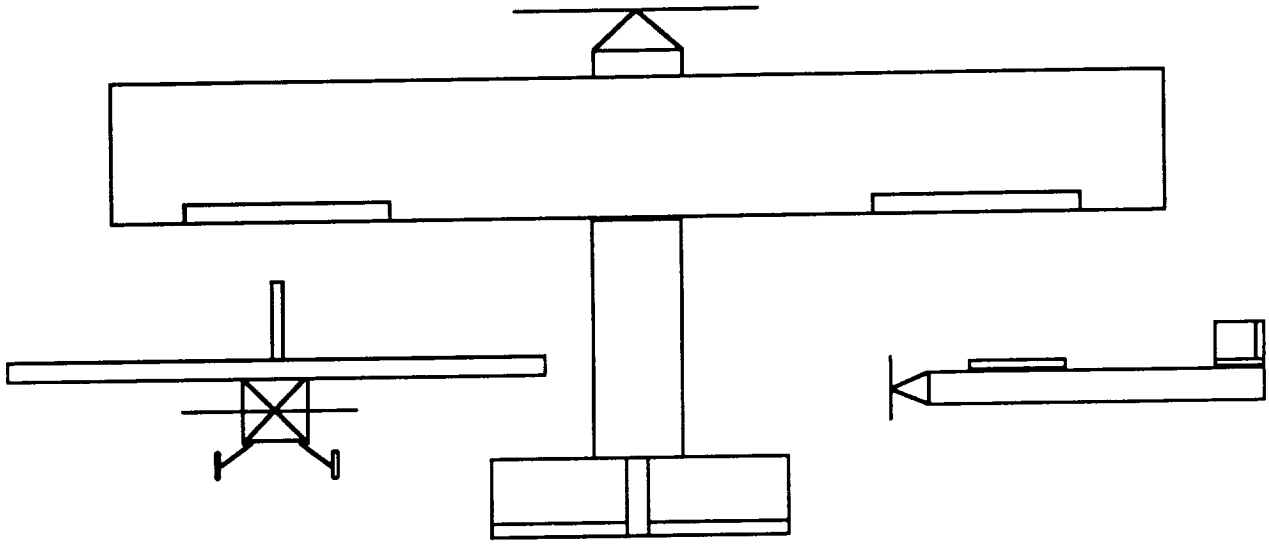

A comparison of the three concepts considered is given in Table C.1. As can be seen, the conventional design is superior to the other concepts considered, with more advantages and fewer disadvantages than the canard and dirigible.

**Table C.1**
**Comparison of Concepts**

| | Advantages | Disadvantages |
|---|---|---|
| Canard | Two Lifting Surfaces | High Construction Cost<br>Stability Problems<br>Aerodynamic Interference |
| Dirigible | Meets Cargo Requirements<br>Short Take-off Distance<br>Low Speed | Too Large For AEROWORLD<br>Too Slow For Overnight<br>Delivery |
| Conventional | Aerodynamic Efficiency<br>Large Data Base<br>2 lb, 1000$in^3$ cargo<br>Low Construction Cost | Large Wing Span |

# D. AERODYNAMIC DESIGN DETAIL

Fuel cost was seen as the biggest factor contributing to the overall cost of the mission. It was well recognized that as fuel consumption decreased, the percent return on investment would increase. Since fuel cost was directly related to the lift to drag ratio of the aircraft, minimizing drag became the single greatest, driving force behind the aerodynamic design. The wing design, airfoil selection, and the drag prediction of the Arrow 227 each demonstrate this motivation as well as the desire for reducing production cost.

## D.1 Wing Design

The wing design took shape after a number of trade studies. The most important of these studies investigated the trends revealed for changing wing area, aspect ratio, as well as taper. The performance of a given wing design was measured in terms of its take-off distance, stall velocity, and, above all, total drag.

Recognizing that the primary importance of the wing was to provide the necessary lift to enable the aircraft to fly, it was decided that sizing the wing would be the first order of business. Fixing the wing area would also eliminate one design variable and thus greatly simplify later studies.

An allowable wing area, S, was found by examining its relation to stall velocity, Vs, and take-off distance , $D_{TO}$. Wing area was related to stall velocity according to,

$$V_S = \sqrt{\left[\frac{2W}{\rho S C_{Lmax}}\right]}$$

With this equation, it was possible to see the effects of changing wing area on stall velocity[1]. Setting W to 6 lb., $C_{Lmax}$ to 1.2, and assuming sea level conditions, it was possible to represent this relation graphically in Figure D.1. Clearly, as the wing area was increased, stall velocity decreased. Figure D.1 also indicates the lower and upper bounds to wing area. The upper bound was estimated knowing that the stall velocity should not fall near the cruise velocity set by the

DR&O at 27 ft/s. The lower bound was estimated through the consideration of the storage requirements imposed on the aircraft.

## Figure D.1

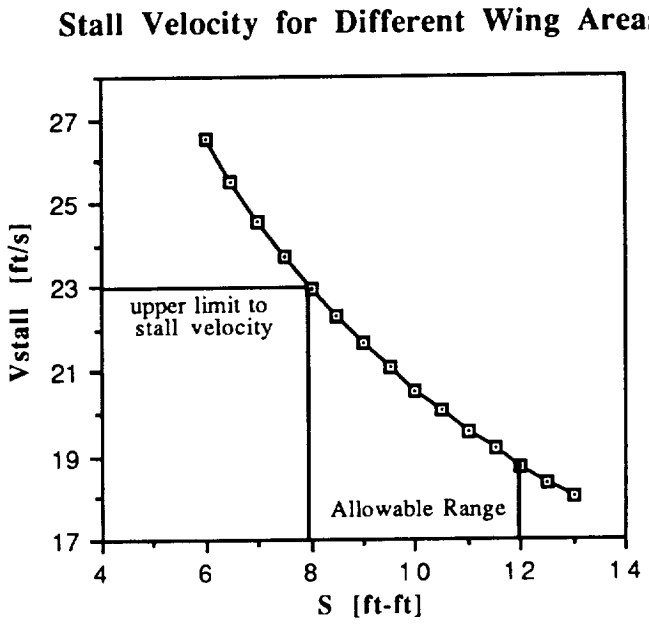


The wing area can also be related to the take-off distance. This relation was illustrated in Figure D.2 using the relation[1],

$$D_{TO} = \frac{1.44W^2}{\rho g S C_{Lmax}(T-(D+\mu(W-L))).7L}$$

The upper bound in this curve was set by the minimum take-off distance of 60 ft. set by the DR&O. The lower bound was set just as it was in the previous study. Together with Figure D.1, Figure D.2 presents a range of possible wing areas. A wing area of 9.5 $ft^2$ was decided upon since it provided a good compromise between the two studies.

## Figure D.2

**Take-off Distance for Different Wing Areas**

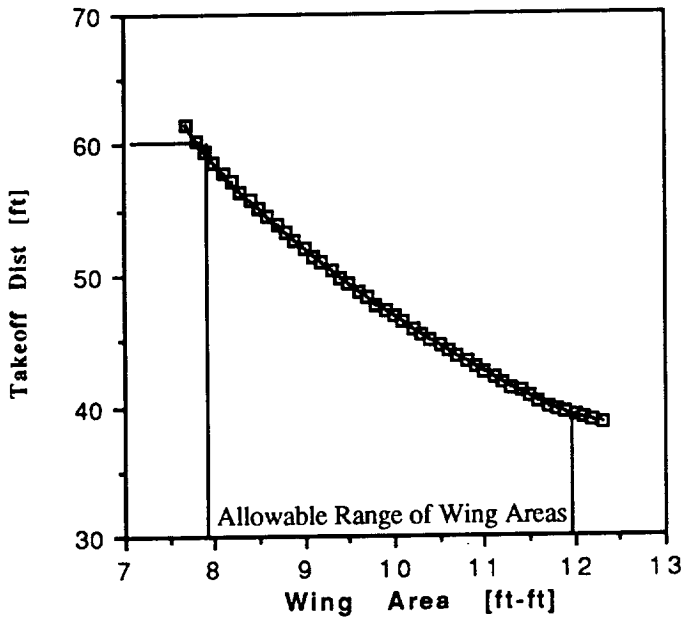


NOTE: In the investigation of wing area, the weight of the aircraft was assumed to remain at a constant value of 6 lb. Considering the small weight of the materials used in the wing construction as well as the small range of possible wing areas investigated, this assumption was deemed satisfactory.

With a wing area set, the next order of business was to find the most aerodynamic distribution of this area. Drag reduction became the primary factor on which a given configuration was measured. Using the software LinAir, by Desktop Aerodynamics Inc., it was possible to arrive at induced drag computations for certain area distributions. In this investigation, it was found that the aspect ratio, AR, was the major design variable. Since AR was a function of span length, b, according to the relation[1],

$$AR = \frac{b^2}{S}$$

the span was also a design variable. For the wing area of 9.5 $ft^2$, two rectangular planforms were compared. They were 9.5ft. by 1 ft. and 10ft. by .95ft. which corresponded to aspect ratios of 9.5 and 10.52 respectively. Figure D.3 demonstrates the effect of this increase in aspect ratio.

## Figure D.3

**Induced Drag for Different Aspect Ratios**

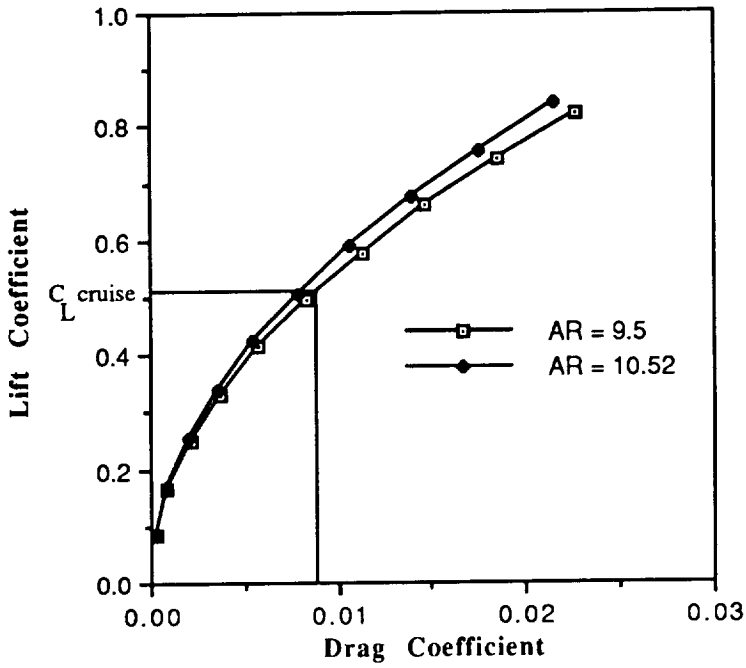


Since induced drag decreased with increasing AR, it was clear that increasing the span length would decrease $C_{Di}$ as well. However, an upper limit to such an increase was imposed by the storage, and flight test constraints set by the DR&O. After considering these constraints and structural constraints, an upper limit of 10 ft. was imposed on the wing span. The span of the Arrow 227 was therefore designed for 10 ft to maximize aspect ratio.

With the span defined, all that remained was to decide on taper. Using computer code, which solves the monoplane equation, it was possible to find the wing loading for various taper ratios. The trend which was revealed was that as the taper was decreased, more of the lift was pushed toward the wing tips. Although, to an extent, this provided a more desirable wing loading, a rectangular wing was chosen. The reasoning behind this decision pointed to the limited

manufacturing skills of the design team. However, as manufacturing skills improve, a movement to a taper giving a suitable wing loading was recommended.

In this manner, the wing design was completed. A dihedral angle of 8° was added to provide the necessary rolling capability to ensure a minimum turning radius under 60ft.. The details of this investigation are provided in section G. The final wing design is illustrated in Figure D.4.

**Figure D.4**

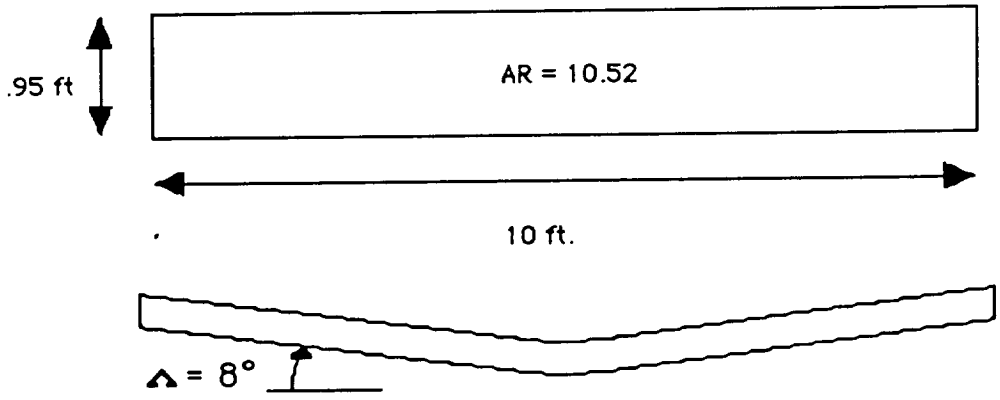


The resulting wing lift curve from this design is recorded in Figure D.5 The linear portion of this graph was estimated using LinAir by modeling the wing as four elements connected in a manner as to resemble the mean camber line of the wing section. The nonlinear portion of the graph was estimated using the computer code described in the previous paragraph. This code enabled the investigation of possible stall at various locations along the span and the resulting loss of lift.

## Figure D.5

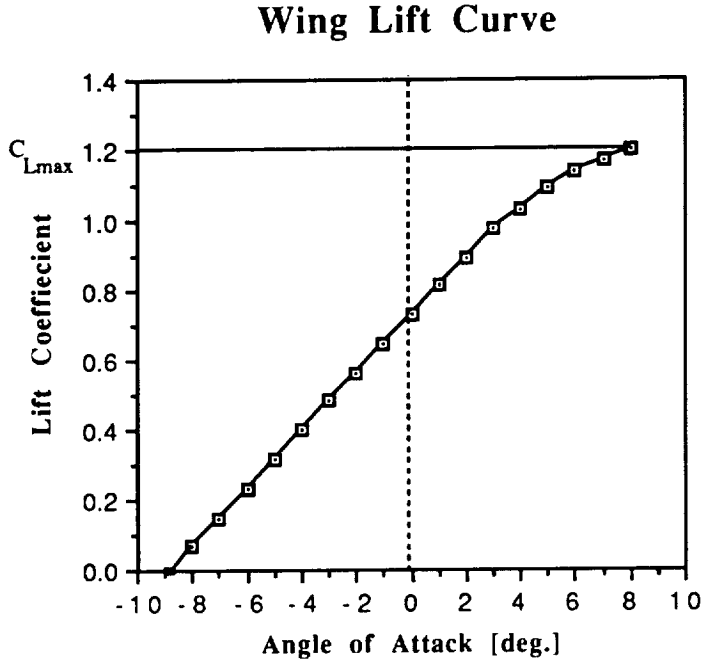


### D.2 Airfoil Selection

Many areas weighed into the selection of the airfoil including drag, lift, stall, and manufacturing. As was the case for the wing design, drag reduction was the most important. In terms of drag, a number of factors were considered. First was the problem of bubble drag resulting from low Reynolds Number flight. This problem could be avoided using a device to trip the flow around the airfoil forcing it to go turbulent. While this method would reduce bubble drag, parasite drag would be increased. Yet, proper design of the airfoil could minimize bubble drag without tripping. Airfoils which avoid the use of a reflexed trailing edge and incorporate a bubble ramp succeed in this respect[2]. Another factor considered in the area of drag was camber. The addition to camber of the airfoil would reduce drag by enabling the aircraft to cruise at an angle of attack which corresponds to the point of minimum drag on the airfoil lift curve[3].

Lift was also considered in the airfoil selection. An airfoil was required that would provide enough lift to allow steady, level flight. Also, a considerably high $C_{Lmax}$ would be required from the airfoil considering the short runways, characteristic of AEROWORLD. Another factor which influenced the airfoil selection was stall. An airfoil with a fat, rounded leading edge would be necessary to provide the gradual stalling needed to minimize impact during landing. One last consideration in the airfoil selection was manufacturing. An airfoil of simple shape would require fewer man hours to construct which would result in lower production cost. Taking all of these factors into consideration, the GO-508 airfoil was selected. The GO-508 succeeded in the following ways:

1. Its minimum point on the airfoil drag curve corresponds to the cruise $C_L$ of the design.
2. It provides satisfactory lift for take-off.
3. Its fat leading edge provides gradual stalling characteristics.
4. Its simple shape allows for easy manufacturing.

These points were demonstrated by the schematic of the GO-508 in Figure D.6 as well as in lift and drag curves for the airfoil recorded in Figures D.7 and D.8.

**Figure D.6**

**The GO-508**

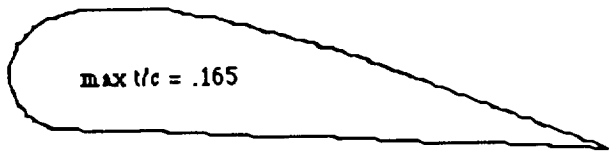

## Figure D.7

### The GO-508 Lift Curve [4]

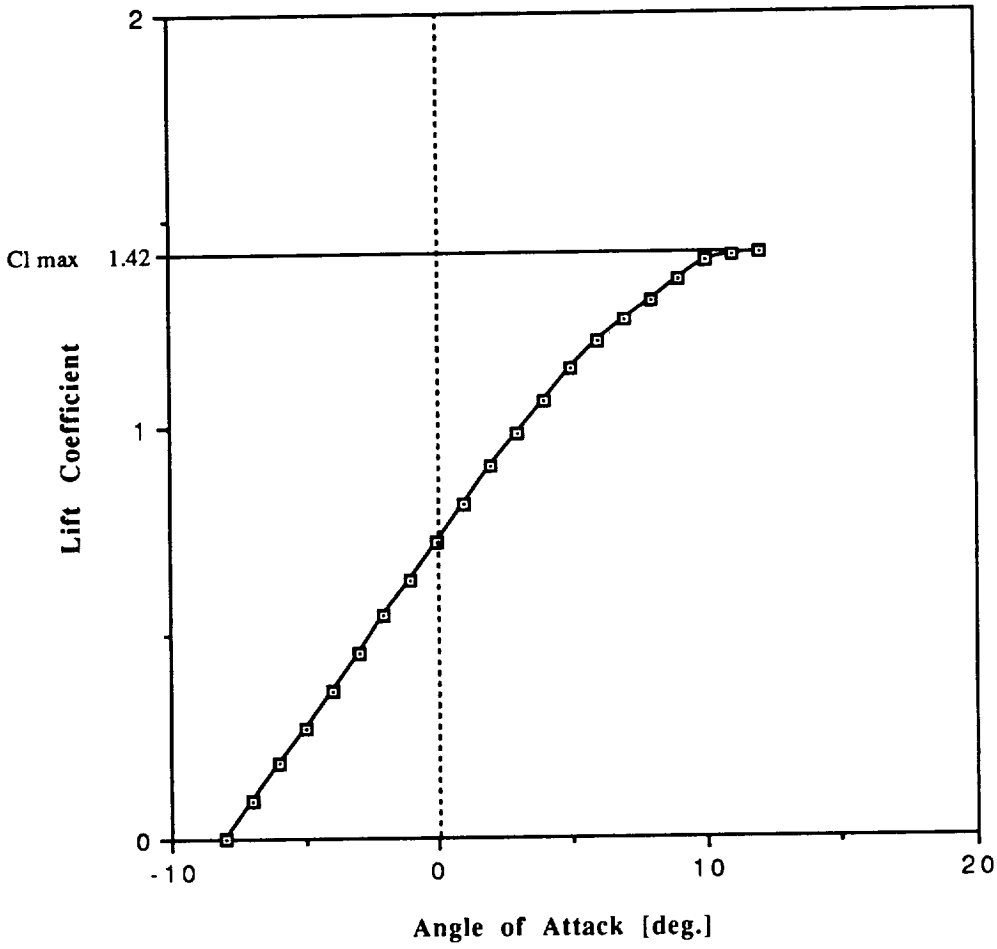

## Figure D.8

**The GO-508 Drag Curve** [4]

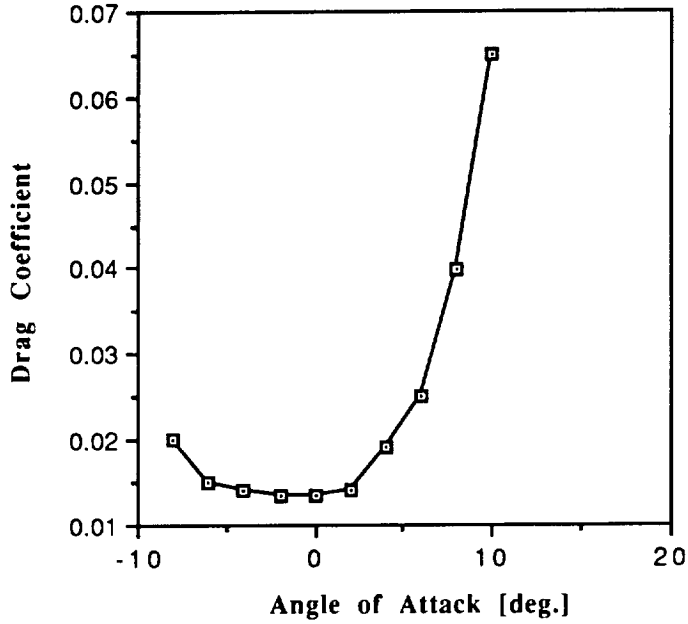


### D.3 Drag Prediction

The drag prediction for the design was performed using the drag breakdown method presented in the notes and lectures of AE 348, Flight Mechanics. According to this method, the parasite drag coefficient of $C_{Do}$ could be estimated by performing the summation,

$$C_{Do} = \Sigma \frac{C_{D\pi} A_{\pi}}{S_{ref}}$$

where $C_{D\pi}$ represents the parasite drag coefficient of an individual component of the aircraft and $A_{\pi}$ symbolizes the area which this $C_{D\pi}$ is based upon. The reference area, $S_{ref}$, used for this drag breakdown was the wing area. With values for $C_{D\pi}$ taken from the above reference, the contributions to the $C_{Do}$ of the aircraft for various components were found. The results were as follows:

| Component | Contribution to $C_{Do}$ |
|---|---|
| Wing | .014000 |
| Fuselage | .002533 |
| Nacelle | .000040 |
| Horizontal Tail | .002640 |
| Vertical Tail | .000890 |
| Landing Gear | .002227 |
| Total | .0230 |
| Roughness and Protuberances | + 15 % |
| $C_{Do}$= | .02645 |

The contribution of each component of the aircraft to the $C_{Do}$ was better visualized using Figure D.9.

**Figure D.9**
**Percent Contribution to the CDo**

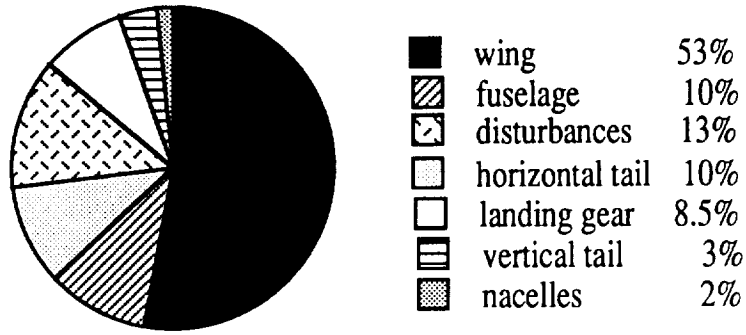

The drag breakdown method also enables the calculation of the Oswald efficiency factor, e, according to the equation,

$$\frac{1}{e} = \frac{1}{e_{fus}} + \frac{1}{e_{wing}} + \frac{1}{e_{other}}$$

In accordance with the method, for a rectangular fuselage and wing, and an aspect ratio of 10.52, the corresponding values for $e_{fus}$ and $e_{wing}$ were 22.9 and .78 respectively[5]. Also, $1/e_{other}$ was given as .05. Plugging these values into the above equation results in an Oswald efficiency factor of .73.

The overall drag of the aircraft could be found using the relation,

$$C_D = C_{Do} + KC_L^2$$

where K is a constant equal to $1/(\pi ARe)$. With the values for $C_{Do}$ and e found using the drag breakdown method, the equation for the overall drag of the aircraft becomes,

$$C_D = .0265 + .04145C_L^2$$

The drag of the overall aircraft was minimized in a number of ways. By maximizing the aspect ratio of the wing, the second term in the drag equation was reduced. Next, the fuselage was designed to have the smallest frontal area possible while still enabling the aircraft to carry the design payload volume of 1000 $in^3$. In this manner, the contribution of the fuselage to the $C_{Do}$ was minimized. Finally, a tail dragger was chosen over a tricycle configuration in order to reduce the contribution of the landing gear to the $C_{Do}$. The tail dragger contributes less to the $C_{Do}$ by minimizing the length of the support rods necessary for landing gear assembly. The overall drag of the Arrow 227 is graphed in Figure D.10.

The lift to drag ratio, L/D, for the Arrow 227 was found by manipulating the overall drag equation. For various angles of attack, the lift to drag ratio was calculated and recorded in Figure D.11. The lift to drag at the cruise angle of attack was also indicated in this Figure. This graph demonstrated clearly, that the Arrow 227 operates at maximum efficiency.

# Figure D.10

## The Arrow 227 Drag Polar

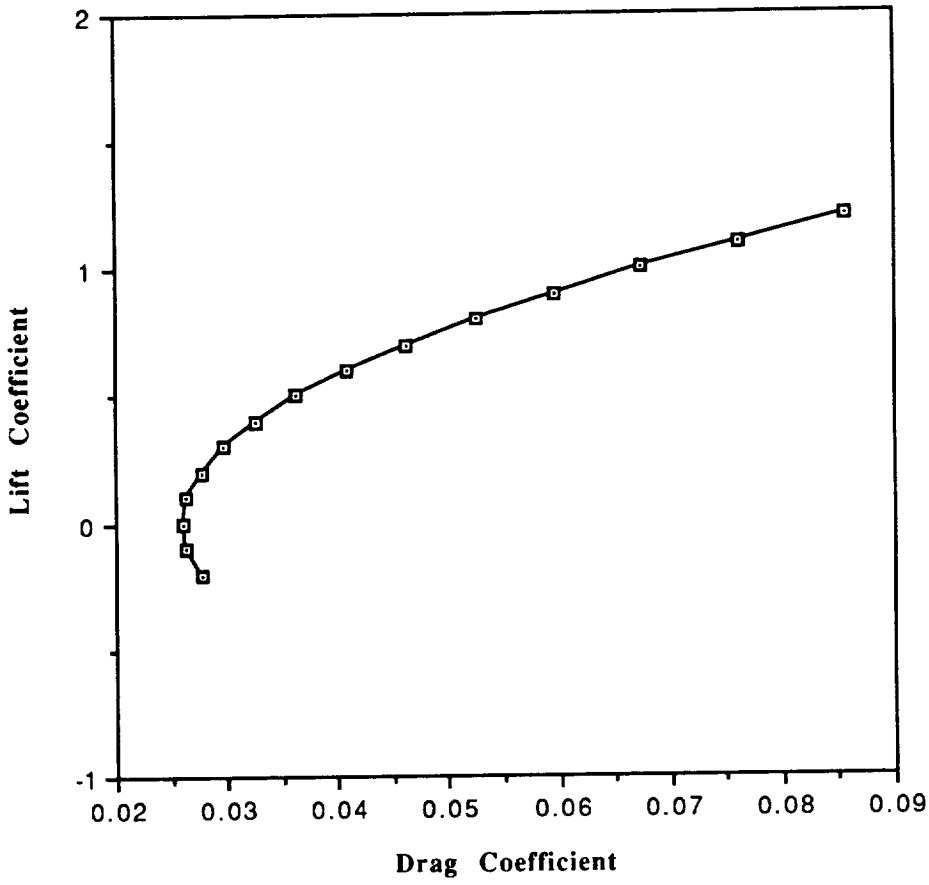

# Figure D.11

## The Arrow 227 Lift to Drag

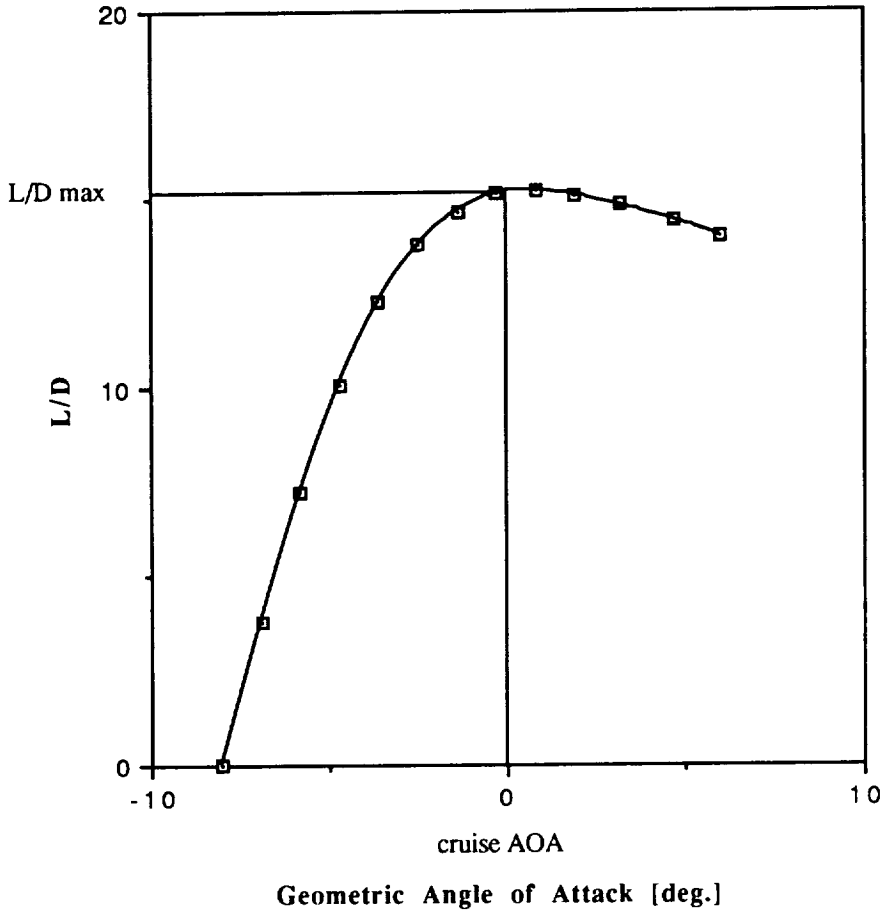

With the configuration of the Arrow 227 set, it was possible to estimate the lift curve for the entire aircraft. The result of this estimation was plotted in Figure D.12. The linear portion of the curve was found in the following manner. First LinAir was used to find the lift curve slope for the wing and tail combination, the result of which was 5.2 $rad^{-1}$. Then, due to interference from the fuselage, this slope was corrected using a correction factor $K_f$ where,

$$K_f = 1 + .025(w/S) - .25(w/S)^2 = .96 \text{ and,}$$

$$C_{L\alpha a/c} = K_f C_{Lawt}$$

The term w in the above equation refers to the width of the fuselage[6]. In this manner, the lift curve slope of the Arrow 227 was found to be 5.0. The nonlinear portion of the graph was estimated using the same method described in the wing design. Joining the two portions, the lift curve for the Arrow 227 was found. Although the method in arriving at this curve was fairly crude, the result does provide a good qualitative look at the aircraft's performance. A curve more suitable for quantitative analysis would best be found through experimental analysis.

## Figure D.12

## The Arrow 227 Lift Curve

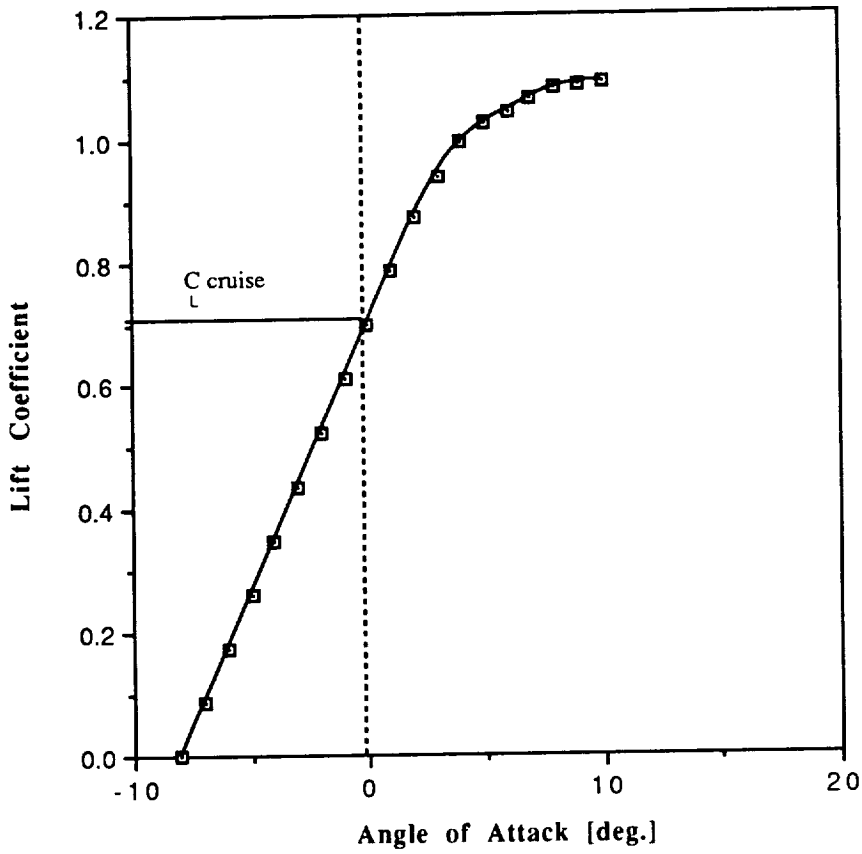

## References:

1. Anderson, John D., Jr., Introduction to Flight, McGraw-Hill Book Company, New York, 1989.

2. Eppler, Richard, Airfoil Design and Data, Springer-Verlag, New York, 1990.

3. Simons, Martin, Model Aircraft Aerodynamics, University of Adelaide Department of Education, North Terrace, Adelaide, South Australia, 1978.

4. Miley, S. J., A Catalogue of Low Reynolds Number Airfoil Data For Wind Turbine Applications, Department of Aerospace Engineering, Texas A&M, TX, 1982.

5. Nelson, R.C., "Notes from AE 348: Flight Mechanics", Department of Aerospace and Mechanical Engineering, University of Notre Dame, IN, 1991.

6. Roskam, Jan, Airplane Design: Part VI, Roskam Aviation and Engineering Corporation, Kansas, 1985.

# E. PROPULSION SYSTEM DESIGN DETAIL

The propulsion system of the Arrow 227 had to satisfy certain criteria set out in the DR & O. These included:

1) Cruise velocity of 27 ft/s
2) Takeoff distance under 60 feet in order to takeoff in AEROWORLD airports
3) Minimum range of 9500 feet (accounting for loiter time and rerouting to nearest airport)
4) Keep system weight to a minimum

## E.1 System Selection and Performance Predictions

The first step in the propulsion system design was to choose an engine. After looking at previous years' designs and noting the complete data base on Astro Cobalt engines, the engine choice was limited to this type of engine. A comparison of maximum power available of the engine, system weight, and takeoff distance was made between the Astro 25, Astro 15 and Astro 05 in order to make the selection. The comparison was made with the Astro 25 using 14 batteries and the Astro 15 and Astro 05 using 12 batteries. The takeoff distance and current draw can be found using the Takeoff Program developed by Dr. Stephen Batill on the Macintosh. The propeller data, which is comparable to that of the Top Flight 10-6, was kept constant throughout the three trials performed.

**Table E.1**
**Engine Statistics**

| Engine | Power Available (W) | System Weight (oz) | Takeoff Distance (ft) | Max Current Draw (amps) |
|---|---|---|---|---|
| Astro 25 | 300 | 38 | 37.7 | 39.14 |
| Astro 15 | 200 | 28 | 52.7 | 26.67 |
| Astro 05 | 125 | 16 | 81.4 | 20.21 |

The Astro 05 was quickly eliminated as a valid engine choice due to its inability to provide enough power to takeoff within 60 feet. The Astro 25 provides the most power and allows for a satisfactory takeoff distance but the system weight and current draw are significantly larger than the Astro 15, which also provides enough power for the aircraft to takeoff under 60 feet. The Astro 15 was selected as the engine for the Arrow 227.

The selection of the batteries was based on the maximum current draw of the engine. Because the maximum current draw is 26.67 amps and the cruise current draw is 4.38 amps, the batteries need only be 400 mah batteries in order to allow for minimum range at cruise current draw and takeoff at maximum current draw. By providing a higher capacity for the system, less battery changes need to occur, therefore, Panasonic 900 mah batteries with nominal voltages of 1.2 volts are selected for the system and are combined in two packs of six batteries each. Motor design restrictions allowed a maximum of 12 batteries for the system. The maximum number of 12 batteries was chosen because providing more voltage helps decrease current draw in the system. Though using 12 of the higher capacity batteries weighs more than using 12 of a smaller capacity battery, the fewer required batteries changes of the former design outweighs the weight drawbacks.

## E.2 Propeller Selection

The propeller for the system was chosen by comparing the performance of several propellers of varying diameter and pitch. Data on the propellers was obtained through a program developed by Mr. Barry Young for an Apple IIe computer. Propeller types were selected and data based on a simple blade element analysis and low Reynolds Number adjustments for a NACA 44XX airfoil was generated. The propellers compared were the Master Airscrew 9-6, Top Flight 10-4, Tornado 10-6, Zinger 10-6, Zinger 12-4 and Top Flight 12-6. The efficiency and RPM at cruise and the takeoff distance of each propeller are the driving factors in the selection of a propeller for the propulsion system. It is desirable to have a propeller operating close to maximum efficiency at cruise. By plotting the efficiency versus the advance ratio (Figure E.1), an overall comparison is first made of how each propeller performs at cruise.

# Figure E.1

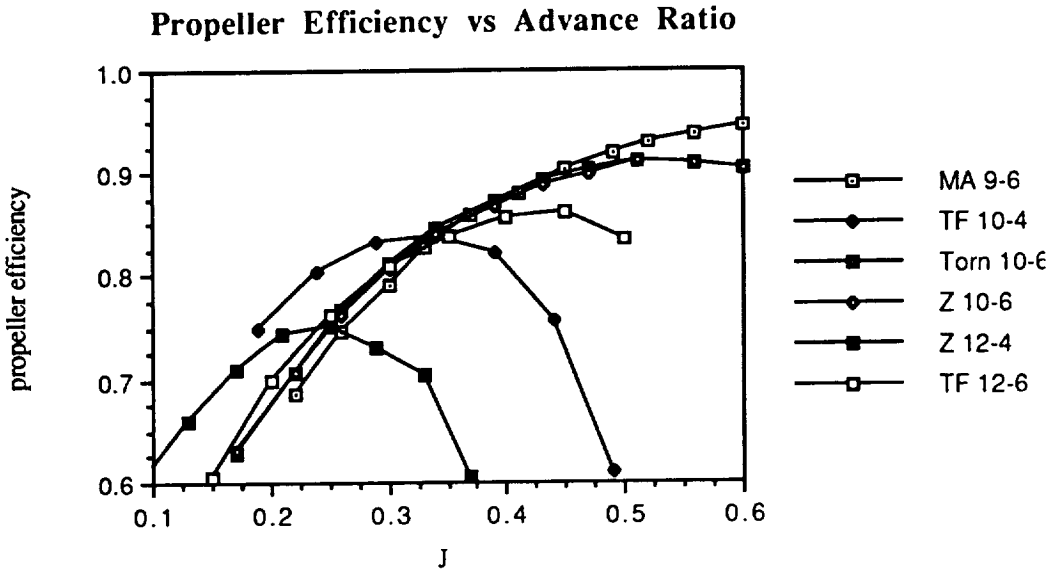
Propeller Efficiency vs Advance Ratio
propeller efficiency
1.0
0.9
0.8
0.7
0.6
0.1
0.2
0.3
0.4
0.5
0.6
J
MA 9-6
TF 10-4
Torn 10-6
Z 10-6
Z 12-4
TF 12-6

Then the thrust required at cruise was calculated and a plot of thrust versus RPM (Figure E.2) was analyzed to find which propeller performed most efficiently at a relatively low RPM in order to decrease current draw and minimize power required at cruise.

**Figure E.2**

**Thrust vs RPM**

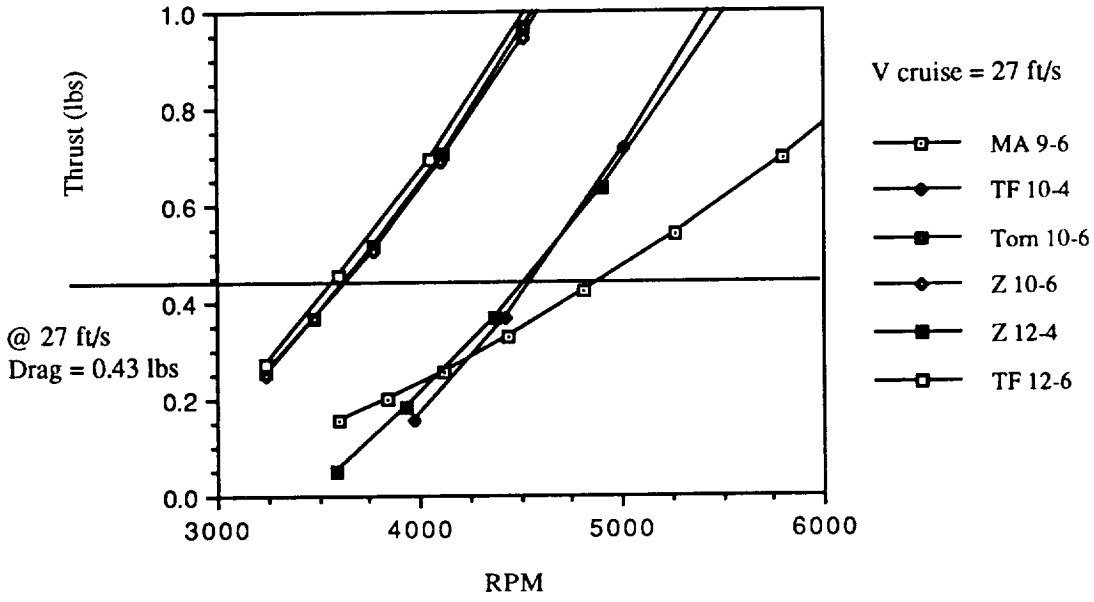

Table E.2 summarizes the data found in the graphs and shows how the final propeller selection was made.

**Table E.2**
**Propeller Statistics**

| Propeller | $\eta$ @ cruise | RPM @ cruise | T.O. Dist. (ft) |
|---|---|---|---|
| Master Airscrew 9-6 | .91 | 3350 | 85 |
| Top Flight 10-4 | .78 | 4300 | 74 |
| Tornado 10-6 | .90 | 3400 | 52 |
| Zinger 10-6 | .90 | 3400 | 52 |
| Zinger 12-4 | .72 | 4300 | 37 |
| Top Flight 12-6 | .86 | 4750 | 34 |

From the above table it can be seen that the Master Airscrew 9-6 and the Top Flight 10-4 did not satisfy the takeoff distance required of 60 feet as stated previously in the criteria for the propulsion system. After eliminating these two propellers, the Tornado 10-6 and Zinger 10-6 had the lowest RPM and, therefore, the lowest current draw on the engine. Although the Zinger 12-4 and the Top Flight 12-6 had exceptional takeoff distances, the amount of thrust they generated at cruise was not needed for the Arrow 227 and they performed at lower efficiencies than the other remaining propellers. The final decision for the propeller selection was between the Tornado 10-6 and the Zinger 10-6 which have equivalent performance. The Tornado propeller is made out of plastic and is several ounces heavier than the wooden Zinger 10-6. Because weight minimization is an important aspect of the design, the Zinger 10-6 was chosen as the propulsion system's propeller.

## E.3 Engine Control

The propulsion system includes the engine, two battery packs, a speed controller, a receiver and receiver battery. The speed controller is the device used to respond to the voltage setting chosen for the aircraft at takeoff and during flight. The voltage setting at takeoff should be the maximum voltage available, 14.4 volts, for the engine which was determined by the type and number of batteries chosen for the Arrow 227. To determine the voltage setting, 8.37 volts, used at cruise, the TK Solver program ELECTRIC PROP was used given flight conditions at 27 ft/s and the Arrow 227 aerodynamics.

The following table is a list of the propulsion system components and performance of the Arrow 227.

**Table E.3**

| Arrow 227 Propulsion System | |
|---|---|
| Engine Type | Astro 15 |
| Propeller | Zinger 10-6 |
| Battery | 12 x 900 mah (Panasonic) |
| System Wt. | 28.47 oz |
| Max Voltage | 14.4 volts |
| Takeoff Dist. | 52 feet |
| Pavail max | 70.00 Watts |
| Preq @ cruise | 14.23 Watts |
| Thrust @ T.O. | 2.21 lbs |
| Thrust @ cruise | 0.37 lbs |
| Current Draw @ T.O. | 6.81 amps |
| Current Draw @ cruise | 4.38 amps |

# F. PRELIMINARY WEIGHT ESTIMATION DETAIL

## F.1 Component Weights

Maximizing the possible payload weight was one of the driving factors behind the design of the Arrow 227. Since the constraints in the request for proposals limited the amount of lift that could be generated, the empty aircraft weight had to be minimized in order to maximize the possible payload weight. Thus, weight entered into almost every decision regarding the design of the Arrow 227. The DR&O established an empty weight of 4 lbs, a payload weight of 2 lbs, and a total weight of 6 lbs.

Table F.1 lists the component weights. The populsion system and avionics weights were determined from data povided by the subcontractor and/or determined by weighing the component if available. The structural weights were determined by the structures department and will be discussed in Section I. The sum of all the component weights including the payload results in a total weight of 5.73 lb. This figure is 4.5% less than the target weight of the DR&O. Table F.1 also lists the súbsystem weights and weight fractions. Figure F.1 depicts the subsystem weight breakdown. Notice that the payload weight comprises 34.9% of the total weight while the structural weight is less than 30% of the total weight. This high payload fraction will make the Arrow 227 a more profitable aircraft.

## F.2 CG Location and Travel

The location of the center of gravity was critical to the pitch stability of the aircraft. The large weight of the payload required that the payload center of gravity be positioned close to the empty aircraft center of gravity. Otherwise the center of gravity would shift considerably when the plane was loaded and unloaded. This would cause the plane to have poor handling qualities or, even worse, be statically unstable in the loaded or unloaded flight mode.

# Table F.1
# Componet and Subsystem Weight Breakdown

| Component | Weight(oz) | X-location(in) | Y-location(in) |
|---|---|---|---|
| Engine | 10.24 | 2.00 | 0.00 |
| Engine mount | 1.16 | 2.00 | 0.00 |
| Engine battery 1 | 7.38 | 29.50 | 2.13 |
| Engine battery 2 | 7.38 | 29.50 | 2.13 |
| Speed controller | 1.77 | 26.30 | 2.31 |
| Propeller | 0.54 | -0.50 | 0.00 |
| Servo-elevator | 0.60 | 32.70 | 2.19 |
| Servo-rudder | 0.60 | 32.70 | 2.19 |
| receiver | 0.95 | 30.80 | 2.03 |
| receiver battery | 2.00 | 28.30 | 1.91 |
| Fuselage | 7.25 | 27.50 | 0.00 |
| Wing CG | 12.00 | 24.50 | 3.50 |
| Empennage | 2.85 | 54.75 | 3.70 |
| Landing gear | 4.73 | 24.00 | -4.46 |
| Payload | 32.00 | 25.43 | -0.25 |
| **Total(lbs)** | 5.72 | | |

| Subsystem | Weight(oz) | Weight-% total |
|---|---|---|
| avionics | 5.92 | 6.5 |
| stucture | 26.83 | 29.3 |
| propulsion | 11.94 | 13.1 |
| fuel | 14.76 | 16.1 |
| payload | 32.00 | 35.0 |

**Figure F.1**
**Subsystem Weight Breakdown**

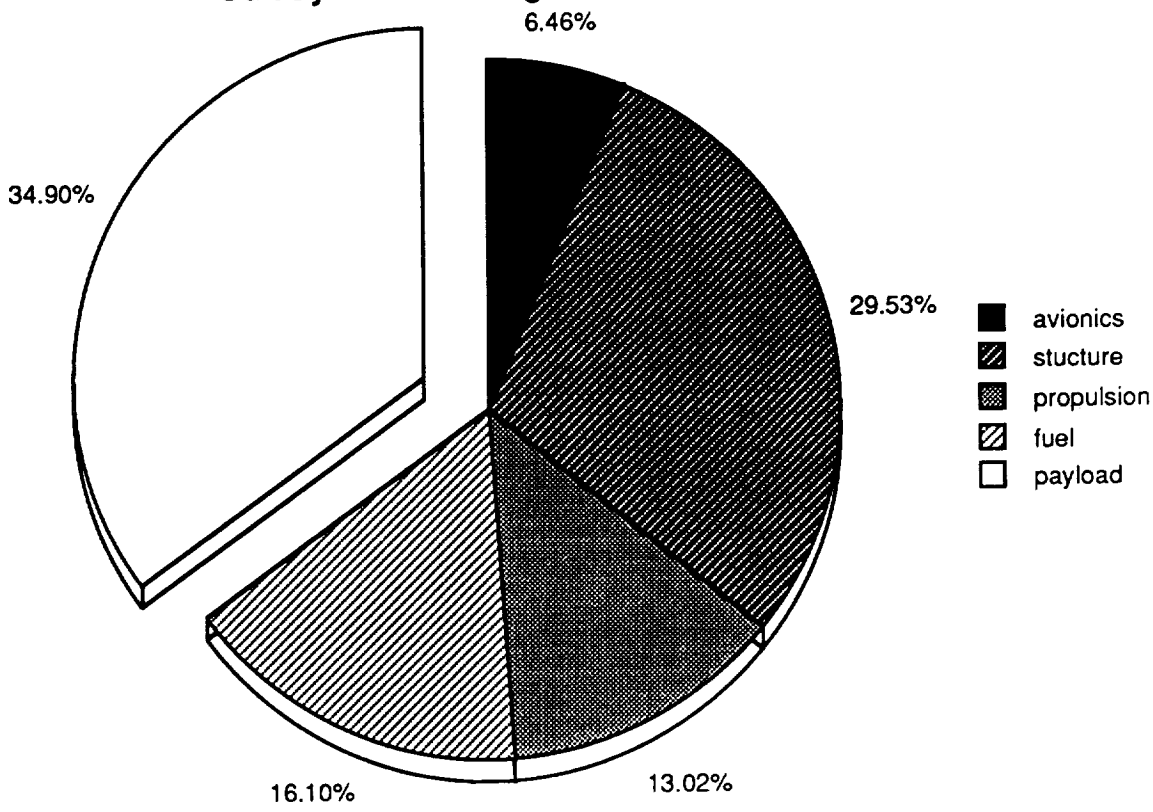


For a small center of gravity shift, the CG of the empty plane must be located near the middle of the fuselage where the center of gravity of the payload would occur. Since the engine was located at the nose of the aircraft, it was a formidable task to move the empty plane CG near the middle of the fuselage. The CG was positioned by properly locating the batteries and avionics in the fuselage. It was desired to place the batteries under the removable wing for easy access. Thus, it was decided to place the engine batteries and avionics in front of the wing trailing edge. For good handling qualities, the center of gravity of the entire plane must be placed near 30% of MAC. Thus, the wing had to be moved towards the center of the fuselage which moved the engine batteries aft and helped move the center of gravity back.

Figure F.2 shows the internal configuration of the aircraft and Table F.1 lists the component locations. A raised platform was placed below the wing to support the engine batteries, servos,

# Figure F.2
## INTERNAL CONFIGURATION

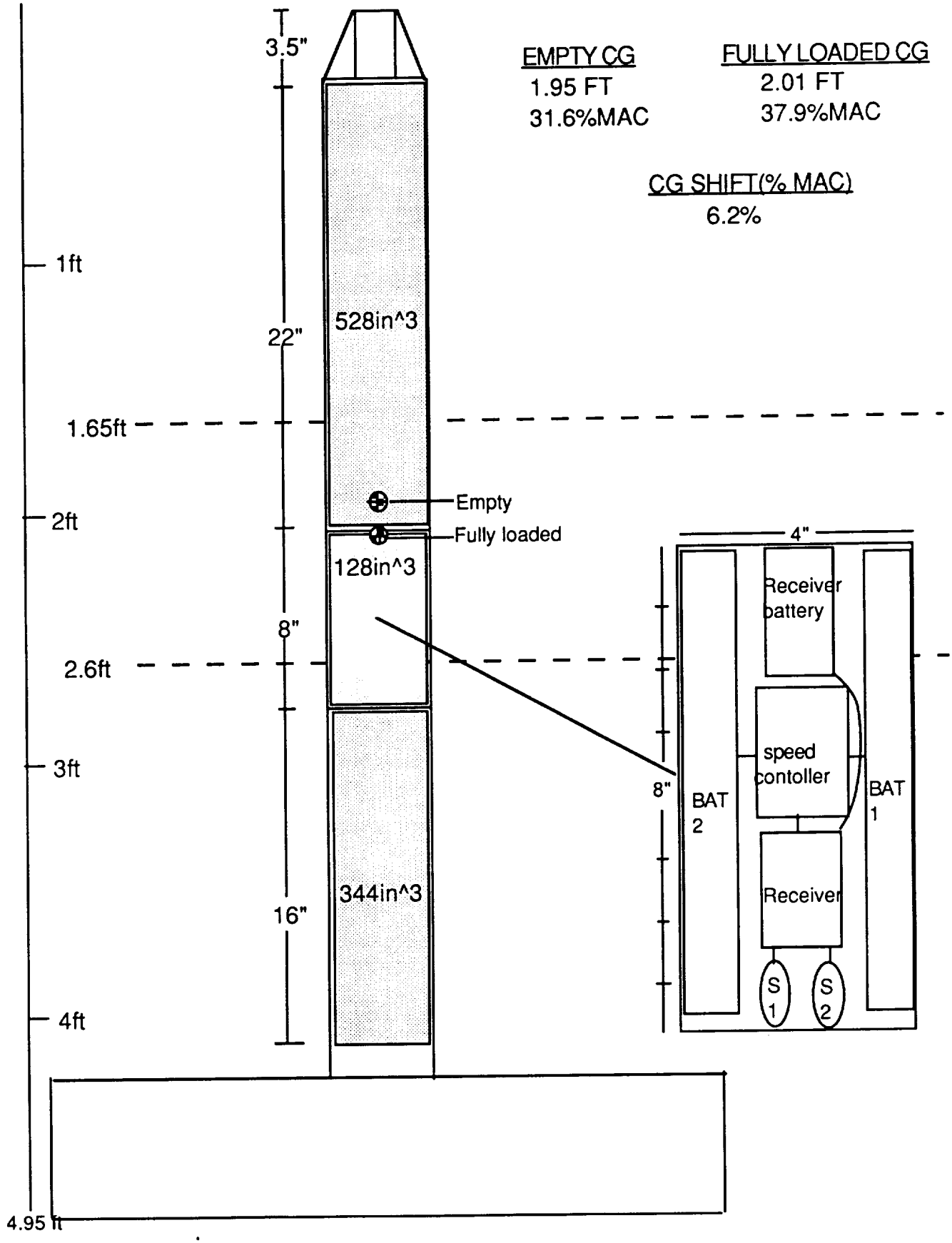

receiver, receiver battery, and speed controller. Cooling vents were cut into the monokote of the fuselage above the platform to expose the batteries. The platform position allowed for a 4"x4" space below the platform which will be used for 128 $in^3$ of cargo. A majority of the cargo will be placed in front of the platform and the remaining cargo behind the platform. The front cargo and batteries could then be accessed by removing the wing. The front and rear cargo could be accessed by a rear cargo door.

The final configuration was arranged to obtain a fully loaded(design) CG location of 2.01 ft or 37.9% MAC. This location was determined by the stability and control department for optimum aerodynamic efficiency for a wing leading edge location of 1.65 ft. The configuration resulted in an empty CG location of 1.95ft or 31.6% MAC and a CG travel of 6.1% of the mean aerodynamic chord. The CG travel could be reduced by moving the CG of the empty aircraft further aft. However, the necessary configuration would move the batteries behind the wing which would make them inaccessible. In addition, moving the engine batteries all the way back would require long wires which would increase the resistance and heat dissipation of the wires.

The forward limit of the C.G. is the empty aircraft C.G. location and the aft limit is the fully loaded aircraft C.G location. Figure F.3 shows the Weight/Balance diagram for the Arrow 227.

Table F.1 also lists the vertical location of the center of gravity from the center of the fuselage. The vertical location of the center of gravity was determined to be 1.3 inches for the empty aircraft and .74 inches for the fully loaded aircraft.

## Figure F.3
## Weight/Balance Diagram

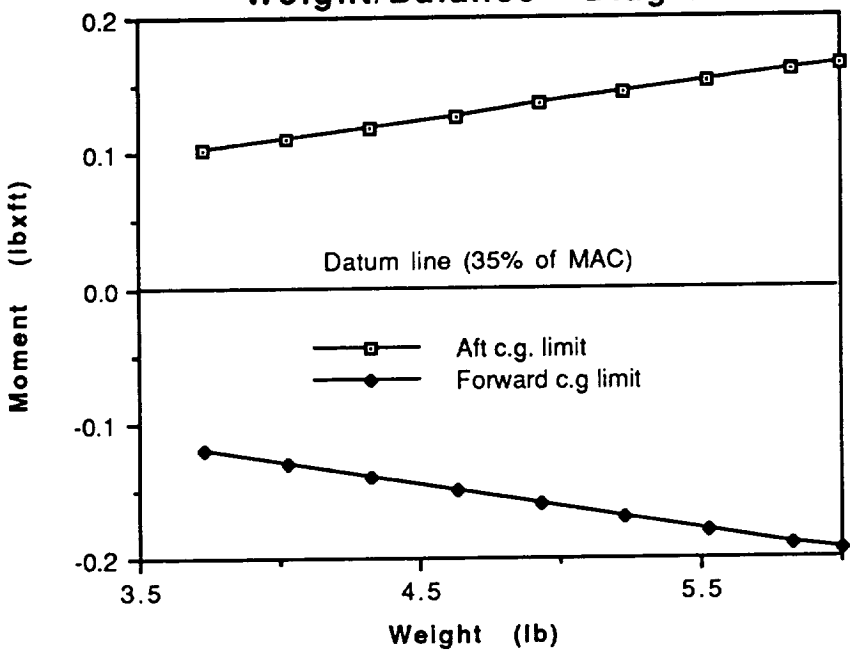

# G. STABILITY AND CONTROL

## G.1 Surface Location and Sizing

Again the driving factors behind the design of the stability and control systems was light weight, low cost, and aerodynamic efficiency. Since the Arrow 227 is a conventional configuration aircraft, stability was attained by employing dihedral, a vertical tail, and a horizontal tail. Flat plates were used in the tail surface design to reduce the cost and the weight. Due to their simple design, flat plates would require fewer man hours to produce and less material.

### G.1.1 Wing and Horizontal Tail

It was necessary to determine the proper sizing and configuration of the lifting surfaces so that the Arrow 227 maintained adequate longitudinal stability and aerodynamic efficiency in both the unloaded and loaded flight modes. As shown in Section F, the large payload weight will cause a CG shift when the plane is loaded and unloaded. Thus, a large static margin is required for the plane to maintain its static stability. However, a large static margin will cause the plane to be nose heavy which would increase trim drag and reduce the aerodynamic efficiency of the Arrow 227.

The internal configuration described in Section F.2 indicates that the maximum center of gravity shift will be 6.1% of the mean aerodynamic chord. Thus, a static margin that is much greater than the usual 5% for transport aircraft is necessary. A static margin that remains between 10% to 20% would provide adequate longitudinal stability in both the loaded and unloaded flight mode. In order to maximize the aerodynamic efficiency of the aircraft, the tail angle of attack at cruise should be approximately zero and no elevator deflection should be necessary to trim the aircraft. This will prevent the tail from developing a down load and trim drag. A tail down load and trim drag would decrease the lift to drag ratio and reduce the aerodynamic efficiency.

Reference 1 provided all the necessary equations to conduct the analysis. The static margin can be determined from the following equations.

$$SM=x_{np}/c - x_{cg}/c \tag{G.1}$$

where

$$x_{np}/c=x_{ac}/c-C_{m\alpha f}/C_{L\alpha w}+\eta V_H C_{L\alpha t}/C_{L\alpha w}(1-d\varepsilon/d\alpha) \tag{G.2}$$

The fuselage contribution to the pitching moment coefficient was neglected in the analysis since the contributions of the large lifting surfaces would dominate at low velocities. In addition, the tail efficiency was assumed to be .9.

The tail angle of attack at cruise could be determined from the following equations.

$$C_{m\alpha}=C_{L\alpha w}(x_{cg}/c-x_{ac}/c)-\eta V_H C_{L\alpha t}(1-d\varepsilon/d\alpha) \tag{G.3}$$

in steady flight

$$0 =C_{mo}+C_{m\alpha}\alpha_w+C_{m\delta e}\delta_e \tag{G.4}$$

and

$$C_{mo}=C_{macw}+C_{Low}(x_{cg}/c-x_{ac}/c)+\eta V_H C_{L\alpha t}(\varepsilon_o+i_w-i_t) \tag{G.5}$$

The tail incidence angle angle can be solved for in Equation G.5 if the characteristics of the wing and tail and the angle of attack of the wing at cruise, $\alpha_w$, are known. The effective angle of attack of the tail can then be determined from

$$\alpha_t=\alpha_w-i_w-\varepsilon+i_t \tag{G.6}$$

**Figure G.1**
**Tail angle of Attack at Cruise VS CG location**

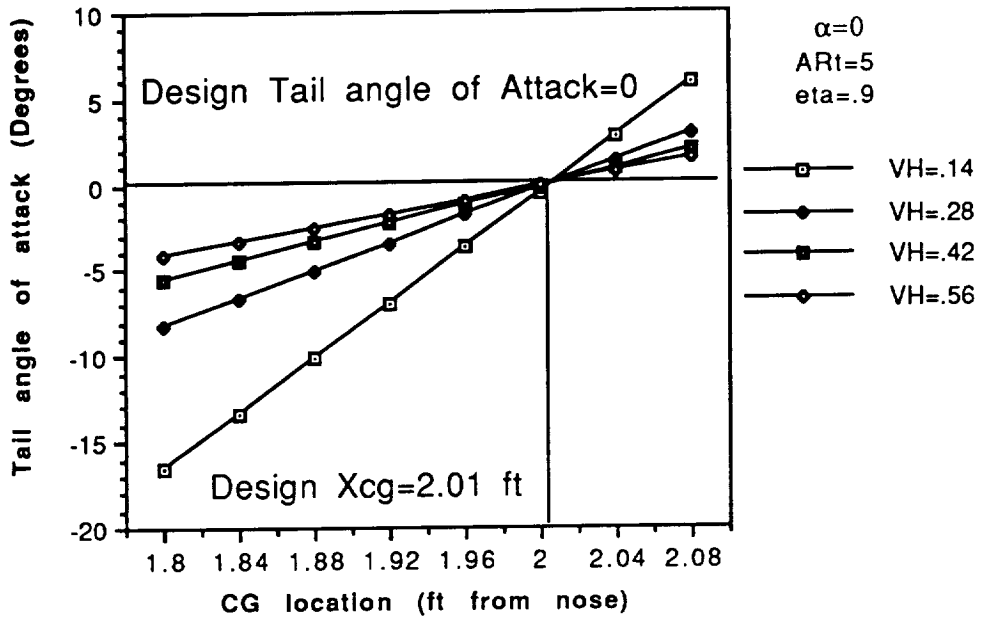


By employing the design parameters determined by the aerodynamics group and choosing a maximum tail aspect ratio of 5 as suggested by Reference 3, the tail angle of attack can be plotted soley as a function of the center of gravity location and the horizontal tail volume ratio. Figure G.1 shows this relationship for a wing leading edge location of 1.65 ft. Notice that a CG location of 2.01 ft from the nose of the aircraft results an a tail angle of attack of $0^{o}$ regardless of the horizontal tail volume ratio. At this location, the aerodynamic center of the wing is far enough ahead of the CG to create a pitch up moment that balances the natural pitch down moment of the cambered wing. Hence no tail load is required to trim the aircraft and the tail angle of attack is zero regardless of the horizontal tail volume ratio. Since no tail load is required, there is no trim drag at the cruise conditions and the plane is more aerodynamically efficient. Thus a CG location of 2.01 ft was set for the design or fully loaded flight mode. This results in a tail incident angle of 2.5 degrees for a wing incident angle of 0 degrees. The incident angle compensates for the 2.5 degrees of downwash caused by the wing and results in a 0 degree tail angle of attack at cruise.

**Figure G.2**
**Static Margin vs CG Location**

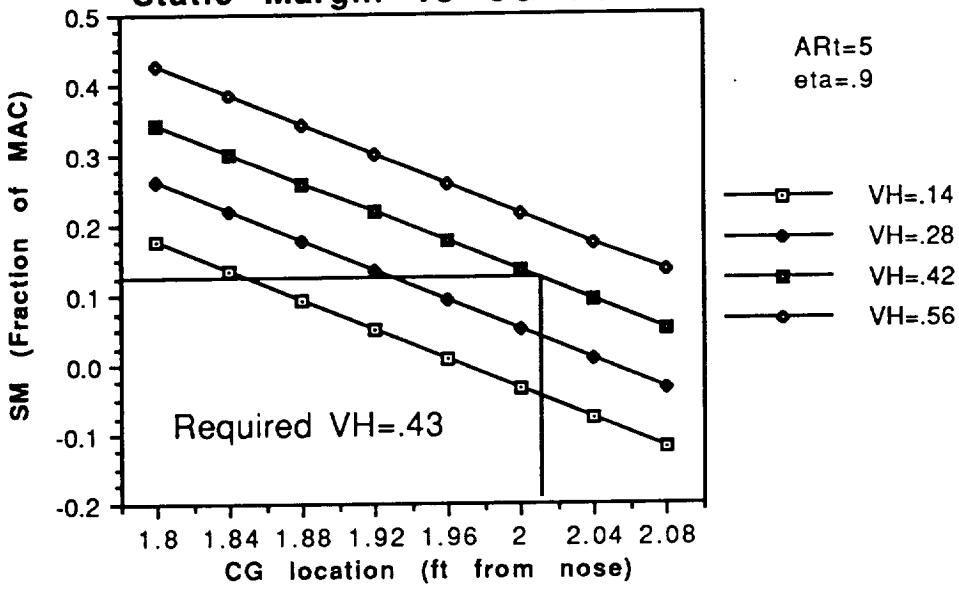


Like the tail angle of attack, the static margin can be plotted as a function of the center of gravity and the horizontal tail volume ratio. Figure G.2 shows this relationship. From this plot, the $V_H$ required to achieve a desired static margin can be determined if the CG location has already been established. Figure G.2 shows that at the design CG location of 2.01 ft, a $V_H$ of .43 is required to achieve a static margin of 12.5% MAC. This horizontal tail volume ratio and an aspect ratio of 5 can be obtain with a tail span of 2.8 ft, a tail chord of .56 ft, and an overall plane length of 2.85 ft.

These values were checked against the simple formulas for tail sizing presented in Reference 2. The formulas suggest a $l_t$ of 2.38 ft and a tail surface area of 2 $ft^2$. The above analysis resulted in a $l_t$ of 2.42 ft and a tail surface area of 1.57 $ft^2$. The tail surface area is less in the above analysis since an emphasis is placed on aerodynamic efficiency.

### G.1.2 Vertical Tail

Adequate directional stability was obtained by employing a properly sized vertical tail. To achieve static directional stability, the derivative of the yawing moment coefficient, $C_n$ with respect to the sideslip angle, $\beta$, must be positive. This will create a restoring moment when the plane is flying at a sideslip angle. The stability coefficient, $C_{n\beta}$, is comprised of a wing-body contribution and a vertical tail contribution. The contributions can be calculated from

$$C_{n\beta wb}=-k_n k_{Rl}(S_{sf}/S_w)(l_f/b) \quad (G.7)$$

$$C_{n\beta v}=V_v \eta_v C_{L\alpha v}(1+d\sigma/d\beta) \quad (G.8)$$

Using Reference 1 to determine the constants $k_n$ and $k_{Rl}$,the wing-body contribution was calculated as -.00019 $rad^{-1}$ which proved to be insignificant compared to the vertical tail contribution.

Since the wing-body was negligible, the magnitude of $C_{n\beta}$ was dependent on the size and location of the vertical tail. It was also determined that the CG shift affected $C_{n\beta}$ by less than 2% and thus the CG shift was ignored in this analysis. Reference 3 suggets that light aircraft stability characteristics are a good initial design point for a low Reynolds number RPV. Appendix B of Reference 1 indicates that the $C_{n\beta}$ of a light general aviation aircraft would be around .071$rad^{-1}$. Thus, a vertical tail with a span of 1.2 ft and a chord of .6 ft was determined. These parameters resulted in a tail surface area of .72 $ft^2$ and a $C_{n\beta}$ of .065 $rad^{-1}$. The simple equation in Reference 2 for sizing the vertical tail suggests a tail area of .82 $ft^2$ which is consistent with the above analysis.

## G.2 Control Mechanisms

In order to control cost and lower the weight, it was decided that only a rudder and an elevator would be used to control the airplane. Lateral control was then achieved by coupling the yaw and roll axis with dihedral. A reduction in the lift coefficient would occur due to additional dihedral. However, estimates indicate that adding 8° of dihedral would result in only a 1.6% reduction in lift. This reduction is tolerable compared to the added production cost and weight of employing ailerons.

### G.2.1 Longitudinal Control

The elevator size was determined by the off design condition in which the aircraft was unloaded and, as a result, nose heavy. With the horizontal tail and wing characteristics determined in Section G.1.1, $C_{mo}$ and $C_{m\alpha}$ can be determined for a CG location. Using Equation G.4, it was determined that in order to be able to trim the aircraft at its maximum angle of attack of 8° when it is unloaded, an elevator control power, $C_{m\delta e}$, of -.65 $rad^{-1}$ is required assuming a maximum elevator deflection of 15°. The flap effectiveness, $\tau$, was determined to be .4 from the following equation.

$$\tau=-C_{m\delta e}/(\eta V_H C_{L\alpha t}) \qquad (G.9)$$

Figure 2.20 of Reference 1 indicates that an elevator area of 20% of the horizontal tail or .31 $ft^2$ is required to trim the aircraft for the off design condition.

### G.2.2 Lateral Control

The maximum sideslip angle at which the aircraft could be trimmed was chosen as 15°. Although, if employed, such a large sideslip angle will create considerable drag, it was necessary in order to

achieve a 60 ft minimum turn radius. The rudder size needed to trim the aircraft at this sideslip angle was determined from the following equations.

at trim $$C_{n\delta r}=-C_{n\beta}\beta/\delta_r \quad (G.10)$$

$$\tau=-C_{n\delta r}/(\eta V_v C_{L\alpha v}) \quad (G.11)$$

Assuming a maximum rudder deflection of 25°, the analysis resulted in a rudder control power, $C_{n\delta r}$, of -.04 $rad^{-1}$ and a flap effectiveness, $\tau$, of .685. Figure 2.20 of Reference 1 shows that a rudder area of 50% of the vertical tail area, or, .36 $ft^2$ is required to achieve the desired sideslip angle.

Next, the amount of dihedral necessary to perform a 60 ft radius turn as required by the DR&O was determined. In order to provide a margin of safety, the aircraft was designed to perform a minimum 50 ft radius turn at its cruise velocity. Since the limit load factor of the Arrow 227 is 1.5, the maximum bank angle is 48°. At this bank angle and a cruise velocity of 27 ft/s, a roll rate of 22 deg/sec will be required to make a 50 ft radius turn. This roll rate coincides with the roll rate suggested by the following equation from Reference 1.

$$\text{roll rate}=.07(2)u_o/b \quad (G.12)$$

The amount of dihedral necessary to make a 50 ft radius turn was determined from Figure G.3. Figure G.3 shows the roll rate as a function of velocity and dihedral for a sideslip angle of 15°. The Figure indicates that 8° of dihedral is necessary for a roll rate of 22 deg/sec at 27 ft/s.

**Figure G.3**
**Roll Rate vs. Flight Velocity**
**sideslip angle = 15 deg**

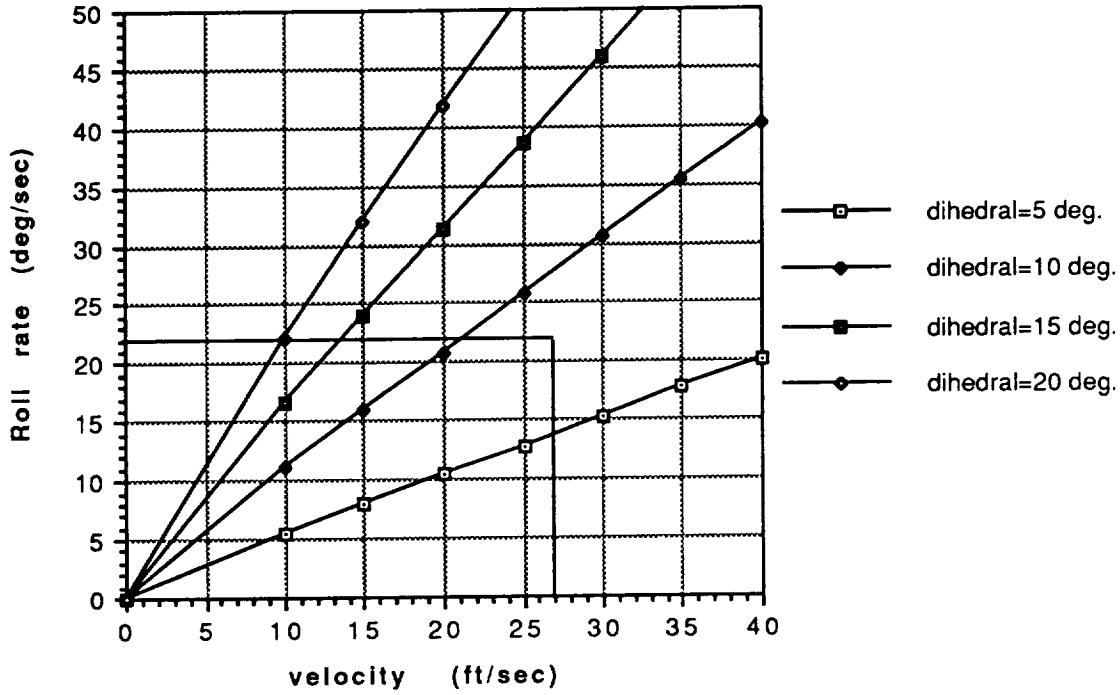


## G.3 Static Stability Analysis

For longitudinal stability, the derivative of the pitch moment coefficient with respect to the angle of attack, $C_{m\alpha}$, must be negative. As previously mentioned, Reference 3 suggests that the stability characteristics of a light general aviation aircraft are good initial design points for low Reynolds number RPV's. Appendix B of Reference 1 indicates that $C_{m\alpha}$ of a general aviation aircraft is approximately -.68 $rad^{-1}$. For the fully loaded Arrow 227, $C_{m\alpha}$ is -.58 $rad^{-1}$ which is within 15% of the initial design point. Figure G.4 shows the pitch moment coefficient curve for the design flight condition. The figure shows that at a cruise angle of attack of $0^o$, the elevator deflection is $0^o$. The tail angle of attack at this cruise condition was also designed to be $0^o$ as shown in section G.1. Thus, when the Arrow 227 is fully loaded, it is flying with optimum aerodynamic at its cruise velocity. Figure G.4 also indicates that a $7^o$ elevator deflection is required to trim the aircraft at its maximum angle of attack of $8^o$.

It was also necessary to insure that the aircraft was statically stable in the off design or unloaded flight mode. Figure G.5 shows the pitch moment curve for this condition. For the unloaded flight mode, $C_{m\alpha}$ is -.9 $rad^{-1}$ and the static margin is 19.5% which indicate increased static stability. However, Figure G.5 shows that an elevator deflection of -4° is necessary to trim the empty aircraft at a cruise angle of attack of 0°. This will result in additional trim drag and a reduction of the aerodynamic efficiency. However, if the aircraft is flying completely empty, aerodynamic efficiency may only be a minor concern. In addition, it was determined that only 2 oz of cargo is required to move the CG to the design point.

Directional stability requires that the derivative of the yaw moment coefficient, with respect to the sideslip angle, $C_{n\beta}$, is positive. In section G.1.2, $C_{n\beta}$ was determined to be .065 $rad^{-1}$ for the Arrow 227 which is within 10% of the stability coefficient for a general aviation aircraft. Thus, the Arrow 227 should have adequate directional stability.

**Figure G.4**
**Design Condition-Fully Loaded**
**Pitch Moment Coefficient vs Angle of Attack**

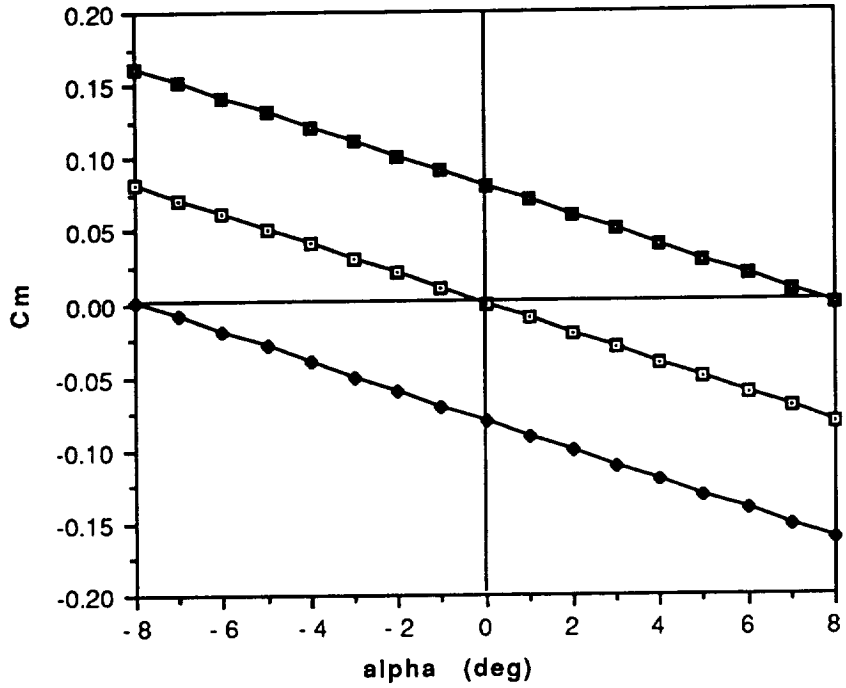


Elevator Control Power=-.65

Elevator Deflection

δ=-7

δ=0

δ=7

Xcg=2.01 ft.

SM=12.5% MAC

Cm alpha=-.58

**Figure G.5**
**Off Design-Unloaded**
**Pitch Moment Coefficient vs Angle of attack**

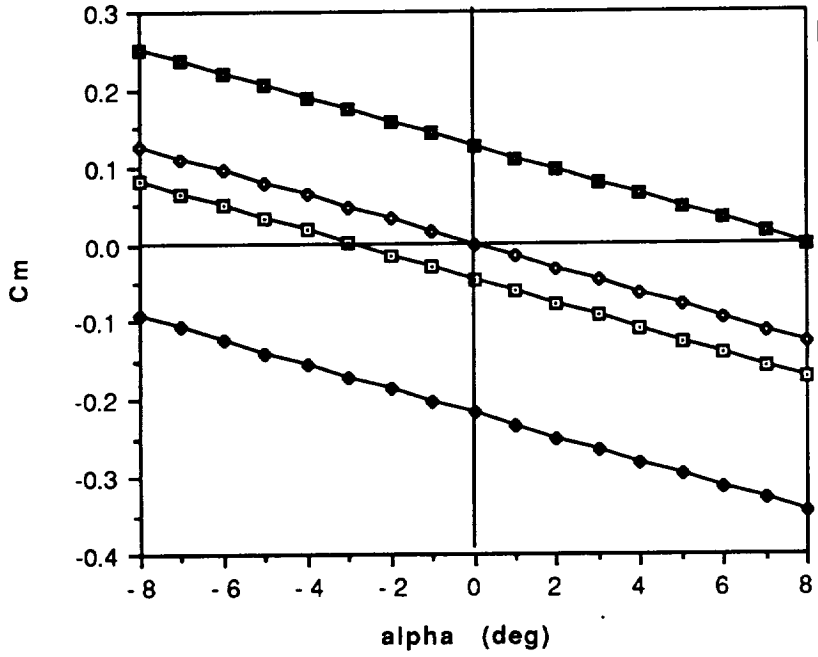


Elevator Control Power=-.65

Elevator Deflection

δ=-15

δ=-4

δ=0

δ=15

Xcg=1.95 ft.

SM=19.5% MAC

Cm alpha=-.9

Roll stability was achieved by employing dihedral. Roll stability requires that the derivative roll moment coefficient with respect to the sideslip angle, $C_{l\beta}$, is negative. $C_{l\beta}$ can be calculated from the following equation.

$$C_{l\beta}=(C_{l\beta}/\Gamma)\Gamma+\Delta C_{l\beta} \qquad (G.12)$$

where $C_{l\beta}/\Gamma$ is determined from Figure 3.9 of Reference 1. For the Arrow 227, $C_{l\beta}$ was determined to be -.12 $rad^{-1}$ which is 62% greater in magnitude than the stability coefficient for a general aviation plane. The large stability coefficient is due to the fact that additional dihedral was required to control the aircraft without ailerons. Hence, the Arrow 227 has more than adequate roll stability. Table G.1 lists the summary longitudinal stablity and control characteristics and Table G.2 lists the summary lateral stability and control characteristics of the Arrow 227.

## Table G.1
## Summary Longitudinal Stability and Control Characteristics

| | Loaded | Unloaded |
|---|---|---|
| Cmo | 0 | -.048 |
| Cma | -.58 $rad^{-1}$ | -.91 $rad^{-1}$ |
| Cmde | -.658 $rad^{-1}$ | -.658 $rad^{-1}$ |
| $\delta_{de}$ max | 15° | 15° |
| $\delta_{de}$ trim | 0° | -4° |
| Static Margin | 12.6% mac | 19.5% mac |
| Horizontal Tail Volume ratio | .42 | .43 |
| Tail Incidence angle | 2.5° | 2.5° |

## Table G.2
## Summary Lateral Stability and Control Characteristics

| | |
|---|---|
| $C_{n\beta v}$ | .065 $rad^{-1}$ |
| $C_{n\delta r}$ | -.039 $rad^{-1}$ |
| $\delta_{r\ max}$ | 25° |
| Vertical Tail Volume ratio | .018 |
| Dihedral | 8° |
| $C_{l\beta}$ | -.12 $rad^{-1}$ |

### References

G.1. Nelson, Robert C. Flight Stability and Automatic Control. McGraw-Hill Book Company, New York 1989.

G.2. Lennon, A.G. R/C Model Airplane Design. Motorbooks International, Osceola 1986.

G.3. Foch, Richard J. Low Reynolds Number Long Endurance Aricraft Design. AIAA, Washington 1992

# H. PERFORMANCE ESTIMATION

## H.1 Takeoff and Landing Estimates

One of the major requirements set on the Arrow 227 was the ability to service cities that have runways that are sixty feet in length. This was determined from a mission and market analysis of AEROWORLD. This requirement, along with an estimation of the aerodynamic drag on the Arrow 227 and the overall maximum weight aided in the decision to employ the Astro 15 engine and the Zinger 10-6 propeller for the Arrow 227. The Astro 15 provides enough power to meet this takeoff requirement with ample margin to adapt should future unforeseen design changes occur.

The takeoff distance was calculated by two different methods in order to validate the calculated values. The first was Dr. Stephen Batill's Takeoff Performance Program. This program takes into account the overall total weight of the Arrow 227, the battery capacity, engine, and propeller used and gives a total takeoff distance of 52 ft. At a takeoff velocity of 27 ft/s the rate of climb was found to be 6.0 ft/s. The second method was equation 6.90 from reference 1. The equation is as follows:

$$\text{Takeoff Distance} = \frac{1.44 \times W^2}{\rho \times g \times S \times Cl_{max} \times \{T - [D + \mu \times (W - L)]_{ave}\}} \qquad \text{(H.1)}$$

The drag and lift parameters were calculated using the Shevell suggestion that the average forces be set equal to the instantaneous value when the velocity reach seventy percent of the takeoff velocity. The weight was assumed to be at its maximum to provide a worst case scenario. The coefficient of friction, 0.15, was determined through experiments performed on the runway's surface. In order to insure enough excess runway would be provided to compensate for any pilot errors that

might occur in takeoff, a maximum value of 0.15 was accepted as the coefficient of rolling friction on the runways. In order to aid in predicting a worst case scenario for the Arrow 227, the assumption of negligible ground effects was also employed, since ground effects benefit an aircraft in takeoff. Applying these criteria resulted in a takeoff distance of 48 ft. The two values obtained for takeoff distance are within 7% error of each other.

Since the same runways will be used for landing the aircraft, the same restrictions must apply to the landing distance required. The landing distance was calculated by using equation 6.100, also from reference 1. The landing equation used was:

$$\text{Landing Distance} = \frac{1.69 \times W^2}{\rho \times g \times S \times Cl_{max} \times [D + \mu \times (W - L)]_{ave}} \qquad \text{(H.2)}$$

Again the drag and lift parameters were calculated using the Shevell suggestion, where instantaneous values of drag and lift are calculated at 70% of the takeoff velocity. The coefficient of rolling friction will also be assumed to be 0.15. Another major assumption is that there will be no thrust control during the landing. The aircraft will be required to rely upon only the coefficient of rolling friction in order to bring it to a complete stop. Using these assumptions a landing distance of 174 feet was calculated. This exceeds are smallest runway length by an excess of 115 feet. In order to reduce this distance it will be necessary to implement a braking system into the Arrow 227 in order to increase the rate of the aircraft's deceleration and therefore reduce the landing distance. One technique to do this would be to apply a braking system to the landing gears tires. Another could be the implementation of spoilers to the wings. Do to time limitations in construction the technical demonstrator will not be implemented any with braking apparatus.

## H.2 Range and Endurance

One of the primary design goals is to have a maximum return on investment. One of the best ways to do that is to reduce daily maintenance costs of the Arrow 227. The objective here was to allow the Arrow 227 to fly as many flights as possible before requiring maintenance, (i.e. a battery change.) The Arrow 227 has been designed for a minimum range of 9720 feet and a minimum endurance of 6 minutes in order to fulfill the requirements for the proposed route. With this criteria the battery will only have to be changed every two flights. If the Arrow 227 flies shorter routes, the batteries can be changed less frequently.

The range and endurance were analyzed over 27 ft/s range in velocity. A maximum range of 22,200 feet occurs at 21 ft/s. A maximum endurance of 13.1 minutes occurs at 39 ft/s. The following graph (Figure H.1) illustrates that the range and endurance are optimum at the cruise velocity of 27 ft/s. Figure H.1 shows the maximum range is attained at a velocity of 21 ft/s and the maximum endurance occurs at approximately 40 ft/s. The velocity at which these two curves intersect is where it is optimal to fly a plane. Because the the range and endurance are considered equally in the design of the Arrow 227, the intersection point corresponds to the velocity at which both properties are considered equally.

## Figure H.1

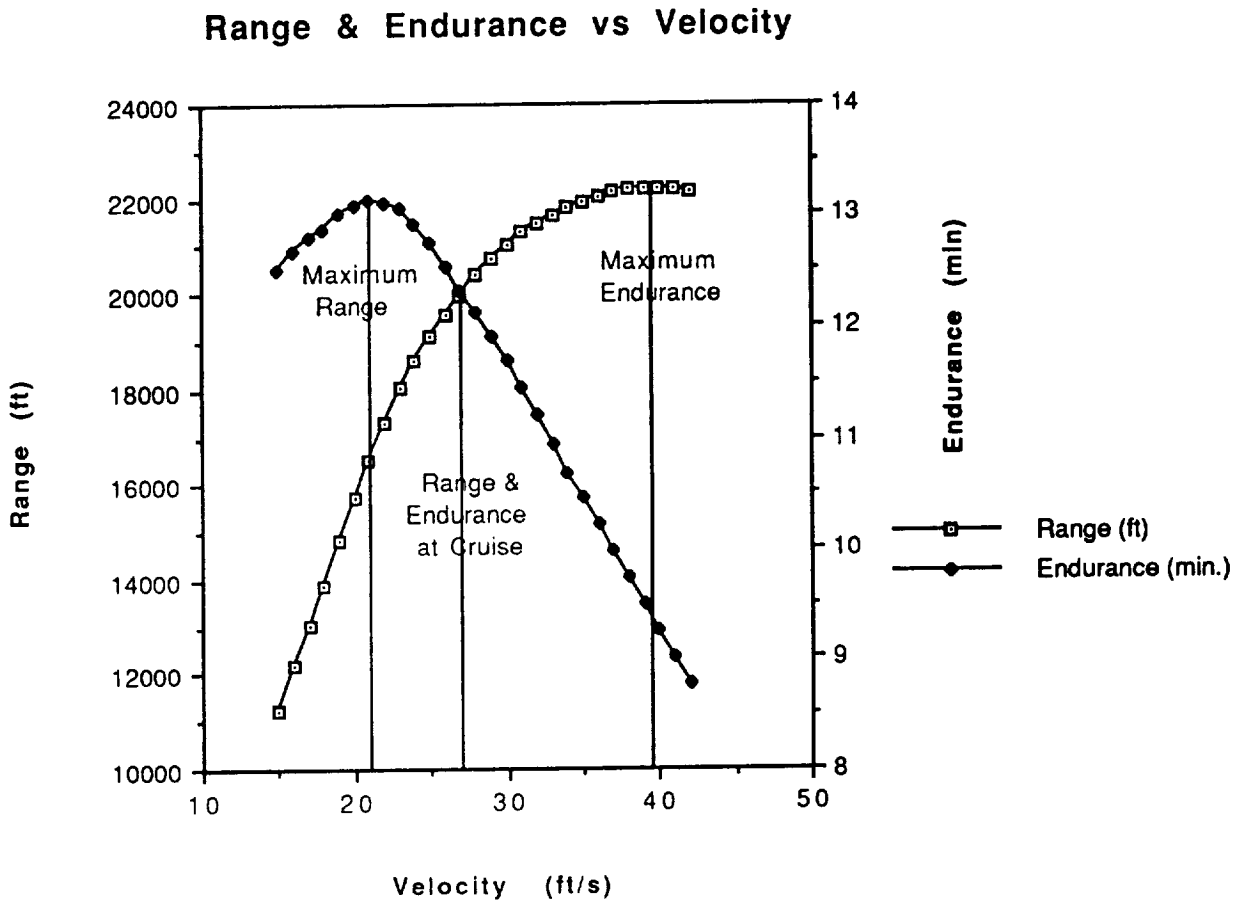


The effects of payload weight on range and endurance, operating with a battery capacity of 0.9 amps, were examined and are displayed in Figure H.2. Examination of the graph reveals that the range decreases by 62 ft/oz of payload.

Figure H.2

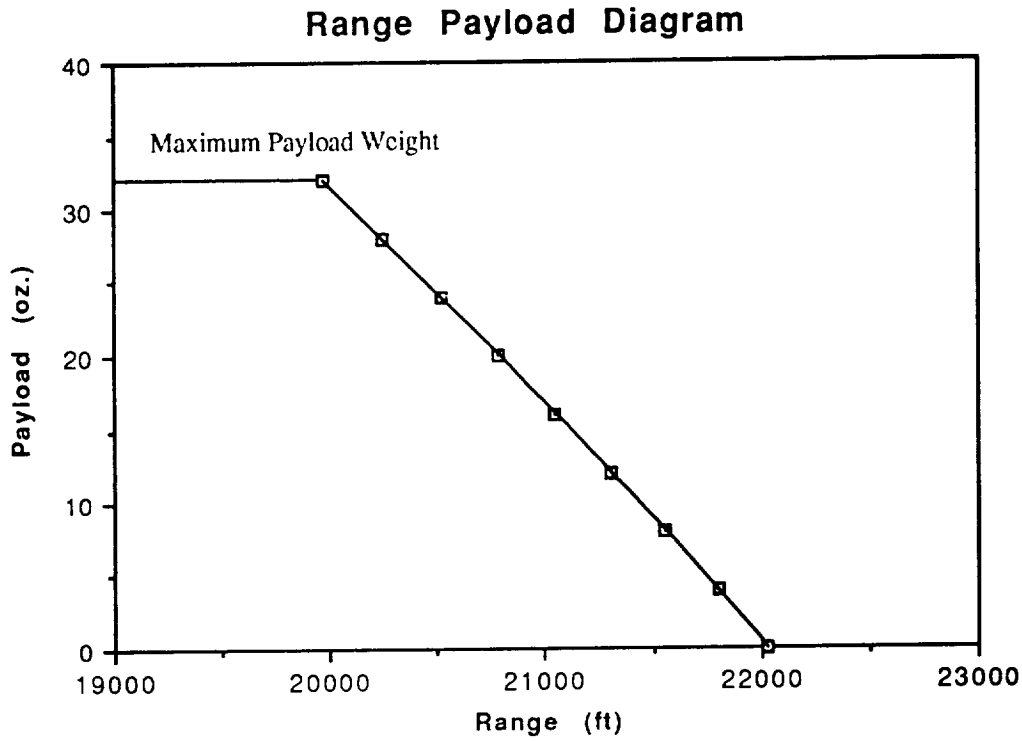
Range Payload Diagram
Maximum Payload Weight
Payload (oz.)
40
30
20
10
0
19000
20000
21000
22000
23000
Range (ft)

## H.3 Power Required and Available Summaries

The Astro 15 provides sufficient power available for takeoff, climb, and maneuverability in flight. The power required and power available at varying voltage settings were analyzed to determine what voltage setting the speed controller should be at for takeoff and cruise. The maximum voltage available is 14.4 volts for the propulsion system and, therefore, this is the voltage setting used for takeoff. The voltage setting that yields equivalent power required and power available at the cruise velocity is where the speed controller should be set at for flight. The voltage setting at cruise for the Arrow 227 is 8 volts. From Figure H.3, the effect of the varying voltage settings on power available can be seen.

Figure H.3

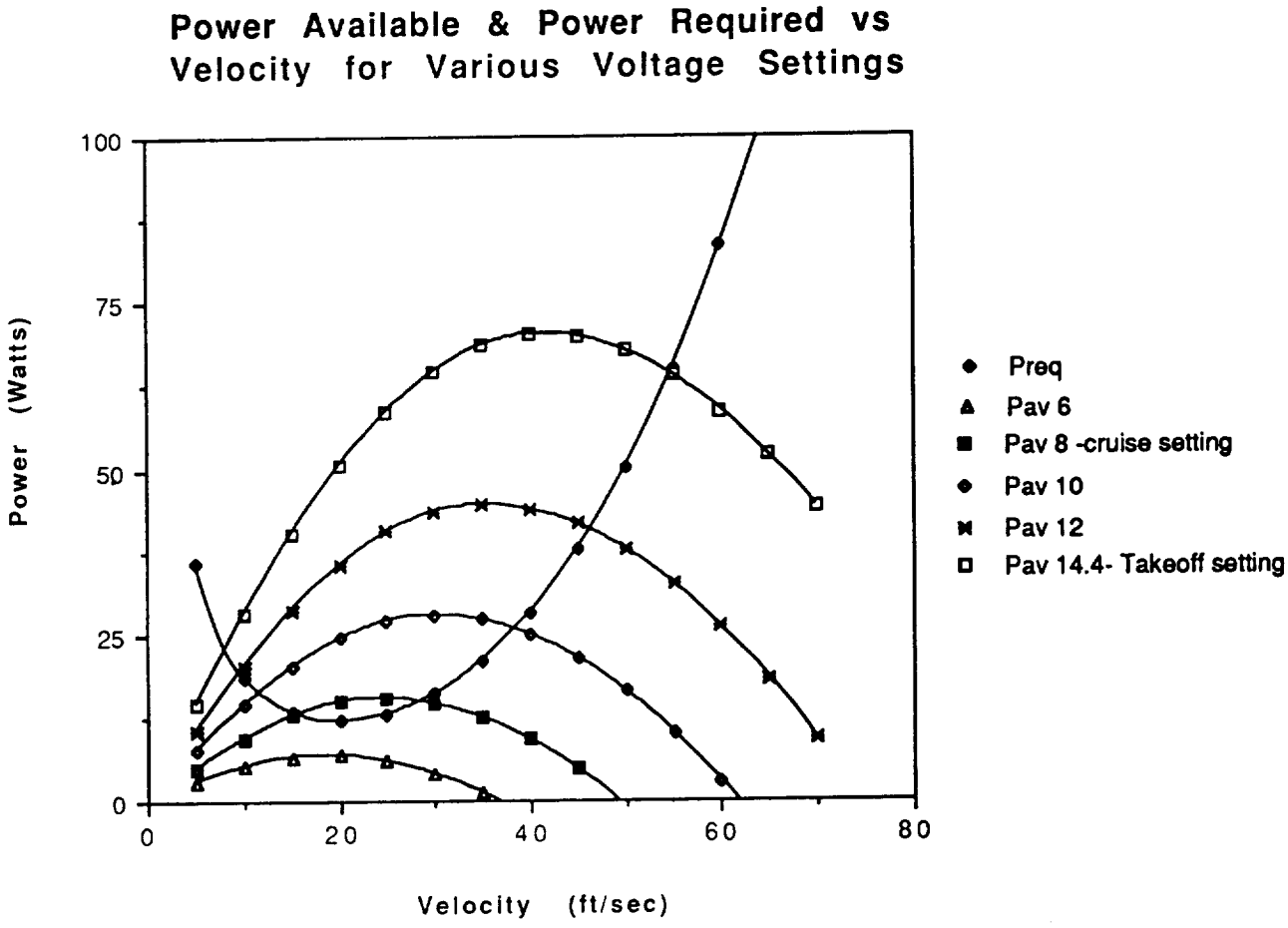
Power Available & Power Required vs
Velocity for Various Voltage Settings
Power (Watts)
100
75
50
25
0
0
20
40
60
80
Velocity (ft/sec)
Preq
Pav 6
Pav 8 -cruise setting
Pav 10
Pav 12
Pav 14.4- Takeoff setting

## H.4 Climbing and Gliding Performance

By examining previous RPV data, a desirable rate of climb would be around 6.0 ft/s. Considering the restrictions of the flight test range, 100 yards long and 40 yards wide, this rate of climb allows for a takeoff distance of approximately 60 feet, enough distance to reach a height of 25 feet and still be able to make a 60' radius turn. The maximum rate of climb for the Arrow 227 was found to be 6.1 ft/sec. Although the actual value is practically equal to our desired value, a rate of climb slightly higher than our desired rate may be advantageous. The elevated rate of climb will allow for the engine to be placed at a lower voltage setting to obtain the desired rate of climb characteristics and thereby reduce fuel costs. Also an elevated rate of climb may prove beneficial should an emergency situation arise or aid in overcoming possible wind shear that may occur during takeoff or landing.

The glide performance of the aircraft is especially important since there it is only a single engine configuration. Should engine failure occur, sufficient glide capabilities will allow the aircraft to fly a considerable distance. The minimum glide angle for the Arrow 227 is -3.72°. This will allow for a glide distance of 385 feet from an altitude of 25 feet before the aircraft touches down. Further studies will need to be conducted to confirm that this will be an adequate distance to perform a successful non-powered landing.

## H.5 Catapult Performance Estimate

The catapult performance of the Arrow 227 was estimated using the catapult system and program designed by Kevin Costello. Information on the RPV was input to the program for this analysis. The program results were that the catapult had to be pulled back 29.5 ft. in order to get the RPV up to Mr. Costello's suggested velocity of 35 ft/s. The program output was that the RPV would take off at a velocity of 23.4 ft/s, and would need only 4.1 feet and .34 seconds to do so.

The maximum velocity during the test of 34.6 ft/s is ideally reached at 13.8 ft. and .66 seconds from the point of launch.

The final results of the program were that the plane should land after traveling 102 ft. in 4.82 seconds. The program also reports an RPV velocity of 31.4 ft/s and a pitch angle of 22° upon landing. These numbers are highly unrealistic. The way the program is written, there is no chance to change the aircraft controls between liftoff and landing, as the plane, as designed, requires. Unless an elevator deflection was input to the program, the pitching motion of the craft would cause the wing to stall rapidly. Once this deflection was input, there was no way to change the angle for level flight, and as the plane should be properly trimmed for proper flight, the program was found to be unpractical.

## H.6 Performance Data Summary

| | |
|---|---|
| Velocity | |
| cruise: | 27.0 ft/s |
| Stall: | 23.0 ft/s |
| Takeoff: | 27.0 ft/s |
| Minimum | 23.0 ft/s |
| Maximum: | 54.14 ft/s |
| Range | |
| @Cruise: | 20200 ft |
| @Rmax: | 22200 ft |
| @Emax: | 15990 ft |
| Endurance | |
| @Cruise: | 12.53 min |
| @Emax: | 13.13 min |
| @Rmax: | 9.3 min |
| Takeoff Distance | |
| Desired: | 60.0 ft |
| Minimum: | 52.0 ft |
| Landing Distance | |
| Desired: | 60.0 ft |
| Minimum: | 174 ft |
| Rate of Climb | |
| Desired: | 6.0 ft/s |
| Maximum | 6.1 ft/s |
| Glide Angle | |
| Minimum | -3.72° |

## Reference

1. Anderson, John D. Introduction to Flight. New York: McGraw-Hill, 1985, pg. 306-311.

# I. STRUCTURAL DESIGN

## I.1 V-n Diagram

The V-n diagram in Figure I.1 illustrates the structural flight envelope for the Arrow 227 operating at the maximum design weight of 6 lbs. The design cruise velocity of 27 ft/s is indicated as well as the maximum velocity of 54 ft/s. The maximum velocity was determined in section H but the aircraft is not expected to fly above 30 ft/s as indicated in the DR&O. The limit load factor was found by computing the maximum load factors expected during flight. The design requirement of a sustained 60 ft. radius turn gave the largest load factor at 1.1 for a velocity of 30 ft/s (from eq. 6.108 Ref. 1). Taking into account the need for a higher velocity turn or a smaller radius turn the limit load was placed at n = 1.5. For comparison this corresponds to a 25 ft. radius turn at 30 ft/s or a 60 ft. radius turn at 46 ft/s which is well within the expected capabilities of the Arrow 227 cargo plane. The flight requirements and performance of this class of aircraft do not include high g-maneuvers and therefore we were able to design a lighter structure while still producing an aircraft which could perform the required mission. In terms of safety, it was felt that the additional boost of the limit load to 1.5 and the incorporation of a factor of safety of 1.5 to place the ultimate load factor at 2.25 was adequate to sustain emergency maneuvers. As a final note the limit and ultimate load factors indicated in figure I.1 represent the values which should not be exceeded to ensure a fatigue life of approximately 700 - 800 flight cycles. It follows then that on early flights load factors exceeding 1.5 or 2.25 could be sustained without damage while at later stages these loads could cause failure as a result of fatigue.

# Figure I.1

## V-n Diagram

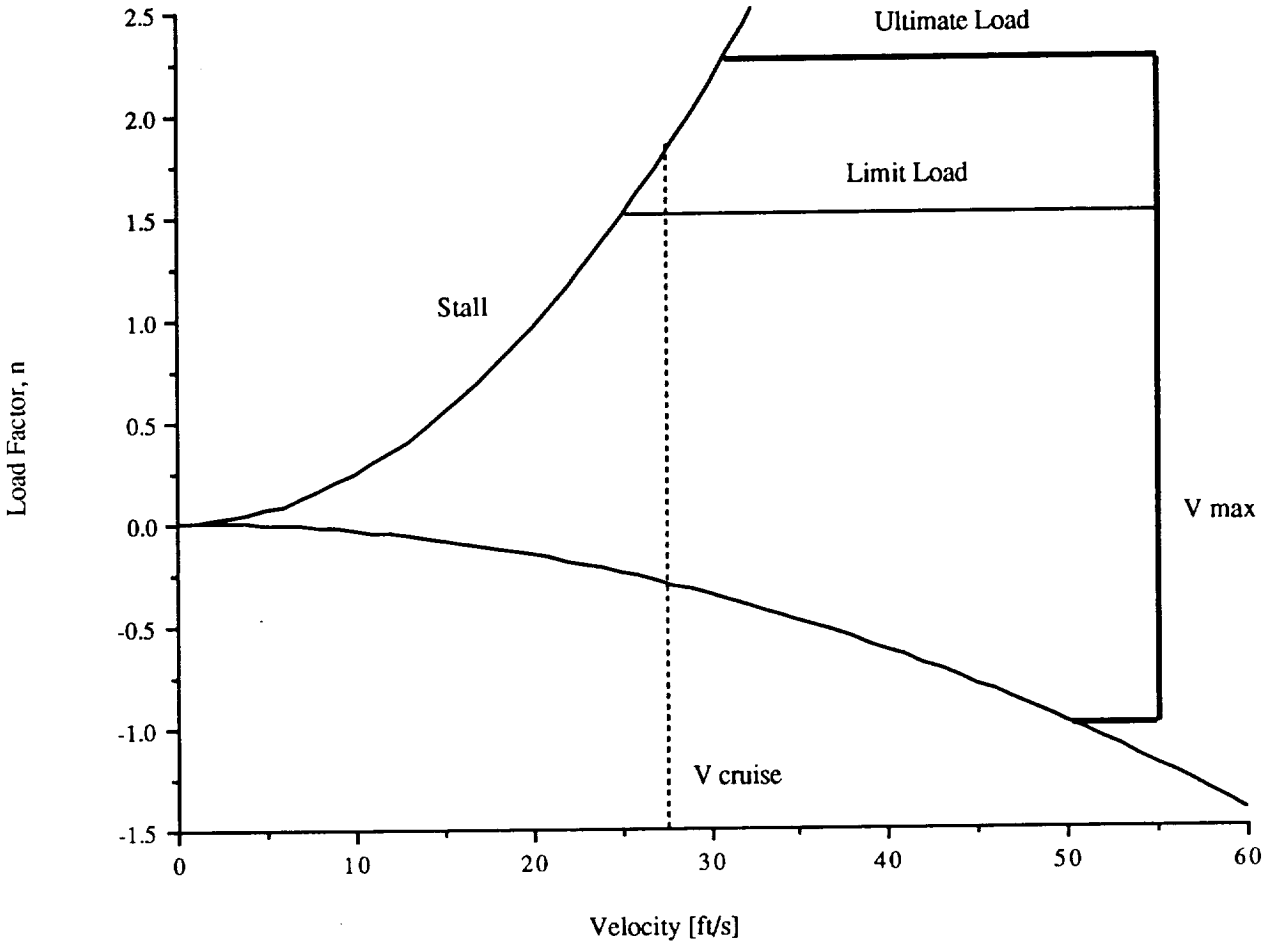

## I.2 Flight and Ground Loads

The ground loads for the Arrow 227 were estimated from the weight and position of each major component including the distributed load of the cargo. The shear and bending moment diagram in figures I.2 and I.3 represent the ground loads with the aircraft pinned at the landing gear. Aside from the cargo the greatest loads came from the engine and the two batteries weighing 10.2 oz and 14.8 oz respectively. The loads produced by these two components during landing was of some concern and drove the design of the fuselage to be addressed later.

**Figure I.2**

**Shear Diagram**

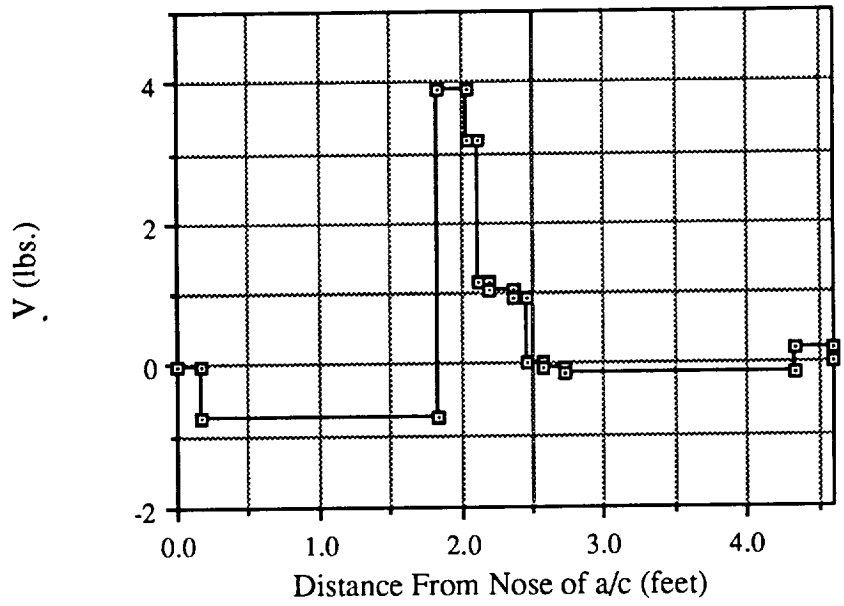


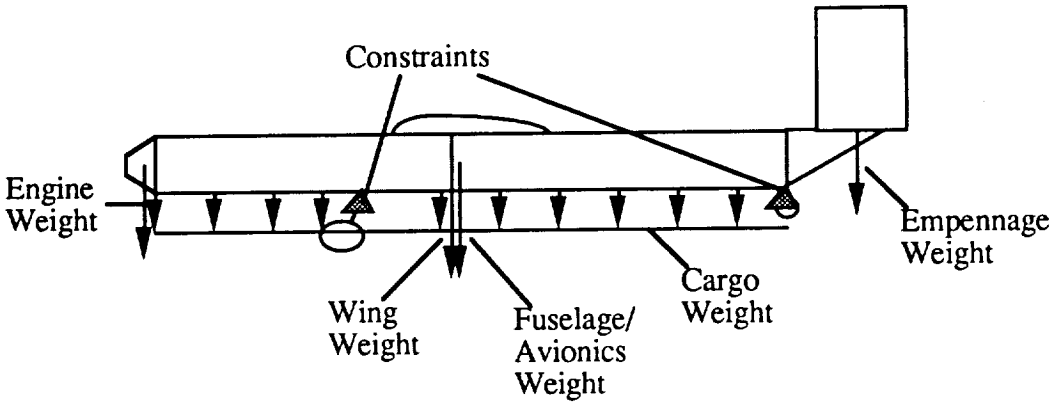

**Figure I.3**
**Bending Moment Diagram**

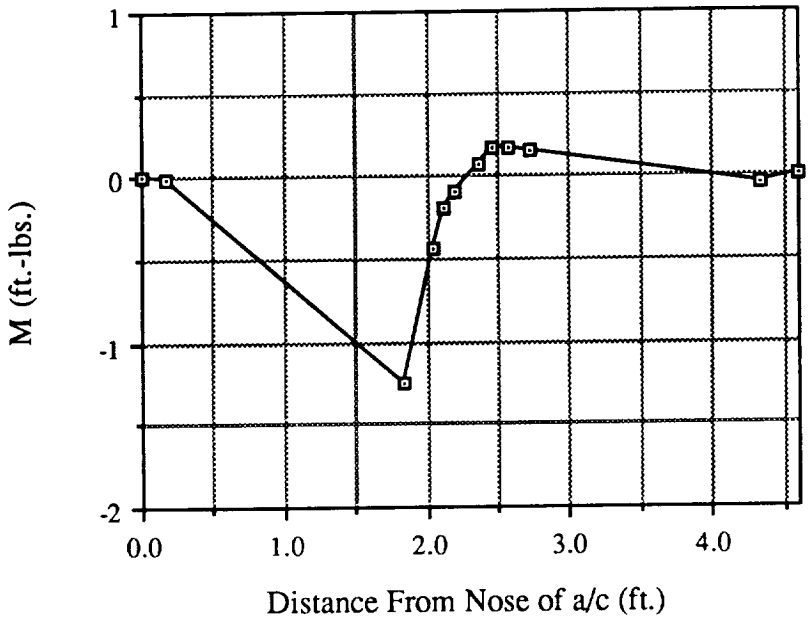


An estimate of the landing force was computed by assuming a sink rate of 5 ft/s and determining the impulse force over 0.1 second. The resulting force was 9.32 for a fully loaded 6 lb. plane which gave a landing load factor of 1.7

The loads on the structure during flight are focused on the main wing with some additional loads produced by the tail especially during maneuvers. Under a limit load of 1.5 the total upward force produced by the wing is 9 lbs and the resulting bending moment distribution is illustrated in figure I.4. The bending moment distribution was found using a computer code WINGLOAD which determined the loadings and stresses of an idealized beam wing given the section aerodynamic lift, drag, and moment coefficients. A listing of WINGLOAD is included in Appendix A. From figure I.4 the maximum root bending moment is 121 lb-in.

**Figure I.4**

**Wing Bending Moment**

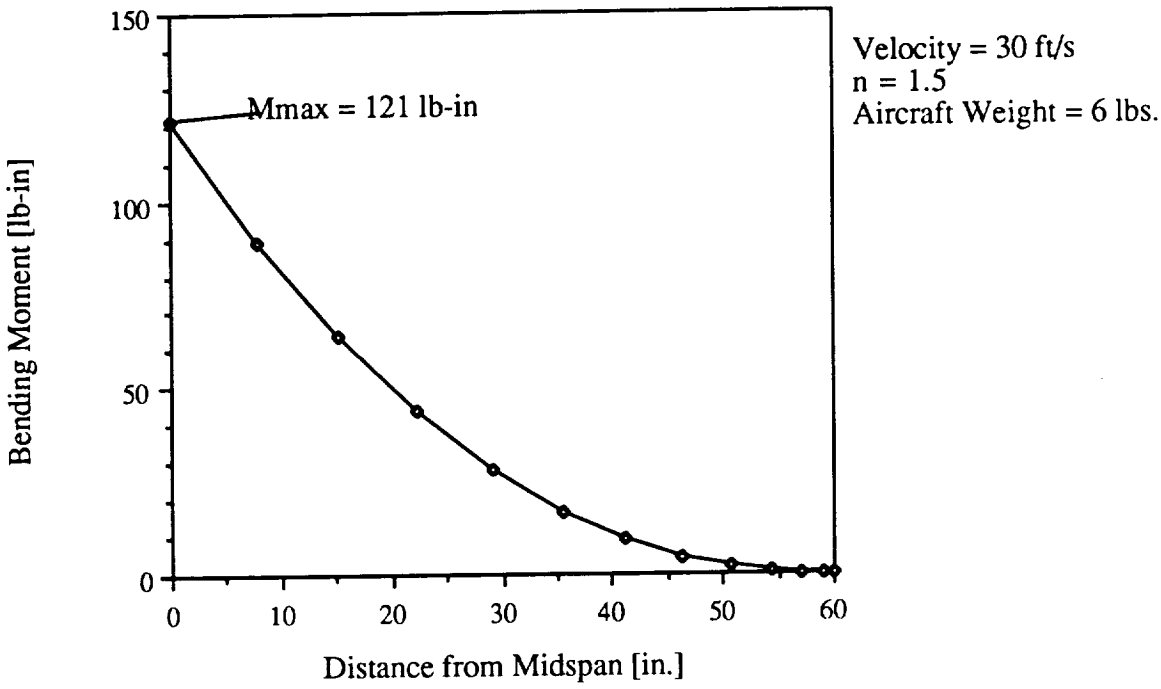


The forces from the horizontal tail were found from stability and control considerations. At cruise the total download on the tail was 0.07 lbs and the maximum expected load due to an elevator deflection was 0.4 lbs. These loads were considered in the design of the fuselage.

## I.3 Materials

The selection of the materials for the aircraft structure focused on the following three parameters:

1. Strength
2. Weight
3. Cost

Since weight was a major concern of the design, standard lightweight woods, balsa and spruce, were chosen for the structure. These woods are common materials for model aircraft construction

and were readily available. This would make construction easier and more cost efficient than using less common woods or composites. Birch plywood was selected for use in areas of high shear stress such as the wing/fuselage connection and the engine firewall. Another lightweight and popular material used for the aircraft covering was Monokote. This was a lightweight, heat shrinkable plastic covering which could be easily applied to the wing and fuselage. Table I.1 lists the properties for the materials selected. (Ref. 2)

**Table I.1**

**Material Properties**

| | | | | Allowable Stresses [psi] | | |
|---|---|---|---|---|---|---|
| **Material** | **E [psi]** | **ν** | **ρ [lb/in$^3$]** | $\sigma_{xx}$ | $\sigma_{yy}$ | $\tau_{xy}$ |
| Balsa | $6.5 \times 10^4$ | 0.08 | 0.0058 | 400 | 600 | 200 |
| Spruce | $1.3 \times 10^6$ | 0.08 | 0.016 | 6200 | 4000 | 750 |
| Birch Plywood | $2.01 \times 10^6$ | 0.36 | 0.0231 | 2500 | 2500 | 2500 |
| Monokote | NA | NA | $1.125 \times 10^{-4}$ [lb/in$^2$] | NA | NA | NA |

## I.4 Wing Design Detail

### I.4.1 Main Spar Design

The design of the wing began with the analysis of the loads carried by the wing. The bending moment distribution is presented in figure I.4 for the limit load factor of 1.5. The design criteria for the wing was the ability to support the maximum root bending moment and resulting stress without failure. In order to simplify the analysis as well as wing construction, one main spar was used as the load carrying member in the wing. Initial estimates indicated that one spar would be more than adequate to support the bending moment and while a leading edge spar and trailing spar

were needed in the wing mainly to hold the shape, they were assumed to carry an insignificant part of the load.

A routine using simple cantilevered beam theory to compute the root axial stress in the main spar was written with the software TK Solver Plus. This routine assumed a uniform lift distribution across the entire span, neglected the weight of the wing, and modeled the spar as a cantilevered beam supported at the midspan. The entire weight of the wing was also computed considering contributions from the ribs, webs and Monokote covering. The formulas in the routine are given in Appendix A. The spar was initially modeled as two flanges (caps) with no connecting web. By varying the height and width of the caps plots of the root axial stress were obtained. Figure I.5 shows the results of changing the spar cap size for the limit load condition. The boundary constraints placed on the figure indicate the maximum allowable stress and a limit on spar size. The maximum stress was computed for spruce wood with a safety factor of 2 (from Table I.1 $\sigma_{allow}$ = 6200/2 = 3100 psi), and the limit at 0.25 in. was intended to narrow the selection range down after noticing that the stress did not decrease greatly for heights greater than approximately 0.25 in.

Spruce wood,although heavier than balsa, was chosen for the main spar material since balsa was not strong enough to withstand the root stress ($\sigma_y$ = 400 psi). A balsa spar would have to be approximately 0.5 x 0.5 in. to reduce the axial stress below 400 psi. This was considered too heavy and unreasonable when less material ( i.e. spruce) would be sufficient. In addition, the modulus of elasticity, E, for spruce was much higher than balsa (see Table I.1) thus producing a more rigid beam with less tip deflection.

## Figure I.5

### Stress vs. Spar Cap Size: No Web

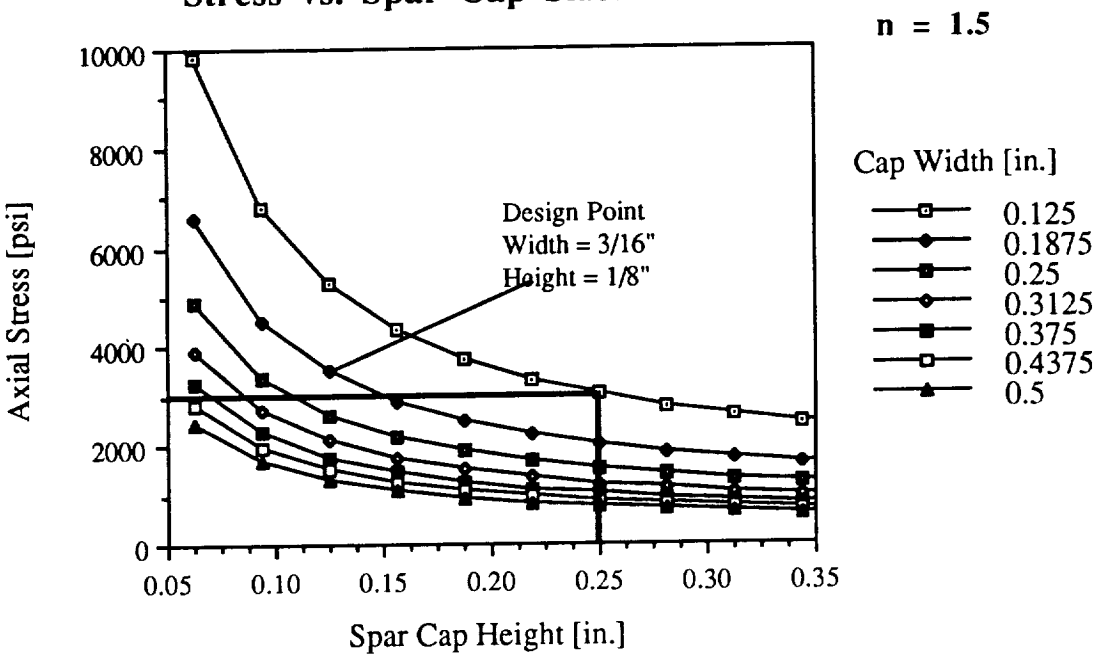


## Figure I.6

### Spar Weight vs. Spar Cap Size

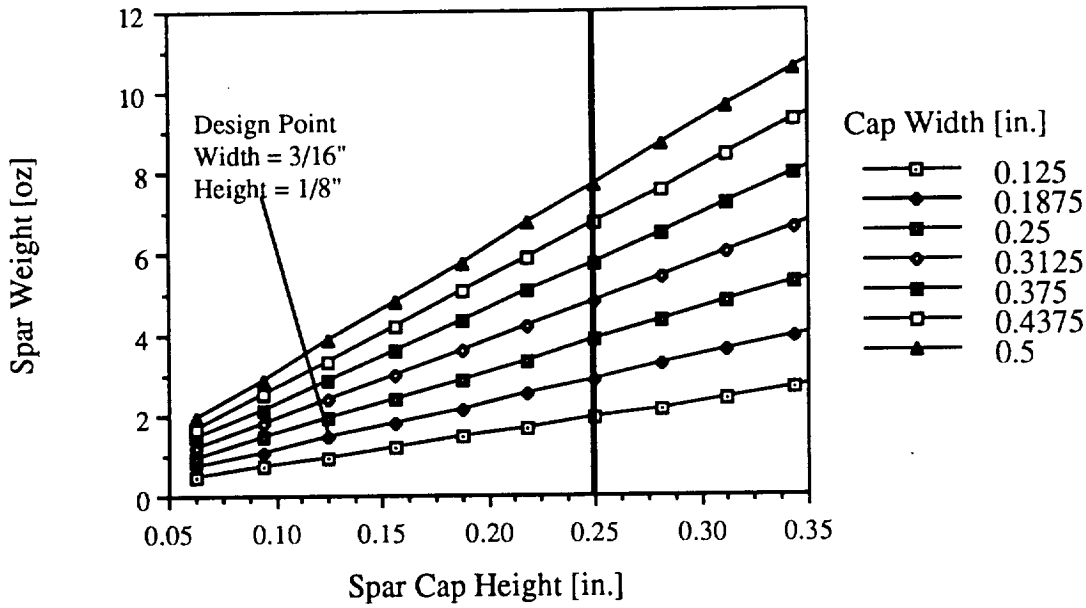

Figure I.5 indicates that there were many different size combinations which would meet the design criteria so figure I.6 was created to show the effect of spar dimensions on the spar weight. Using these two figures the objective was to select the lightest weight spar which met the stress criteria. Initially this was selected at width = 3/16" (0.1875)and height = 5/32" (0.15625). However, further analysis included the contribution of a web between the two caps which increased the moment of inertia of the spar and greatly decreased the axial stress for the same load conditions. The new results are illustrated in figure I.7. With this new information the spar car size was dropped to 3/16" x 1/8".

**Figure I.7**

**Stress vs. Spar Cap Size: With Web**

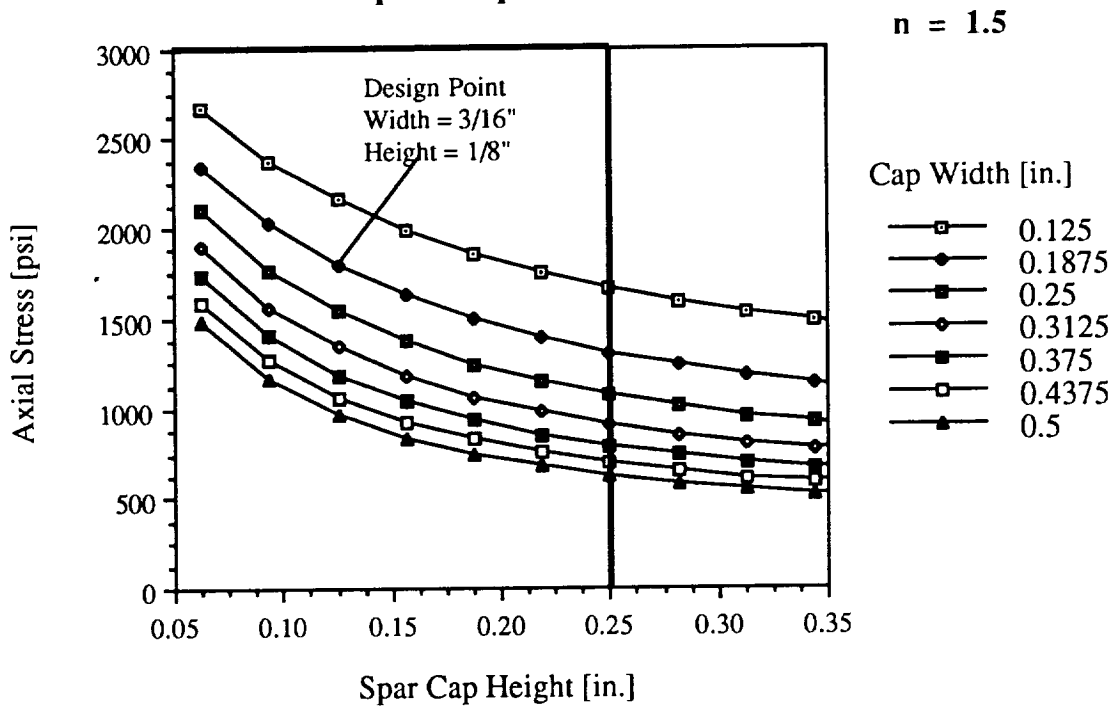


While figure I.7 indicated that a further reduction in spar cap size was possible this was not done because smaller dimensions seemed unreasonable when compared to the sizes of previous designs. In addition, smaller beams would be susceptible to buckling, the web was not intended to cover the entire span, and the analysis was still only an ideal case estimate. Time did not permit testing of

the spar structure to determine how accurate the ideal estimations were so some overcompensation was deemed necessary.

### I.4.2 Other Components and Substructures

The spacing of the ribs throughout the wing was determined based on the need to hold the leading edge shape of the airfoil. The Monokote covering has a tendency to shrink inward between ribs upon heat shrinking. Since the addition of a solid balsa sheet covering over the leading edge would be too heavy, a spacing of 4 in. was set after studying the database of previous models and consulting Mr. Joe Mergen. Since the ribs do not carry much of the wing load but merely keep the shape of the airfoil, the rib thickness was set at 1/16". The small thickness was an attempt to keep the weight of the wing down.

The leading and trailing edge spars were constructed of balsa and included to hold the shape of the wing and the spacing between ribs. The leading edge was a 1/4 x 1/4 in. square section and the trailing edge a 3/16 x 3/4 in. triangular section.

The wing will be constructed of three sections, one 56" middle section and two 32" end sections in order to conform to the size restriction stated in the DR&O. The joint between the sections is illustrated in figure I.8 and is composed of a solid block of balsa glued securely to the outboard wing section and able to slide into the sheath created by the spar caps and webs on the inboard section. A smaller pin of balsa wood will hold the trailing edges of the two sections together.

## Figure I.8

## Wing Joint Detail

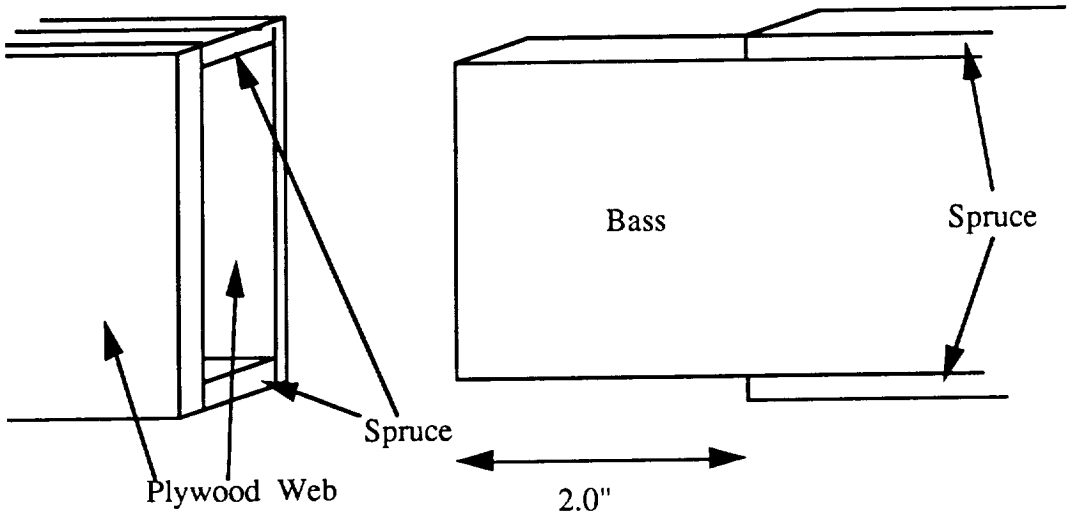


Finally, the wing will be connected to the fuselage through a single wooden pin as illustrated in figure I.9. Two 1/16" plywood sheets will hold the center of the wing at the proper dihedral angle and the wooden dowel will be inserted into a hole in the fuselage bulkhead. A nylon screw will be inserted through the trailing edge to prevent the wing from slipping out. Almost the entire load from the wing will be transferred to the fuselage through the wooden dowel connection, therefore plywood was used to support the large shear stresses around the insertion hole.

# Figure I.9

## Fuselage/Wing Connection

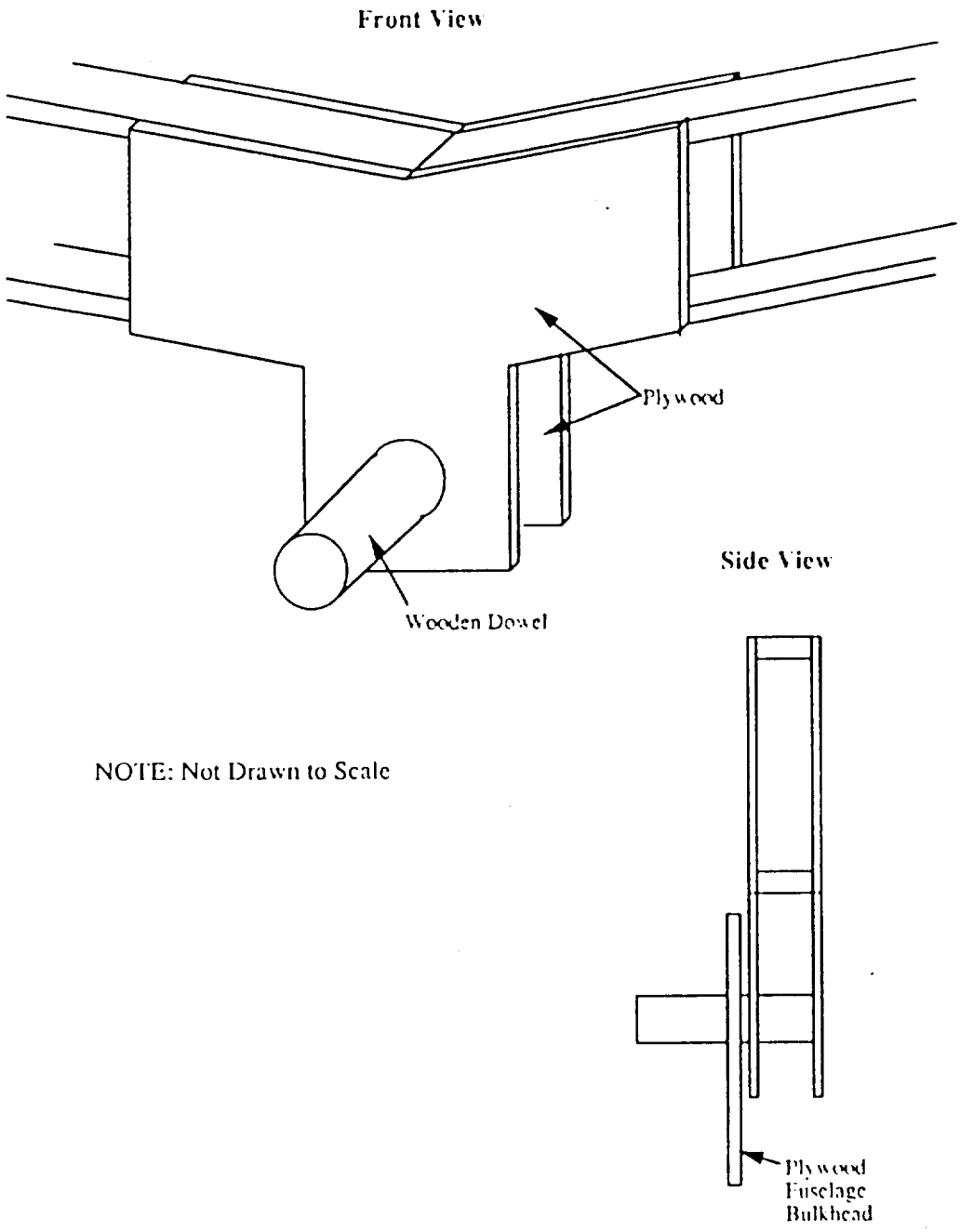


NOTE: Not Drawn to Scale

### I.4.3 Wing Weight Breakdown

Table I.2 summarizes the weight breakdown of the wing.

**Table I.2**

**Wing Weight Breakdown**

| Component | Weight (oz) |
|---|---|
| Main Spar Caps | 1.44 |
| L.E Spar | 0.7 |
| T.E. Spar | 0.78 |
| Ribs | 1.93 |
| Web | 0.85 |
| Wing/Fuselage Connection | 1.16 |
| Joints | 0.26 |
| Monokote | 4.9 |
| Total | 12.0 |

## I.5 Fuselage Design Detail

The initial concept for the fuselage was a simple truss design based on four main beams placed at the corners of the fuselage cross section. The truss concept was chosen due to its light weight and ability to be modeled be finite element methods. The entire truss will be constructed of balsa wood. Balsa was selected over spruce (mainly for the four main beams) since the expected loads did not require the extra strength and weight of spruce wood. Using a landing load factor of 1.7 and figure I.3 the maximum fuselage bending moment was approximately 25 lb-in. well under the 121 lb-in. in the wing.

The fuselage was initially analyzed using only the four main beams as a simple cantilevered beam to get a size estimate. Then the finite element code SPACETRUSS was used to model the entire truss. Figure I.10 is a diagram of the final fuselage truss design. The driving load condition for

the fuselage was landing. The fuselage needed to be strong enough to support the inertial loads from the major weight components especially the engine and the batteries. Using a landing load factor of 1.7 the maximum loads were tested on the finite element model. It was found that although the axial stress in each member could be sustained with little difficulty, the internal force could cause buckling in some members. The critical buckling load for a member constrained at both ends was given by eq 11-6 of reference 3

$$P_{cr} = \frac{4\pi EI}{L^2}$$

This criteria drove the size of the cross braces to 3/16" x 3/16". While some braces did not require as much strength as others, uniformity was kept as much as possible to make construction easier as well as accounting for other loadings which were not modeled on SPACETRUSS.

# Figure I.10

## Fuselage Truss Design

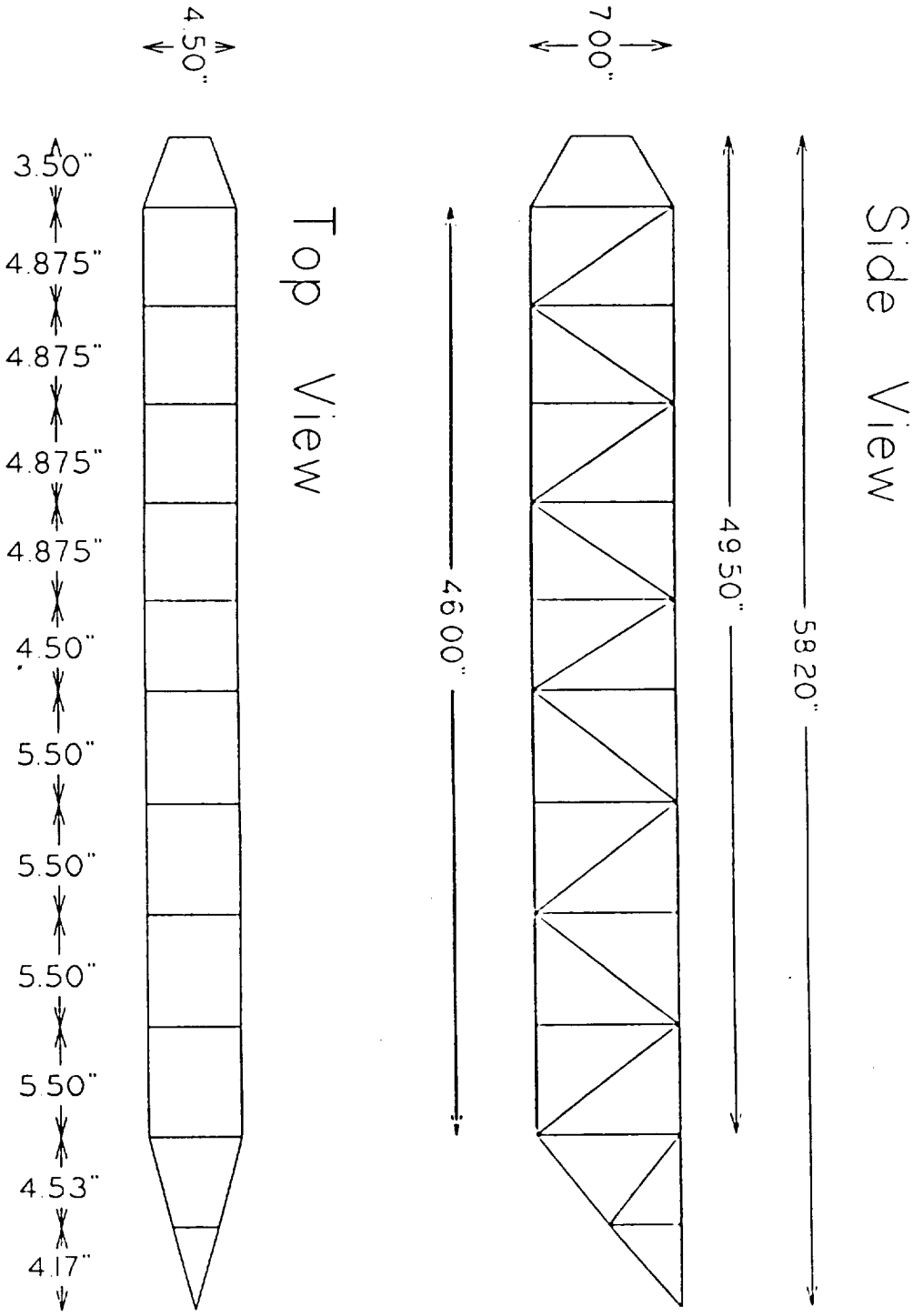

## I.6 Fatigue Life

The working stress reduction factor after a given number of flight cycles is given in figure I.11. This information can be used to determine the reduced maximum allowable stress to achieve a set fatigue life or to determine the fatigue life based on the maximum stress in a existing structure. Throughout the design of the wing and fuselage keeping the stress down below $\sigma_y$ was considered in order to achieve a fatigue life of approximately 700 cycles. After the design has been set and the maximum stresses in the components calculated, the final fatigue life was calculated. Using a safety factor of 2 the original $\sigma_y$ for spruce and balsa were reduced to 3100 psi and 200 psi, respectively. Then the stress reduction factor was found by

$$\text{stress reduction factor} = \frac{\sigma_{max}}{\sigma_y}$$

where $\sigma_{max}$ is the maximum expected stress in the structure

Using the TK Solver Plus routine for the wing the at n = 1.5 gives $\sigma_{max}$ = 1792 psi. Then the stress reduction factor = 0.6. The maximum stress in the fuselage occurred during landing and was found to be 103 psi. This gave a reduction factor of 0.515. The limiting case then is due to the wing which gives a fatigue life of approximately 750 cycles using figure I.11.

**Figure I.11**

**Working Stress Reduction Factor**

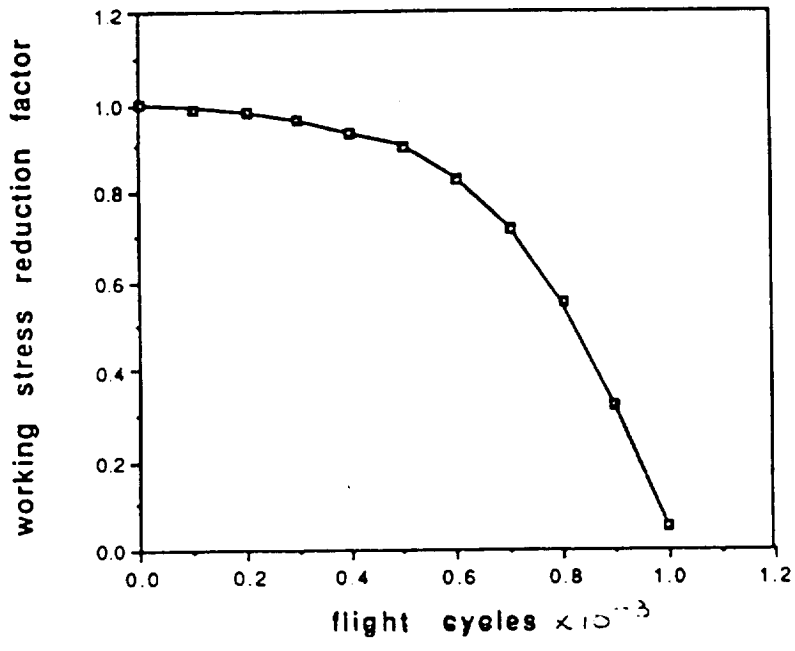

## I.7 Landing Gear Design

The landing gear of the Arrow 227 was driven by five main factors. The tricycle landing gear first was designed to be able to withstand over 700 landings of a fully loaded, 6 pound Arrow 227. Secondly, the gear must provide stability in landing for ground friction and for up to a 30° roll on landing. The third consideration for the landing gear was that the weight should be minimized without losing any durability or stability. It was also desired by the designers that gear be mounted such that the wings be at an incidence angle of approximately 6° to the runway (for the desired takeoff angle). Finally, the landing gear is required to meet any and all ground handling capabilities needed at every airport at which it will operate.

To withstand the strength and durability requirements, the gear uses as struts 1/8 inch diameter steel music wire. The other considered wire diameter was 5/32", which would have been more durable, but with substantially large parasite drag and weight penalties (36% weight saving with 1/8" wire). The extra strength of the thicker wire was not needed, as the 1/8" wire will last through the entire service life of the Arrow 227. The wire will flex slightly upon landing, and ease the load on the fuselage by doing so. The pilot should not be able to land the plane hard enough to flex the wire so greatly that the propeller hits the ground. Flight testing will validate this aspect of the landing gear design.

Runway stability for ground friction is done by two means, minimizing friction and keeping the main gear at greater than a 15° angle forward of the center of gravity (As dictated by aerospace enginner Joe Mergen). Reduction of friction is done by the choice of wheels - two foam 2.5" diameter wheels are used. A 15° angle in front of the CG is maintained by placing the gear at 18 1/8" from the nose, 5 1/2" (31°) in front of the CG at its foremost position. Stability for a roll during landing is provided by having the outer edge of the wheel out from the CG at an angle of

30°. The outside of the wheel is 6.2" out from the center of gravity, which provides an angle of 33° for the highest (worst case) position of the CG.

To minimize the weight of the landing gear, the gear is attached to a strong point on the fuselage, through which the force and moments associated with landing can be readily accommodated. This, coupled with the need for friction roll stability left the main gear to be placed at the 18 1/8" position. To have the front gear at this point, coupled with the tail wheel intersection with the ground at 1 1/2" below the fuselage at a position 49 1/2" from the nose, the front wheels need to be 4.8" down from the bottom of the fuselage. This distance provides the optimal 6° incidence angle between the wing and the runway.

To meet the ground handling qualities of every airport, the tail dragging gear is movable and controllable by the pilot. This is done by one of two methods. The first method entails simply running a second control bar off of the rudder servo and to the tail wheel. This may, however, require unnecessary control weight as it may be possible to directly link the tail wheel to the rudder. Doing this may slightly complicate the design , but so minimally so that the weight savings would well be worth the extra time.

The landing gear as designed will prove to be sufficient for the entire service life of the Arrow 227, and at a weight of 3.9 ounces. The performance includes the maintenance of stability in all directions given the expected loads of landing and ground handling. The tricycle gear is mounted to provide the optimal take off angle for the Arrow 227 while meeting desired stability parameters. The landing gear as finally designed, will be able to meet all ground handling needs as well as the above performance characteristics.

## References

1. Anderson, John D. Introduction to Flight. New York: McGraw-Hill, 1989.

2. Aerospace Design Lab Notebook

3. Gere, James & Timoshenko, Stephen. Mechanics of Materials. Monterey, CA: Brooks/Cole, 1984.

# J. CONSTRUCTION PLANS

## J.1 Major Assemblies

### J.1.1 Wing

The wing spar is composed of spruce spar caps and balsa webs covering the middle 6.5 ft of the span. A diagram of the main spar cross section is shown in figure J.1. Ribs are composed of balsa and are spaced every 4 in. All ribs are 1/16" thick except the ribs on all exposed ends of the wing (i.e. wing tips and joint location) which are 1/8" thick to resist bending from the Monokote covering. The webs are all 1/16" thick balsa except for the center section and the region around the wing joint which are 1/16" plywood. Detailed drawings of the wing/fuselage connection and wing joint connection were presented in section I.4.2. Finally the leading and trailing edge spars are both balsa beams with cross sectional areas of 0.0625 $in^2$ and 0.07 $in^2$, respectively.

**Figure J.1**

**Main Wing Spar**

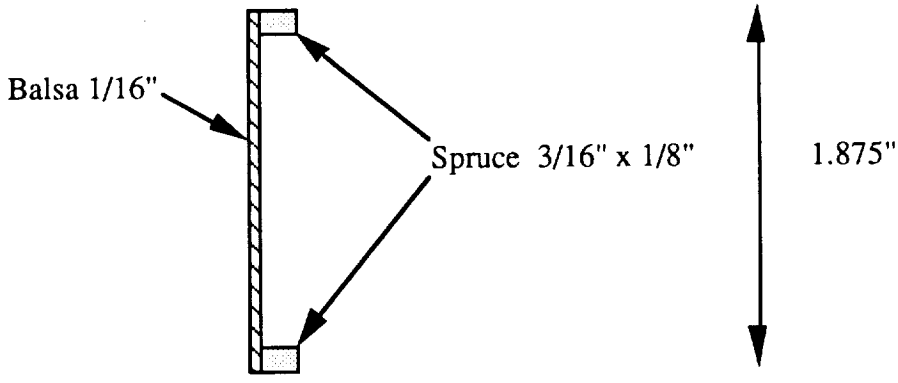

### J.1.2 Fuselage

The fuselage is an all balsa wood truss design composed of four main beams at the corners supported by cross braces along the sides, top and bottom. A diagram of a typical fuselage bay section is shown in figure J.2. The nose of the fuselage includes a plywood firewall across the width of the fuselage to attach the engine mount. A platform slightly behind the wing and approximately 2 in from the top of the fuselage holds the batteries and avionics.

**Figure J.2**

**Typical Fuselage Bay**

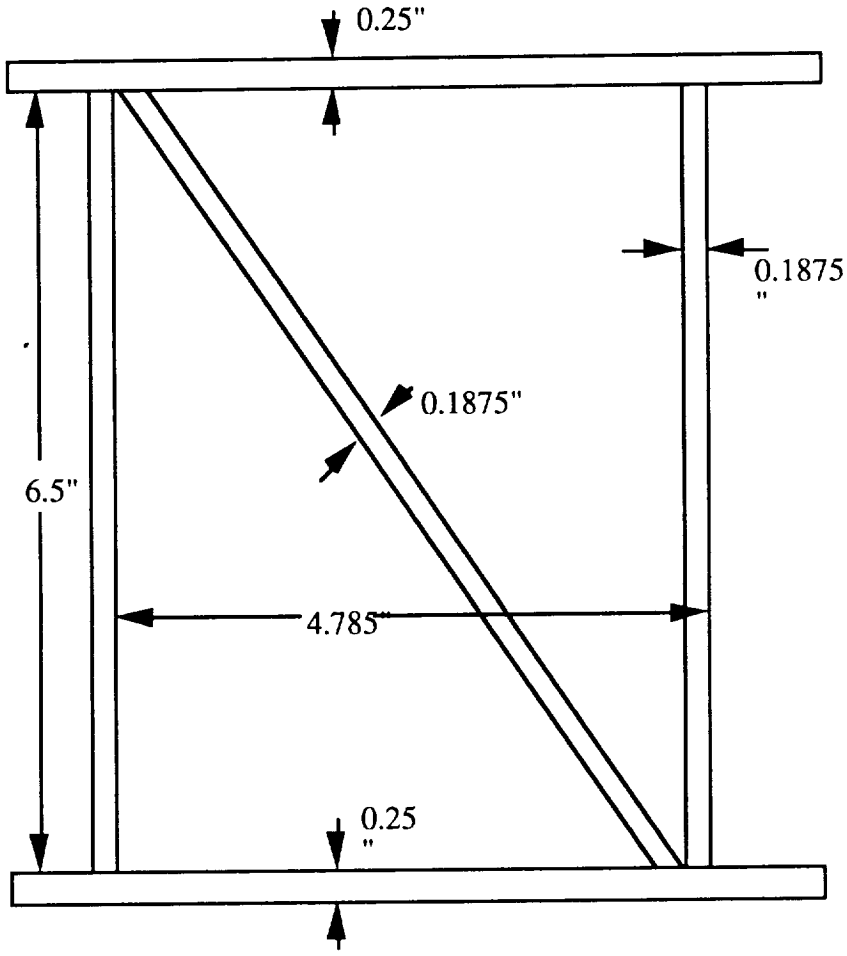


Side View

### J.1.3 Horizontal and Vertical Tail

Flat plates were used in the design of the horizontal and vertical tails since past aircraft have proven that they are effective and can be produced cheaply due to their simple design. A maximum load of .6 lb was used in the design of the horizontal tail. Two balsa spars, 2.8'x.5"x.25", resist the bending moment of the load while 8 flat balsa ribs, 4.38"x1/8"x1/8", keep the shape of flat plate and connect the two spars. The elevator, a 2.8'x1.3"x1/16" stip of balsa with bored holes, is connected to the rear spar with two hinges.

The vertical tail was designed the same as the horizontal tail with the exception that the rudder was not a single piece of balsa. The lack of ailerons created a need for a rudder that is 50% if the vertical tail area. Thus, the vertical tail consists of two equally sizes flat plates that are attached by two hinges. Each flat plate consist of two balsa 1.2'x.5"x1/4" spars and four balsa3.6"x1/8"x1/8" ribs.

## J.2 Complete Parts Count

The following table lists the numbers of parts for the entire aircraft excluding the propulsion system and the avionics (table J.1). These parts are purchased as packages containing an abundant amount of parts. The basic components are provided in the material cost breakdown (Appendix 2).

**Table J.1**

| CATEGORY | COMPONENT | MATERIAL | QUANTITY |
|---|---|---|---|
| MISCELLANY | nose cone | Balsa | 8 |
| | engine mount | Plywood | 1 |
| FUSELAGE | hatches | Balsa | 10 |
| | longitudinal | Balsa | 4 |
| | lateral | Balsa | 19 |
| | vertical | Balsa | 20 |
| | side diagonals | Balsa | 18 |
| | battery platform | Balsa/Plywood | 6 |
| EMPENNAGE | | | |
| main body: | top(longitudinal) | Balsa | 2 |
| | lateral | Balsa | 2 |
| | vertical | Balsa | 2 |
| | side diagonals | Balsa | 2 |
| Tails: | vertical tail | Balsa | 6 |
| | rudder | Balsa | 7 |
| | horizontal tail | Balsa | 11 |
| | elevator | Balsa | 1 |
| WING | main spar | Spruce | 8 |
| | leading edge | Balsa | 4 |
| | trailing edge | Balsa | 4 |
| | ribs | Balsa | 34 |
| | webs | Balsa | 20 |
| | joints | Balsa/Plywood | 4 |
| | wing/fuse. connection | Plywood | 4 |
| | trailing edge screw | Nylon | 2 |
| LANDING GEAR | wheels | Foam/Rubber | 3 |
| | extensions | Music wire | 2 |
| | fuse. reinforcement | Balsa/Plywood | 8 |
| | brackets & mounts | Nylon | 5 |
| AVIONICS | | | |
| | r/c unit | --------- | 1 |
| | engine | --------- | 1 |
| | batteries | NiCd | 12 |
| | servos | --------- | 2 |
| | propeller | Wood | 1 |
| | control rods | Plastic | 2 |

## J.3 Assembly sequence

The first step of the assembly process will be the construction of the structural components. These components consist of the wing, the fuselage, the horizontal tail, the vertical tail, and the nose cone. Each component will be assembled by a team or an individual, allowing several components to be assembled at one time. The process will consist of the following general steps:

1. Plot full-scale drawing of component
2. Cut wood pieces
3. Pin base member of component on top of drawing
4. Glue other members to foundation of component
5. Apply Monokote to frame of component

After the aforementioned structural components are constructed, the next step will be to attach each component to each other (i.e., assembling "the plane"). The wing will be the only component that will not immediately be attached since the batteries, remote control unit, servos, etc. need to be positioned underneath the wing first. Next, the engine will be mounted to the nose's firewall, the propeller will be attached, and the control surfaces will be hooked up to the servos. Finally, the landing gear will be assembled then attached to the fuselage using the appropriate braces.

# K. ENVIRONMENTAL IMPACT AND SAFETY ISSUES

## K.1 Disposal Costs

The majority of the material used in the ARROW 227 can be disposed of at either no cost or even a slight profit if done properly. The main cost in disposal is expected to come from the glue holding the structure together and from the NiCd batteries. The cost for the environmentally sound disposal of these materials is unknown and will require further study. It is believed that these costs can be frayed significantly by wisely choosing an environmentally and economically sound disposal plan for the rest of the RPV materials.

The monokote and the plastics from the servos, motor and wheel hubs have the potential of becoming environmental problems, if not disposed of in an acceptable fashion. It is suggested by the design team that G-Dome look into signing a contract with a plastics recycling company which would strip the RPV's of their plastics for free in return for only the plastic itself. Such a contract would be mutually beneficial to both companies.

The foam tires would not necessarily have to be disposed of. The foam could be ground up by the overnight company and reused as fill for packaging. The one time cost of a shredder should be recouped and may well prove profitable to the company over the shredder lifetime by the savings in packaging costs.

The infrastructure is built with spruce and balsa, two woods which could be taken away at no cost, and with the gratitude of the local communities. The proposed method for disposal of wood is to have the local AeroScout chapter dismantle the plane and cart away the wood. The scouts should be more than pleased to have wood for their bonfires and woodworking projects with no detrimental effects on the local forests.

Another material in the RPV's is steel. Steel is used for the control rods as well as the landing gear struts. It should prove possible to sell off the unusable steel as scrap - further salvaging the manufacturers investment in materials.

## K.2 Noise Characteristics

An important consideration of the Arrow 227 was to keep the cruise velocity below 30 fps, the speed of Aerosound. The Arrow 227 was thus designed to maintain a cruise velocity of AeroMach 0.9. This keeps the RPV from breaking the Aerosound barrier and from making a sonic boom which would disturb communities over which the plane will fly.

The other key factor in the noise characteristics of the Arrow 227 is that of the propulsion system, namely the motor and the propeller. An electric motor was chosen and is expected to run far more silently than would a gas engine of similar power output. The propeller noise is the one unknown factor in the aircraft sound characteristics. The combination of the silent flight (low velocity) and electric motor creates the expectation that the propeller will be the loudest of the aircraft subsystems. However, the propeller is not expected to attain a very high decibel level at all as its tips travel nowhere near the speed of true sound (as tip speed is an exception to the speed of AeroSound). The overall noise characteristics of the Arrow 227 are expected to be among the best in AEROWORLD. Flight tests are expected to prove the validity of this claim.

## K.3 Waste and Toxic Materials

There will be no waste materials emitted during the course of a regular flight of the Arrow 227, as the system uses electric rather than gas power. As mentioned above, the two problematic materials are the glue and the Nickel-Cadmium batteries. These materials may prove to be too toxic for normal disposal, and special guidelines may have to be followed in their disposal at the end of their useful lives. Further research needs to be done to find a suitable means for the disposal of these potentially troublesome materials.

# L. ECONOMICS

## L.1 Introduction

The primary goal of the Arrow 227 was to provide the customer with the greatest potential return on investment. This goal was imperative because economic feasibility, not simply performance, determines a product's marketability. As will be shown by the subsequent market analysis, the Arrow 227 maximizes the profit an overnight package delivery service can attain by minimizing production costs, maintenance costs, and operation costs. As a result, the delivery service can increase sales by decreasing the cost per package since the expenses it incurs to purchase the fleet will be minimal. Overall, the Arrow 227 provides a cost efficient design that benefits both the manufacturer and the customer.

## L.2 Production Costs

**Figure L.1**

**Production Cost Breakdown**

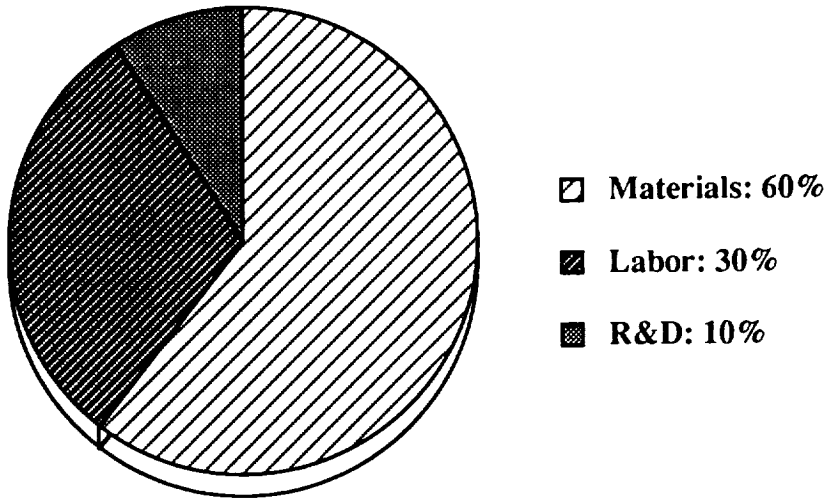

An important way in which the Arrow 227 minimizes charging costs per customer while still attaining a profit is through minimization of the production costs. The total production cost for the Arrow 227 is $5,737,600. The two major components that constitute the production cost of the Arrow 227 are the materials and the labor (Figure L.1).

Based on the detailed structural plans, it was calculated that the total cost of the materials needed to construct the Arrow 227 prototype is $565. The cost breakdown for each component is shown in Appendix B. In the PDR, this cost was approximated as $500 based on the available database. The inflation of the component costs, however, is responsible for the underestimation. As can be seen, the remote control unit constitutes the majority of the expense ($249). This amount is standard for the operation of all transport aircraft in AEROWORLD. The propulsion system is also a major component of the material cost but its selection was dictated by the takeoff and landing requirements. It is the least expensive system that meets these demanding requirements.

The labor cost is the money necessary to pay the workers to construct the aircraft. The construction time was estimated to be 100 man-hours from the database of past aircraft with similar designs. It is felt that this value will most likely decrease for the construction of the actual fleet since the prototype will be the first run through the manufacturing process. With the experience of building the prototype, the construction crew will suggest revisions to the process, thereby increasing their efficiency during the construction of the actual fleet. The research and development cost corresponds to the profit G-Dome Enterprises will receive. This was simply ten percent of the total production cost.

## L.3 Maintenance Costs

As can be seen in figure L.2, maintenance costs contribute a fairly insignificant amount in comparison to the fuel costs over the fleets lifetime. Despite this fact, it still played a role in the design of the Arrow 227.

Maintenance costs are a function of the time it takes to replace the twelve batteries used by the engine. To minimize this time, the batteries had to be easily accessible. For the Arrow 227, the batteries are located on an elevated platform beneath the wing. The actual placement of the platform was dictated by center of gravity requirements, but it also turned out to be advantageous. Such a configuration will provide an exchange time of approximately half a minute. Since the wing had to be removeable due to storage requirements, this location provided a means of accessing the batteries without having to construct another hatch on the plane. Thus, this configuration reduced construction costs. The elevated platform also served several purposes. First, it allowed easier access to the batteries and servos since the hatch is located on the top of the fuselage. Second, cargo can be stored underneath the battery platform, permitting more cargo to be carried.

## L.4 Operation Costs

Along with the maintenance costs, the operation costs the Arrow 227 incurs are minimal with respect to the fuel costs (figure L.2). The operation cost for a flight is equal to the product of the time of the flight and the number of servos used to operate the aircraft. This had a significant influence on the decision to eliminate ailerons from the design since they necessitate an additional servo. To avoid this cost penalty, the dihedral effect is used to effect a turn through a rudder deflection. In addition, the high cruise velocity of the Arrow 227 (27 ft/sec) ensured the minimization of the flight time without having an adverse effect on the fuel consumption.

## L.5 Market Analysis

To ascertain the economic viability of the Arrow 227, a market analysis was performed that proposed a delivery route, determined plausible shipping charges, and evaluated the likelihood of profit.

The proposed itinerary necessitates 16 planes which will carry 30930 $in^3$ of freight each night (Figure B.2). The fleet will perform 58 ground-air-ground cycles daily. The average distance of the daily flights is 2690 feet. Since the Arrow 227 can complete 700 cycles before fatigue failure, the fleet is expected to have a life of 193 days. Over the entire fleet life, the fleet will cost $22,913,592 to operate. This value is based on the assumption that the cost of fuel will equal $12.50/milli-amp hour. As can be seen in figure L.2, the fuel constitutes the major portion of this total cost.

**Figure L.2**

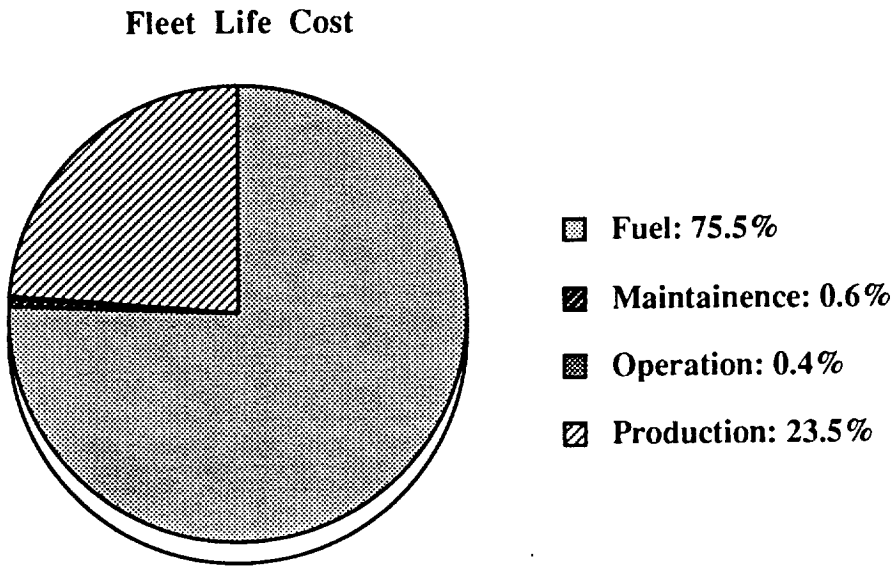

The determination of the shipping rates constituted the majority of the market analysis. The rates must be competitive while still providing a quick return on investment. It was concluded that the most practical pricing system would depend upon the distance the freight must be carried and the volume of the freight. The shipping rates were divided into three categories depending upon their length:

A. Intracontinental shipment: $\$3.69/in^3$

B. Transcontinental shipment: (to/from hub continent): $\$6.29/in^3$

C. Other transcontinental shipment: $\$8.99/in^3$

The minimum rate corresponds to the intracontinental shipment since it is the shortest flight on average. The second rate corresponds to a shipment that involves one transcontinental flight while the third rate involves two transcontinental flights. To obtain the actual monetary values, it was assumed that the break even point would be attained if, over its lifetime, the fleet filled 60% of if its volume capacity. It should be noted that if this system was implemented the rates would most likely change upon evaluation of delivery distribution. It was assumed that the total daily cargo would be distributed equally among each type of flight (i.e., each type of flight will carry 1/3 of the total daily cargo volume). If the services do not correspond to this distribution then the rates will be adjusted accordingly to satisfy the 60% break even point.

The profits acquired through implementation of this system validate the feasibility of the concept. A 28% profit accumulates from the given investment if the fleet carries an average of 64% of its maximum payload volume over its lifetime. Operating at this volume, the investment will be returned within 150 days. The investment will be doubled if the fleet carries an average of 75%. The fastest return of the investment would be 50 days if the fleet operated at maximum capacity.

Without a doubt, this study shows that the concept is presently economically feasible. In addition, the concept provides an opportunity to increase the already substantial profit margin with future

fleets. The profits for the subsequent fleets will increase since many of the components from the preceding fleet can be recycled (e.g., servos, engines, control rods, transmitter and receivers). These components fatigue at a slower rate in comparison to the actual aircraft structure which can only withstand 700 flight cycles. Profits will also increase for subsequent fleets since the man-hours will decrease. The first production run is a trial-and-error process. The manufacturing process will speed up as the skill of the workers increases.

# M. Results of Technology Demonstrator Development

## M.1 Configuration Data

No serious problems were encountered during the development of the Arrow 227. The geometry of the technology demonstrator was, for the most part, in strict accordance with the final design. The aircraft length increased from 4.85 ft to 4.95 ft since the horizontal tail was mounted 1.3 inches further back to free the elevator from the fuselage. Table M1 lists the important technology demonstrator geometries. The geometry required by the final design is also listed for reference.

**Table M.1**
**Configuration Data-Geometry**

| | Technology Demonstrator | Final Design Requirements |
|---|---|---|
| Wing Span | 10 ft | 10 ft |
| Wing Cord | .94 ft | .95 ft |
| Dihedral | 8.2° | 8° |
| Sweep | 0° | 0° |
| Wing Incidence angle | 1° | 0° |
| Horizontal Tail Span | 2.79 ft | 2.8 ft |
| Horizontal Tail Chord | .56 ft | .56 ft |
| Horizontal Tail Incidence angle | 2° | 2.5° |
| Vertical Tail Span | 1.11 ft | 1.2 ft |
| Vertical Tail Chord | .6 ft | .6 ft |
| Overall Length | 4.95 ft | 4.85 ft |
| Dist. from nose to Wing LE | 1.66 ft | 1.65 ft |
| Max Fuselage Width | 4.5 in | 4.5 in |
| Max Fuselage Hidth | 7 in | 7 in |

The only major discrepancy between the completed aircraft and the final design was the empty weight. The technology demonstrator weighed in at 4.5 lb compared to the design 4 lb. This weight increase was caused by a mistake by a subcontractor and increased structural weight. The

batteries delivered by a subcontractor had a capacity of 1000mah and weighted a total of 18 oz. The batteries ordered had a capacity of 900mah and weighed 14.8oz. This resulted in a .2 lb increase in the total weight. In addition, the wing incurred a weight increase of 3.5oz. Another increase in the Arrow 227 weight was the use of 5/32" diameter wire for the landing gear rather than the 1/8" wire to increase landing gear strength. The remainder of the extra weight was introduced by structural weight added to the fuselage to better support various subsystems.

The weight increases resulted in the empty aircraft center of gravity location moving aft. This shift in the CG threatened the longitudinal stability of the Arrow 227 and thus a means of moving the CG forward needed to be determined. This was accomplished by moving the platform that supported the avionics and batteries forward. Table M2 lists the completed technology demonstrator weight break down and CG location.

## Table M.2
## Component Weight Breakdown

| Component | Weight(oz) | X-location(in) | Y-location(in) |
|---|---|---|---|
| Engine | 8.90 | 1.75 | 0.00 |
| Engine clamp | 0.75 | 1.00 | 0.00 |
| Engine mount | 1.16 | 2.00 | 0.00 |
| Engine battery 1 | 9.27 | 27.80 | 2.75 |
| Engine battery 2 | 9.27 | 27.80 | 2.75 |
| Speed controller | 2.66 | 25.50 | 2.75 |
| Propeller | 0.54 | -0.50 | 0.00 |
| Servo-elevator | 0.60 | 31.57 | 2.25 |
| Servo-rudder | 0.60 | 31.57 | 2.25 |
| receiver | 0.95 | 29.88 | 2.65 |
| receiver battery | 2.01 | 27.88 | 2.53 |
| Fuselage | 11.00 | 27.50 | 0.00 |
| Wing CG | 15.50 | 24.50 | 3.80 |
| Empennage | 3.40 | 54.75 | 3.80 |
| Landing gear | 5.00 | 24.00 | -4.46 |
| Payload | 32.00 | 25.43 | -0.25 |
| **Total(lbs)** | 6.48 | CG-empty(ft) | CG-w/pld(ft) |
| | | 1.993 | 2.032 |
| | %cord | 35.014 | 39.128 |

## M.2 Flight Test Plan and Safety Considerations

The flight test plan involved both the taxi tests and the actual flight test. The taxi test was done three days prior to the flight test in order to determine how the Arrow 227 ground handled. A preliminary flight check list was given to the design group by senior management to complete prior to the tests.

Before both tests, the receiver batteries and the engine batteries were charged and the propulsion and avionics systems were checked to make sure they were securely in place and would not shift in flight due to vibration and aircraft maneuvering. The platform containing the batteries and avionics was directly under the wing, therefore, once the wing was in securely in place, there was still a need to access the on/off switches for the speed controller and receiver. To insure safety, the on/off switches were placed outside of the fuselage and under the wing. Now, the wing could be assembled and, once the aircraft was prepared for flight, the switches could be turned on. This allowed for safe assembly and easy access of the systems' power.

When these switches were turned on and off, no person was allowed to stand near to the propeller in case it was not secured correctly or if charge was left over in the wires after the system was turned off. Prior to putting on any throttle, the elevator and rudder were checked to assure full range of desired motion.

Finally, before the Arrow 227 began accelerating, all people moved away from the aircraft and anyone not designated to be on the takeoff range at that time had to move behind a safety net at one end of the flight test ground.

## M.3 Flight Test Results

The taxi tests were performed on April 28, 1992. The purpose of the test was to verify that the technology demonstrator was ground controllable. An attempt would also be made to fly the aircraft for a very short period of time to verify that it was flyable.

The taxi test was a success. The Arrow 227 was both ground controllable and flyable. Joe Morgan who piloted the aircraft was able to take-off, land, and taxi the Arrow 227 back to its original starting position.

The controlled flight tests were performed on May 1, 1992. Again, the Arrow 227 successfully completed the flight test. Initially the pilot seemed to have a slight problem controlling the aircraft after take off. However, he soon became familiar with the dynamics of the Arrow 227 and had no problem controlling the aircraft. The pilot was able to trim the aircraft at a throttle setting and fly the aircraft without using the controls which indicated that the Arrow 227 was indeed longitudinally and lateral stable. The Arrow 227 was flown a second time and pilot further demonstrated the controllability and stability of the Arrow 227 as the aircraft flew smoothly from take off to landing. From a performance standpoint, the aircraft took off in approximately 38 ft when it was unloaded and at 85% of maximum throttle. The Arrow 227 also performed turns that appeared to be well below the minimum 60 ft turn radius.

## M.4 Manufacturing and Cost Details

The development of the Arrow 227 technology demonstrator was begun on April 7, 1992 and completed on April 30. Full scale drawings of the fuselage and wing were made so that construction could proceed by simply building on top of the drawings. This method made

construction easy and quick and the frame for the main body of the fuselage was completed in about six hours. Construction time for the wing was longer than expected, mainly due to the lack of experience of the construction team. The exact construction times, along with costs, for each major component are listed in the following table.

**Table M.4**
**Construction Time and Cost**

| COMPONENT | HOURS | COST($) |
|---|---|---|
| fuselage | 28 | 37.20 |
| wing | 37 | 55.59 |
| empennage | 15 | 11.35 |
| control system | 7 | 12.41 |
| landing gear | 7 | 14.05 |
| integration | 13 | 11.24 |
| Total | 107 | 141.84 |

The transformation of the structural design to the actual physical product complicated by the need to consider the thickness of support beams in the total overall dimensions. On paper the spacing between beams or ribs was set as if the beam was simply a line. However, careful planning was required to account for the actual thickness of the beams or ribs and some dimensions needed to be slightly altered. Other unforeseen complications included the addition of extra plywood supports for the landing gear, the integration of the steerable landing gear, and the placement of the wing trailing edge screw supports outside of the fuselage due to interference on the inside from the engine batteries and avionics.

The integration of the tail-dragger wheel to the rudder control system was not fully considered during the design phase, and when the prototype was built this posed a problem since the rear wheel was at least six inches forward of the rudder and the control rod ran along the outside of the cargo bay. A few control integration methods were considered but in the end the decision was

made to leave the tail dragger uncontrollable. This greatly simplified the attachment of the tail dragger and effective control was still easily obtained through the rudder.

# APPENDIX A
## Computer Tools to Analyze Wing

### 1. WINGLOAD Progam

```
c       Tim Cashin
c       Program to determine section properties, stress resultants,
c       axial stress, and shear flow in a discrete area wing section.
c       December 13, 1991
c
        parameter(dim=20)
        real x(dim),cl(dim),cd(dim),cm(dim),w(dim),py(dim),pz(dim),mx(dim),q(0:20)
        real vy(dim),vz(dim),my(dim),mz(dim),mm(dim),l,mo,n,lift

        implicit real(i,m)
        dimension a(20),z(20),y(20),e(20),alpha(20),t(20),stress(20,20),z2(20),y2(20)
        character*20 filen
c
c       Initialize Values
c
        write(6,1)
1       format(' Enter filename containing wing geometric data: ',$)
2       read(5,'(a)')filen
        open(20,file=filen,status='old',err=5)
        goto7
5       write(6,6)
6       format(' File does not exist; Re-enter: ',$)
        goto2
7       read(20,*)ne
        read(20,*)(a(j),y(j),z(j),e(j),alpha(j),t(j),j=1,ne)
        open(21,file='wingload.results')
        write(6,8)
8       format(' Enter filename containing wing aerodynamic data: ',$)
        read(5,'(a)')filen
        open(30,file=filen,status='old')
        read(30,*)npts
        read(30,*)(x(j),cl(j),cd(j),cm(j),w(j),j=1,npts)
        rho=.0023769
        write(6,*)' Enter velocity (ft/s), load factor and angle of attack'
        read(5,*)v,n,aa
        qq=(.5*rho*v**2)/144.
        write(21,*)'V  =',v,'ft/s'
        write(21,*)'Angle of attack =',aa
        write(21,*)'n  =',n
        write(21,*)

        write(6,*)'Enter Reference value for E'
        read(5,*)er
c
```

```
c       Find Moments of Inertia.  Ref axis MUST be at trailing edge
c
        do 10 j=1,ne
              area=area+(e(j)/er)*a(j)
              iy=iy+(e(j)/er)*z(j)*a(j)
              iz=iz+(e(j)/er)*y(j)*a(j)
10      continue
        zbar=iy/area
        ybar=iz/area
        do 20 j=1,ne
              z2(j)=z(j)-zbar
              y2(j)=y(j)-ybar
              iyy=iyy+(e(j)/er)*z2(j)**2*a(j)
              izz=izz+(e(j)/er)*y2(j)**2*a(j)
              iyz=iyz+(e(j)/er)*y2(j)*z2(j)*a(j)
              pt=pt+e(j)*alpha(j)*t(j)*a(j)
              mtz=mtz+e(j)*alpha(j)*t(j)*a(j)*y2(j)
              mty=mty+e(j)*alpha(j)*t(j)*a(j)*z2(j)
20      continue
        write(21,*)' Modulus Weighted Values, Er =',er
        write(21,200)ybar,zbar
        write(21,*)'Iyy =',iyy
        write(21,*)'Izz =',izz
        write(21,*)'Iyz =',iyz

c
c       Find Section Lift, Drag, and Moment (about centriod)
c       Assume cg is at modulus weighted centriod
c
        write(6,*)' Enter wing chord (in.)'
        read(5,*)c
        lac=.75*c-zbar
        do 30 j=1,npts
              l=qq*cl(j)*c
              d=qq*cd(j)*c
              mo=qq*cm(j)*c**2
              py(j)=l*cosd(aa)+d*sind(aa)-n*w(j)*cosd(aa)/12.
              pz(j)=l*sind(aa)-d*cosd(aa)-n*w(j)*sind(aa)/12.
              mm(j)=-l*cosd(aa)*lac-d*sind(aa)*lac-mo
              lift=lift+2*(l*(x(j+1)-x(j)))
30      continue
        write(21,*)
        write(21,*)'Total lift =',lift

c
c       Trapezoidal Integration
c
        vz(npts)=0.
        vy(npts)=0.
        mz(npts)=0.
        my(npts)=0.
        do 40 j=npts-1,1,-1
              vz(j)=vz(j+1)+(pz(j+1)+pz(j))/2*(x(j+1)-x(j))
              vy(j)=vy(j+1)+(py(j+1)+py(j))/2*(x(j+1)-x(j))
```

```
            mx(j)=mx(j+1)+(mm(j+1)+mm(j))/2*(x(j+1)-x(j))
            my(j)=my(j+1)-(vz(j+1)+vz(j))/2*(x(j+1)-x(j))
            mz(j)=mz(j+1)+(vy(j+1)+vy(j))/2*(x(j+1)-x(j))
40      continue
        write(21,*)' Wing Loading'
        write(21,100)
        do 50 j=1,npts
            write(21,101)x(j),vy(j),vz(j),mx(j),my(j),mz(j)
50      continue

c
c       Direct Stress at each Point
c
        do 500 k=1,npts
        do 60 j=1,ne
          stress(k,j)=e(j)*(p+pt)/(er*area) -e(j)/er*((mz(k)-mtz)*iyy+(my(k)+mty)*iyz)/(iyy*izz-
iyz**2)*y2(j)    +e(j)/er*((my(k)-mty)*izz+(mz(k)+mtz)*iyz)/(iyy*izz-iyz**2)*z2(j
e(j)*alpha(j)*t(j)
60      continue
500     continue

        write(21,201)
        do 80 k=1,npts
            write(21,*)' x =',x(k)
            do 70 j=1,ne
                write(21,202)y(j),z(j),stress(k,j)
70          continue
80      continue
c
c       Shear Flow
c
        write(21,*)'Shear Flow'
        y2(ne+1)=y2(1)
        z2(ne+1)=z2(1)
        do 90 k=1,npts
            c1=(-vy(k)*iyy+vz(k)*iyz)/(iyy*izz-iyz**2)
            c2=(-vz(k)*izz+vy(k)*iyz)/(iyy*izz-iyz**2)
            do 95 j=1,ne
                q(j)=q(j-1)+e(j)/er*(c1*y2(j)*a(j) + c2*z2(j)*a(j))
                aj=abs(y2(j+1)*z2(j)-y2(j)*z2(j+1))
                a2=a2+aj
                c3=c3+q(j)*aj
95          continue
            j=0
            q(0)=(vy(k)*zbar-vz(k)*ybar+mx(k)-c3)/a2
            write(21,*)' x =',x(k)
            write(21,203)j,q(0)
            do 300 j=1,ne-1
                q(j)=q(j)+q(0)
                write(21,203)j,q(j)
300         continue
90      continue
```

```
100   format('x (ft)',t10,'Vy (lb)',t20,'Vz (lb)',t30,'Mx (lb-in)',t41,'My (lb-in)',t52,'Mz (lb-
in)')
101   format(f4.1,t10,f7.2,t20,f7.3,t30,f8.2,t41,f8.2,t52,f7.1)
200   format(' Centroid at (',f5.2,','f6.3')')
201   format('Point',t20,'Axial Stress [psi]')
202   format(' (',f5.2,',',f5.2,')',t22,f12.2)
203   format(' q(',i2,') = ',f10.2,' lbs/in')

      close(20)
      close(21)

      end
```

## 2. TK Solver Plus Program

**Rules**

```
zbar=t/2-h/2
I=2*(zbar^2*A + b*h^3/12)+tweb*t^3/12
Mroot=(span/4)*(L/2)
zmax=t/2
t=c*tc
stress=Mroot*zmax/I
Q=b*h*(t/2-h/2)+tweb*t^2/4
Vroot=L/2
taumax=Vroot*Q/(I*tweb)
A=h*b
L=n*Wtot
numrib=round(span/ribspace)+1
Srib=t*c/2
Wspar=2*A*span*rhospar*16
Wrib=Srib*trib*rhobalsa*numrib*16
Wweb=tweb*t*span*rhobalsa*16
Wle=Ale*span*rhobalsa*16
Wte=Ate*span*rhobalsa*16
Wsur=2*span*c*rhomonokote*16
Wtotal=Wspar+Wrib+Wle+Wte+Wsur+Wweb
```

**Output for n = 1.5**

| Input | Name | Output | Unit | Comment |
|---|---|---|---|---|
| .1875 | b | | in. | width of spar cap |
| .125 | h | | in. | height of spar cap |
| 120 | span | | in. | wing span |
| 11.4 | c | | in | chord |
| .165 | tc | | | t/c ratio |
| 1.5 | n | | | load factor |
| 6 | Wtot | | lb | Est. total plane wieght |
| .0625 | trib | | in | thickness of rib |
| .0625 | Ale | | in^2 | area of leading edge spar |
| .09375 | | Ate | | in^2 area of T.E. spar |
| 4 | ribspac | | | in spacing between ribs |
| .625 | tweb | | in | web thickness |
| .0001125 | | rhomono | | |
| .016 | rhospar | | | lb/in^3 |
| .0058 | rhobals | | | lb/in^3 |
| | I | .07085914 | | in^4 I for spar |
| | A | .0234375 | | in^2 Area of one spar cap |
| | Mroot | 135 | lb in | Moment at root |
| | L | 9 | lb | total wing lift |
| | stress | 1791.8294 | | psi stress at root |
| | t | 1.881 | in | airfoil thickness |
| | zbar | .878 | in | |
| | zmax | .9405 | in | point of max stress (t/2) |
| | Q | .07586189 | | |
| | Vroot | 4.5 | lb | |
| | taumax | | 77.083293 | psi |
| | numrib | | 31 | number of ribs |
| | Srib | 10.7217 | | in^2 |
| | Wspar | 1.44 | oz | |
| | Wrib | 1.9277617 | | oz |
| | Wweb | 1.309176 | | oz |
| | Wle | .696 | oz | |
| | Wte | 1.044 | oz | |
| | Wsur | 4.9248 | | oz |
| | Wtotal | 11.341738 | | oz |

# APPENDIX B

## MATERIAL COST BREAKDOWN FOR PROTOTYPE

| CATEGORY | UNIT | KIND | SUBTOTAL($) |
|---|---|---|---|
| PROPULSION: | | | |
| | geared motor | Astro Cobalt 15 | 124.95 |
| | speed controller | Tekin | 70.00 |
| | batteries | Panasonic 900 mah | 24.99 |
| | propeller | Zinger 10-6 | 2.49 |
| AVIONICS: | | | |
| | r/c unit: (transmitter, servo, receiver, batteries) | Futaba system | 244.95 |
| | control rods | Sullivan plastic | 3.99 |
| | nylon control horns | DuBro | 1.78 |
| | velcro fasteners | | 3.45 |
| | threaded rods | | 0.69 |
| STRUCTURES: | | | |
| | MonoKote | | 40.56 |
| | glue | Insta-cure | 9.98 |
| | balsa wood | | 42.69 |
| | spruce | | 4.72 |
| | threaded blocks | | 1.15 |
| | nylon wing screws | | 0.89 |
| | birch dowel | | 0.88 |
| | plywood | | 7.77 |
| LANDING GEAR: | | | |
| | Music wire | 5/32" & 3/32" | 1.73 |
| | front wheels | Lite Wheels (2.5") | 4.25 |
| | tailwheel bracket | DuBro | 2.25 |
| | wheel collars | DuBro | 1.49 |
| | screws | #4X3/8" | 1.59 |
| | tail wheel | Foam (1") | 1.45 |
| | landing gear clamps | | 1.29 |
| TOTAL ($) | | | 599.98 |

| | |
|---|---|
| t/c | 0.1 |
| Incidence angle (root) | 0 |
| Hor. pos of 1/4 MAC | 1.89 ft. |
| Ver. pos of 1/4 MAC | 3.5 in. |
| e- Oswald efficiency | 0.93 |
| CDo -wing | 0.0136 |
| CLo - wing | 0.72 |
| CLalpha -wing | 4.76 |

FUSELAGE

| | |
|---|---|
| Length | 4.85 ft. |
| Diameter - max | 7 in. |
| Diameter - min | 4.5 in. |
| Diameter - avg | 5.75 in. |
| Finess ratio | |
| Payload volume | 1000 in3 |
| Total volume | 1587 in3 |
| Planform area | 238825 in2 |
| Frontal area | 31.5 in2 |
| CDo - fuselage | 0.00253 |
| CLalpha - fuselage | 0 |

EMPENNAGE

Horizontal tail

| | |
|---|---|
| Area | 1.57 ft2 |
| span | 2.8 ft. |
| aspect ratio | 5 |
| root chord | 0.56 ft. |
| tip chord | 0.56 ft. |
| taper ratio | 1 |
| l.e. sweep | 0 |
| 1/4 chord sweep | 0 |
| incidence angle | 2.5 degrees |
| hor. pos. of 1/4 MAC | 4.43 ft. |
| ver. pos. of 1/4 MAC | 3.5 in. |
| Airfoil section | plate |
| e - Oswald efficiency | - |
| CDo -horizontal | 0.00264 |
| CLo-horizontal | 0 |
| CLalpha - horizontal | 4.34 |
| CLde - horizontal | 1.736 |
| CM mac - horizontal | 0 |

Vertical Tail

| | |
|---|---|
| Area | 0.72 ft2 |
| aspect ratio | 2 |
| root chord | 0.6 ft. |
| tip chord | 0.6 ft. |
| taper ratio | 1 |

| | |
|---|---|
| l.e. sweep | 0 |
| 1/4 chord sweep | 0 |
| hor. pos. of 1/4 MAC | 4.4 in. |
| vert. pos. of 1/4 MAC | 3.5 in. |
| Airfoil section | plate |

SUMMARY

| AERODYNAMICS | |
|---|---|
| Cl max (airfoil) | 1.42 |
| CL max (aircraft) | 1.2 |
| lift curve slope (aircraft) | 5 |
| CDo (aircraft) | 0.0265 |
| efficiency - e (aircraft) | 0.73 |
| Alpha stall (aircraft) | 8 degrees |
| Alpha zero lift (aircraft) | neg. 8 degrees |
| L/D max (aircraft) | 15.2 |
| Alpha L/D max (aircraft) | 0 |

| WEIGHTS | |
|---|---|
| Weight total (empty) | 91.7 oz. |
| C.G. most forward-x&y | 1.95 ft., 1.28 in. |
| C.G. most aft- x&y | 2.01 ft., 0.74 in. |
| Avionics | 4.15 oz. |
| Payload (max) | 32 oz. |
| Engine & Engine Controls | 13.17 oz. |
| Propeller | 0.54 oz. |
| Fuel (battery) | 14.76 oz. |
| Structure | 27.1 oz. |
| Wing | 12 oz. |
| Fuselage/emp. | 7.25/3.1 oz. |
| Landing gear | 4.73 oz. |
| Icg - max weight | - |
| Icg - empty | 0.185 slugs*ft2 |

| PROPULSION | |
|---|---|
| Type | Astro 15 |
| number | 1 |
| placement | nose |
| Pavil max @engine | 70 watts |
| Preq cruise | 14.23 watts |
| max. current draw | 6.81 amps |
| cruise current draw | 4.38 amps |
| Propeller diameter | 10 in. |
| Propeller pitch | 6 |
| Number of blades | 2 |
| max. prop. rpm | - |
| cruise prop. rpm | 3400 |
| max. thrust | 1.82 lbs. |
| cruise thrust | 0.37 lbs. |

| | |
|---|---|
| battery type | Panasonic-90SCR |
| number | 12 |
| individual capacity | 900 mah |
| individual voltage | 1.2 volts |
| pack capacity | 900 mah |
| pack voltage | 14.4 volts |

## STAB AND CONTROL

| | |
|---|---|
| Neutral point | 0.5 |
| Static margin %MAC | 12.50% |
| Hor. tail volume ratio | 0.42 |
| Vert. tail volume ratio | 0.018 |
| Elevator area | 0.31 ft2 |
| Elevator max deflection | 15 degrees |
| Rudder Area | 0.36 ft2 |
| Rudder max deflection | 25 degrees |
| Aileron Area | 0 |
| Aileron max deflection | 0 |
| Cm alpha | neg. 0.58 /rad |
| Cn beta | 0.065 /rad |
| Cl alpha tail | 4.34 |
| Cl delta e tail | 1.756 |

## PERFORMANCE

| | |
|---|---|
| Vmin | 23 ft/s |
| Vmax | 54 ft/s |
| Vstall | 23 ft/s |
| Range max - Rmax | 22,198 ft. |
| Endurance @ Rmax | 9.3 min. |
| Endurance Max -Emax | 13.13 min. |
| Range at @Emax | 15,990 ft. |
| ROC max | 6.1 ft/s |
| Min Glide angle | neg. 3.72 degrees |
| T/O distance | 52 ft. |
| T/O rotation angle | 15 degrees |
| Landing Distance | 174 ft. |
| Catapult Range | 102 ft. |

## SYSTEMS

| | |
|---|---|
| Landing gear type | tail-dragger |
| Main gear position | 18.1 in. |
| Main gear length | 4.8 in. |
| Main gear tire size | 2.5 in. |
| nose/tail gear position | 49.5 in. |
| n/t gear length | 1.5 in. |
| n/t gear tire size | 1.0 in. |
| engine speed control | Tekin |

| Control surfaces | Rudder/Elevator |
|---|---|
| **TECH DEMO** | |
| Payload volume | 1008 in3 |
| Payload Weight | 2 lbs. |
| Gross Take-Off Weight | 6.58 lbs. |
| Empty Operating Weight | 4.58 lbs. |
| Zero Fuel Weight | 3.46 lbs. |
| Wing Area | 9.48 ft2 |
| Hor. Tail Area | 1.57 ft2 |
| Vert Tail Area | 0.71 ft2 |
| C.G. position | 1.99 ft. |
| 1/4 MAC position | 1.9 ft. |
| Static margin %MAC | 17% |
| V takeoff | 25 ft/s |
| Range max | 20000 ft. |
| Endurance max | 12 min. |
| V cruise | 30 ft/s |
| Turn radius | 60 ft. |
| Airframe struct. weight | 31.9 oz. |
| Propulsion sys. weight | 29.4 oz. |
| Avionics weight | 7.3 oz. |
| Landing gear weight | 4.7 oz. |
| Est. Catapult range | |
| **ECONOMICS:** | |
| unit materials cost | $91.00 |
| unit propulsion system cost | $222.00 |
| unit control system cost | $252.00 |
| unit total cost | $565.00 |
| scaled unit total cost | $358,600.00 |
| unit production personhours | 100 person hrs. |
| scaled production costs | $326,000 |
| total unit cost | $565.00 |
| cargo cost ($/in3) | avg=6.39 |
| single flight gross income | max=$3410.00 |
| single flight op. costs | max=$7.90 |
| single flight profit | max=$1876.00 |
| #flights for break even | min=50 days |